UNIVERSITÉ DE SHERBROOKE
Faculté de génie
Département de génie chimique et de génie biotechnologique

Quiescent and flow-induced crystallization of poly(lactic acid)

La cristallisation statique et induite par écoulement du poly(acide lactique)

Thèse de doctorat
Spécialité : génie chimique et de génie biotechnologique

Amirjalal Jalali

Jury: Prof. Michel Huneault (directeur)
Prof. Saïd Elkoun (codirecteur)
Prof. Mathieu Robert
Dr. Pascal Vuillaume
Prof. Jocelyn Veilleux

Sherbrooke, Québec, Canada Janvier 2017

To my parents for their love, support and patience

RÉSUMÉ

Le poly(acide lactique), PLA, est un polymère biocompatible et biodégradable, qui peut être produit à partir de ressources renouvelables. En conséquence, il a soulevé une attention toute particulière en tant que remplacement éventuel des polymères à base de pétrole. C'est un polyester aliphatique ayant des propriétés telles que module élevé, haute résistance, biocompatibilité et est donc un matériau prometteur pour diverses applications telles que les implants, l'encapsulation de médicaments et l'emballage. A cause de sa faible température de transition vitreuse, le PLA a une faible résistance thermique et les applications sont donc limitées à celles qui ne sont pas associées à des températures élevées. En outre, ce polymère souffre d'un faible degré de cristallinité. L'augmentation du taux de cristallinité dans de nombreuses techniques de mise en forme, telles que le moulage par injection, est nécessaire.

Il y a plusieurs façons d'augmenter le niveau de cristallinité du PLA. Ces procédés comprennent l'utilisation d'agents nucléants, de plastifiants, ou de combinaisons d'agents plastifiants et de nucléation. La cristallisation du PLA à l'état fondu se présente sous deux formes cristallines légèrement différentes connues sous les noms α et α'. Cette étude compare la capacité d'auto-nucléation de ces deux formes cristallines par auto-nucléation. Ceci est réalisé en comparant les températures de cristallisation lors du refroidissement des échantillons préalablement cristallisés à diverses températures, puis de nouveau chauffé à une température dans la plage de fusion partielle du PLA. Dans la deuxième étape, l'effet des paramètres cinétiques et le poids moléculaire du PLA sur l'efficacité de nucléation des PLA phases cristallines a été étudié. Cette partie de l'étude ouvre une nouvelle voie pour comprendre le rôle des modifications cristallines du PLA qui mènent aux conditions optimales pour la cristallisation du PLA. La mise en forme des polymères implique des contraintes de cisaillement et d'élongation, ce qui implique une cristallisation induite par l'écoulement et la solidification qui s'en suit. Les propriétés mécaniques des produits finals dépendent du degré de cristallisation et de la nature des cristaux formés. Par conséquent, l'optimisation du procédé nécessite une bonne compréhension de la façon dont l'écoulement influence la cristallisation. Le type d'écoulement peut jouer un rôle important sur la cristallisation. Par exemple, l'écoulement élongationnel provoque l'orientation et l'étirement des molécules dans le sens de l'extension, comme dans le cas de la mise en forme de fibres et le soufflage de film, en aidant le processus de cristallisation induite par l'écoulement. Une littérature abondante existe sur la

cristallisation des thermoplastiques classiques induite par l'écoulement. Cela dit, moins d'attention a été accordée à l'effet de l'écoulement de cisaillement et d'allongement sur la cristallisation du PLA. Comme étudié dans la dernière partie de ce document, l'effet du poids moléculaire sur la cristallisation induite par cisaillement du PLA est rapporté. Pour cela, trois différents PLA à faible, moyen et haut poids moléculaire ont été préparés par réaction d'hydrolyse. Ensuite, en utilisant un rhéomètre oscillatoire, l'effet du cisaillement sur la cinétique de cristallisation du PLA a été examiné.

Mots -clés: Poly(acide lactique), la cristallisation, l'auto-nucléation, la cristallisation induite par écoulement.

SUMMARY

Poly(lactic acid), PLA, is a biocompatible and biodegradable polymer that can be produced from renewable resources. As a result, it has raised particular attention as a potential replacement for petroleum-based polymers. It is an aliphatic polyester with properties such as high modulus, high strength, and biocompatibility and is thus a promising material for various applications such as implants, drug encapsulation, and packaging. In the wake of low glass transition temperature, PLA has a low heat resistance and its application is limited to those not associated with high temperatures. In addition, this polymer suffers from a low degree of crystalinity. Increasing the crystallization rate in many processing operations, such as injection molding, is required.

So far, many routes have been found to improve the crystallinity of PLA. These methods include using nucleating agents, plasticizers, and combination of nucleating agents and plasticizers together. PLA crystallization in the melt state results in two slightly different crystalline forms known as α and α'forms. This thesis compares the self-nucleation ability of these two crystal forms by self-nucleation. This is achieved by comparing crystallization temperatures upon cooling for samples previously crystallized at various temperatures and then re-heated to a temperature in the partial melting range for PLA. In the second step, we study the effect of molecular weight of PLA on the nucleation efficiency of PLA crystalline phases. This part of the investigation opens a new pathway to understand the role of PLA crystalline phases on the optimal condition for its crystallization kinetics.

Polymer processing operations involve mixed shear and elongational flows and cause polymer molecules to experience flow-induced crystallization during flow and subsequent solidification. The mechanical properties of the final products are significantly dependent upon the degree of crystallization and types of formed crystals. Therefore, optimization of any polymer process requires a good understanding of how flow influences crystallization. The type of flow can play a significant role in affecting crystallization. For example, elongational flow causes molecules to orient and stretch in the direction of extension, as in the case of fiber spinning and film blowing, helping the process of flow-induced crystallization. An extensive body of literature exists on flow-induced crystallization of conventional thermoplastics. Having said that, less attention has been paid to the effect of shear and elongational flow on the PLA crystallization kinetics. As investigated in the final part of this thesis, the effect of

molecular weight on the shear-induced crystallization of PLA is reported. For this, low, medium and high molecular-weight PLAs were prepared from a high molecular weight one by a hydrolysis reaction. Next, by means of a simple rotational rheometry, effect of the shear flow was examined on the crystallization kinetics of these three PLAs.
Key words: Poly(lactic acid), crystallization, self-nucleation, flow-induced crystallization.

ACKNOWLEDGEMENT

Firstly, I would like to express my sincere gratitude to my advisor Prof. Michel Huneault for the continuous support of my Ph.D. study and related research, for his patience, motivation, and immense knowledge. I am also thankful to him for encouraging the use of correct grammar and consistent notation in my writings and for carefully reading and commenting on countless revisions of this thesis. I could not have imagined having a better advisor and mentor for my Ph.D. study.

My gratitude is to my co-advisor, Prof. Saïd Elkoun. I have been fortunate to have a co-advisor who gave me the freedom to question thoughts and express ideas. His patience and support helped me overcome many crises and finish this dissertation.

Dr. Shant Shahbikian is one of the best friends that I have had in my life. He sets high standards for his work and he encourages and guides all his colleagues to meet those standards. He introduced me to rheometry and his teachings inspired me to work on rheology profoundly. I am indebted to him for his continuous encouragement and guidance.

I am grateful to Florent Gauvin, Christian Lubombo and Thomas Mazerolles for their encouragement and practical advice for the French abstracts of my thesis. I am also thankful to them for reading my abstracts; commenting on my views and helping me understand and enrich my French.

I thank my fellow labmates for the stimulating discussions, for working together and for all the fun that we have had in the last four years.

Most importantly, none of this would have been possible without the love and patience of my family. My immediate family, to whom this dissertation is dedicated to, has been a constant source of love, concern, support and strength all these years. I warmly appreciate the generosity and understanding of my family.

TABLE OF CONTENTS

LIST OF FIGURES

LIST OF TABLES

LIST OF SYMBOLS

Symbol	Definition
t	time
$X(t)$	Degree of crystallinity
$t_{1/2}$	Crystallization half-time
T_m	Melting temperature
T_g	Glass transition temperature
T_s	Partial melting temperature
T_{CC}	Cold crystallization temperature
T_C	Crystallization temperature
T_{ic}	Isothermal crystallization temperature
T_{Cmin}	Minimum crystallization temperature
T_{Cmax}	Maximum crystallization temperature
ΔH_t	Enthalpy generated at time t
ΔH_∞	Enthalpy generated at infinite time
ΔH_m	Melting enthalpy
ΔH_{CC}	Cold crystallization enthalpy
ΔH_{m0}	Melting enthalpy of 100% crystalline PLA
n	Avrami exponent
K	Avrami constant
N	Nuclei density
G	Spherulite growth rate
D	Average spherulite size
U^*	Activation energy
M_n	Number-average molecular weight
M_w	Weight-average molecular weight
G'	Storage modulus
G''	Loss modulus
$\lvert\eta^*\rvert$	Complex viscosity
T_{ref}	Reference temperature

a_T	Shift factor
C_1	WLF parameter
C_2	WLF parameter
T_0	Reference temperature in WLF equation
T_r	Glass transition temperature in WLF equation
η_0	Zero-shear viscosity
$\eta+$	Stress growth coefficient
Wi	Weissenberg number
$\dot{\gamma}$	Shear rate
λ	Relaxation time
W_{rep}	Reptation Weissenberg number
Ws	Stretch Weissenberg number
λ_{rep}	Reptation relaxation time
λ_R	Rouse relaxation time
ω	Angular frequency
M_e	Molecular mass between entanglements
$H(\lambda)$	Relaxation time distribution

LIST OF ACRONYMS

Acronym	Definition
PLA	Poly(lactic acid)
PLLA	Poly(L-lactic acid)
PDLA	Poly(D-lactic acid)
WAXD	Wide Angel X-ray Diffraction
TEM	Transmission Electron Microscopy
PET	Poly (ethylene terephthalate)
PBT	Poly(butylene terephthalate)
PBS	Poly(butylene succinate)
PES	Poly(ethylene succinate)
PEEK	Poly(ether ether ketone)
DSC	Diffrential Scanning Calorimetry
XRD	X-ray Diffraction
PCDI	Polycarbodiimide
TNPP	nonylphenyl phosphite
DNA	Deoxyribonucleic
EBS	Bis-stearamide
C60	Fullerene
TPS	Thermoplastic starch
PGA	Polyglycolide
CNC	Cellulose nanocrystals
CD	Cyclodextrin
PHB	Poly(hydroxybutyrate)
PHBV	Poly(hydroxybutyrate valerate)
PBA	Poly(butylene adipate)
OA	Orotic acid
ZnCC	Zinc citrate complex
BTA	1,3,5-benzene tricarboxyamide
TBC8-eb	P-tert- butylcalix

DBS	Dibenzylidene-D-sorbitol
NA	N,N'-Bis(benzoyl) acid dihydrazide
CNT	Carbon nanotubes
MWCNT	Multiwall carbon nanotube
CB	Carbon black
MCB	Modified carbon black
PPZn	Zinc phenylphosphonate
PPA-Zn	Phenylphosphonic acid zinc
POSS	Polyhedral oligosilsesquioxane
BF	Bamboo fiber
PEG	Polyethylene glycol
PPG	Polypropylene glycol
TPP	Triphenyl phosphate
CO2	Carbon dioxide
ATC	Acetyl triethyl citrate
NES	Nucleation efficiency scale
PC	Polycarbonate
PP	Polypropylene
PB	Polybutylene
FTIR	Fourier transform infrared spectroscopy
PVDF	Poly (vinylidene fluoride)
SSA	Self-nucleation and Annealing
PPDX	Poly(p-dioxanone)
SAXS	Small-Angle X-ray Scattering
BOPP	Biaxially oriented Polypropylene
iPB	Poly (1-butene)
WLF	Williams-Landel- Ferry equation
NLREG	Non-linear regression software
B-PLA	Branched PLA

CHAPTER 1 INTRODUCTION

Context

PLA is a versatile biobased linear polyester that has found multiple applications in recent years. Its use, however, could be further expanded if its crystallization rate could be increased. Higher crystallinity in PLA could lead to enhanced temperature resistance, a typical drawback of PLA for industrial applications. To date, several routes have been explored to increase the level of the crystallinity of PLA. The majority of these studies have been performed in quiescent conditions. However, even in these simple conditions, determination of the optimum crystallization conditions remains a challenge. From a crystallographical and chemical point of view, the most efficient nucleating agents for the crystallization of a semi-crystalline polymer are the crystal nuclei of the same polymer. Hence, studying the "self-nucleation" of PLA in the melt state can give us valuable information about its optimum crystallization conditions. Furthermore, two crystalline phases known as α' and α may form, depending on the crystallization temperature. The α' is favored at low crystallization temperature (< 100 °C) while the α phase is favored at high crystallization temperatures (> 120 °C). Within the crystallization temparture range of 100-120 °C, a mixture of these crystalline phases might co-exist.

PLA-based products are produced by conventional polymer processing techniques (e.g. injection molding, extrusion, film blowing). Crystallization in polymer processing conditions involves dynamic flow and heat transfer. For example, in injection molding, the polymer melt is subjected to high deformation rates during mold filling. Thus, crystallization upon cooling takes place in static mode but upon highly stretched polymer chains, which is very different from the quiescent crystallization used in calorimetric studies. Another interesting example is that of film blowing. In this process, the polymer melt experiences elongational flow leading to highly enhanced crystallization rates. Overall, the PLA crystallization kinetics in the presence of shear and elongational flow is still, to a large extent, poorly understood.

1.1 Research questions and objectives

Depending on the crystallization temperature, PLA has two crystalline phases, α and α'. The effect of these crystalline structures on the self-nucleation behavior of PLA has not been investigated yet. The first focus of this work will therefore aim at determining how the crystal phases differ in terms of nucleating efficiency and their role on the final sample morphology. The second question will be in relation with the effect of molecular weight. It is well recognized that molecular weight plays an important role on the mobility of polymer chains. In turn, this will play a role on crystal growth rates and on the overall crystallization rate. The research question that deserves to be tackled concerns the role of molecular weight on the crystallization dynamics and furthermore on the nucleation efficiency and phase morphology (α vs α' forms) genereated upon cooling and after self-seeding. This will provide a better understanding on means to promot the crystallization kinetics of PLA.

The third research question that will be addressed will be regarding the effect of flow on crystallization. As mentioned previously, manufacturing of thermoplastics always implies flow conditions that in turn influences crystallization kinetics. Hence, understanding the crystallization behavior of semi-crystalline polymers, like PLA, in the presence of flow is critical for both academic and industrial viewpoints. Consequently, the research has sought to determine how crystallization can occur upon continuous shear flow and how crystallization can be promoted through strong pre-shearing flows. Since the chain relaxation is strongly molecular-weight dependant, these last questions were answered for a range of molecular weight giving this study a more general scope.

Hence, in summary the main objective of this project is to further improve the basic understanding of:

"**Quiescent and flow-induced crystallization of PLA"**

with specific objectives being:

- To study the self-nucleation behavior of pure PLA, in particular on the effect of α and α' crystalline phases on nucleation efficiency.

- To investigate the effect of molecular weight on the self-nucleation efficiency of PLA.

- To investigate the effect of continuous shear flow and strong pre-shearing flow on the crystallization behavior of PLA with varying molecular weight.

1.2 Thesis organization

The thesis has been organized in the following manner. In chapter 2, a literature review on PLA crystallization has been presented in two parts. A general knowledge on crystallization of PLA, its crystalline phases and the ways that have been employed so far to improve the crystalinity of PLA is reflected in the first section. The second part focuses on the flow-induced crystallization of PLA. Chapters 3 to 5 cover the three distinct core experimental parts responding to the three main objectives described previously. Chapter 3 presents a study on the effect of thermal protocol on the self-nucleation of PLA. In chapter 4, effect of molecular weight on the nucleation efficiency of PLA crystalline phases is demonstrated. Chapter 5 presents the effect of molecular weight on the shear-induced crystallization of PLA. Finally, chapter 6 briefly outlines the most significant concluding remarks and presents recommandations for the future works in this area.

1.3 Original contribution

This work exhibits several original contributions to the subject of PLA crystallization. In the first section of the work, which addresses the quiescent crystallization of PLA, a successive heating and cooling thermal protocol to study the self-nucleation of PLA was illustrated. In addition, the optimum condition for the crystallization kinetics of PLA was reported. For the first time, a double crystallization peak for the self-nucleated PLA was reported. These peaks were ascribed to the formation of the α and α' phases. Changing the proportion of these two peaks by slightly changing the temperature within the partial melting range of PLA was another originality of the first section of the study. In the second part, the effect of thermal process and molecular weight on the nucleation efficiency was intended using the same applied thermal protocol in the first part. The self-nucleation experiments revealed that for the high-molecular weight PLA the maximum crystallization temperature upon cooling after self-seeding is a dependent function of the isothermal crystallization temperature. However, for the low-molecular weight PLA, it is rather equivalent, irrespective of the isothermal crystallization temperature. Furthermore, the double crystallization peak previously observed

in the first part of study was detected for the self-seeded low-molecular weight PLA on a given partial melting temperature range. The last phase of project regarding the shear-induced crystallization of PLA was original because it was not explored prior to the attempts reported in this thesis. It showed that crystallization kinetics of PLA was accelerated with molecular weight in the presence of shear flow.

CHAPTER 2 LITERATURE SURVEY

2.1 Preface

This section is dedicated to a review on crystallization kinetics of PLA, published methods for increasing its crystallinity, some aspects of stereocomplex PLA, self-nucleation and flow-induced crystallization of PLA. The last two subjects are the basis of the current research.

2.2 Lactic acid and lactide

Due to the existence of a chiral carbon in its backbone, PLA possesses two stereoisomers, L-PLA and D-PLA, which are called PLLA and PDLA, respectively. PLA can be synthesized by ring opening of lactide; a cyclic lactic acid dimer is produced in the first step (**Figure 1**) and this structure is polymerized to obtain high molecular weight PLA. Meso-lactide can also be produced by the combination of *L*- and *D*- units (**Figure 1**). The L:D ratio in PLA is a crucial parameter to control its biodegradability, mechanical properties as well as the degree of crystalinity and the melting point [1].

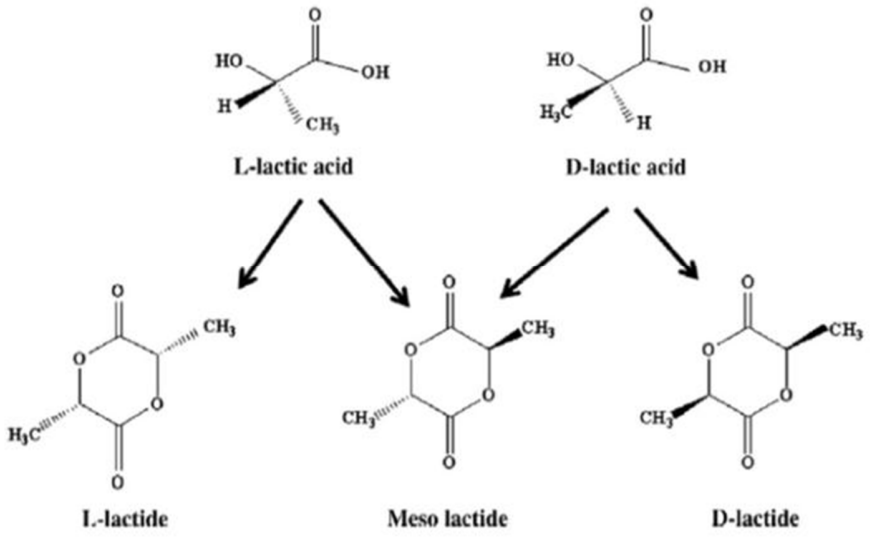

Figure 1. Stereoforms of lactide [2].

Details on synthesis of this polymer including the effect of temperature, catalysts, and kinetics of polymerization reactions can be found elsewhere [3]. We only focus on the crystallization of PLA. Before reviewing the main aspects of PLA crystallization, the crystallinity of polymers is briefly discussed.

2.3 Polymer crystallization

A two-phase model traditionally describes semi-crystalline polymers. In this model, every amorphous and crystalline phase demonstrates different characteristics. However, Menczel *et.al* [4] provided the first experimental evidences indicating the presence of a third intermediary phase. This interfacial layer is regarded as rigid amorphous fraction (RAF). Characteristics and properties of RAF are beyond the scope of this study and afterwards we mainly focus on the role of PLA crystalline phases.

The process of crystallization of polymers from the melt is divided into three parts: primary nucleation, crystal growth, and secondary crystallization [5]. In primary nucleation, a crystalline nucleus is formed in the molten state. This nucleus might form homogeneously by means of statistical fluctuation in the melt phase or heterogeneously by the presence of heterogeneities. Nucleation is often heterogeneous and takes place on surfaces, cavities, or cracks of insoluble impurities. After the formation of nuclei, crystalline lamellae establish and 3D structures form. The most commonly observed morphology on solidification from the melt is the spherulite; however, formation of the other structures such as hedrites or dendrites has been reported as well [6]. Crystallization does not stop with the growth of the crystals, and a process, which is called “secondary crystallization”, occurs. Here, the level of crystalinity as well as thickness of the already formed lamellar crystals increase, as reported in polyethylene [7] or poly(3-hydroxybutyrate) [8]. **Figure 2** shows a spherulite of isotactic polypropylene (iPP), which represents the organization of the crystalline lamellae and the amorphous phase.

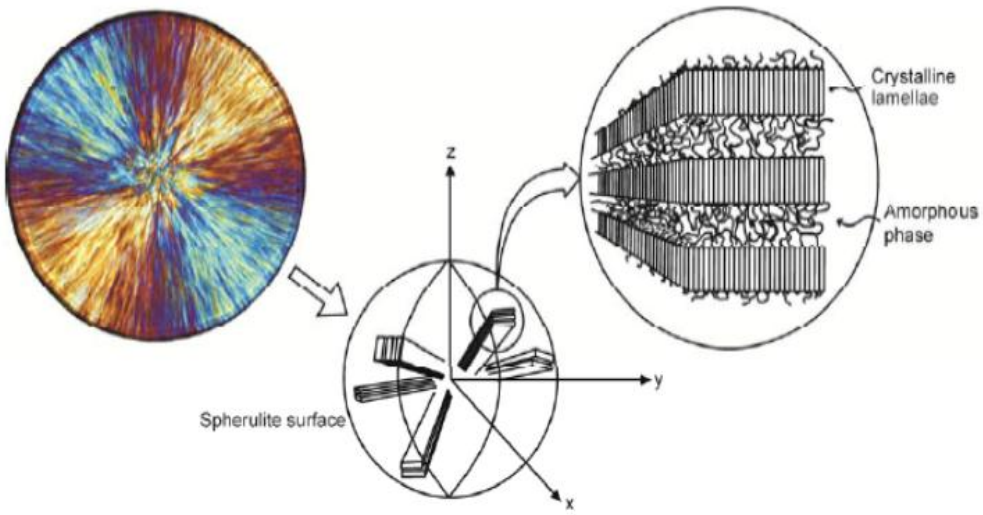

Figure 2. A spherulite of iPP as observed in the optical microscope [9].

Polymer crystallization is usually described by Lauritzen–Hoffman model, which explains three different regimes of crystallinity when log (G) + U^*/k (T-T_0) is plotted as a function of $(T\Delta T)^{-1}$[10].In this model, G is the spherulite growth rate, U^* is the activation energy and k is the constant. Covering the fundamental aspects of this theory is impossible in this review. **Figure 3** presents the Lauritzen–Hoffman plot for PLA with different molecular weights [11].

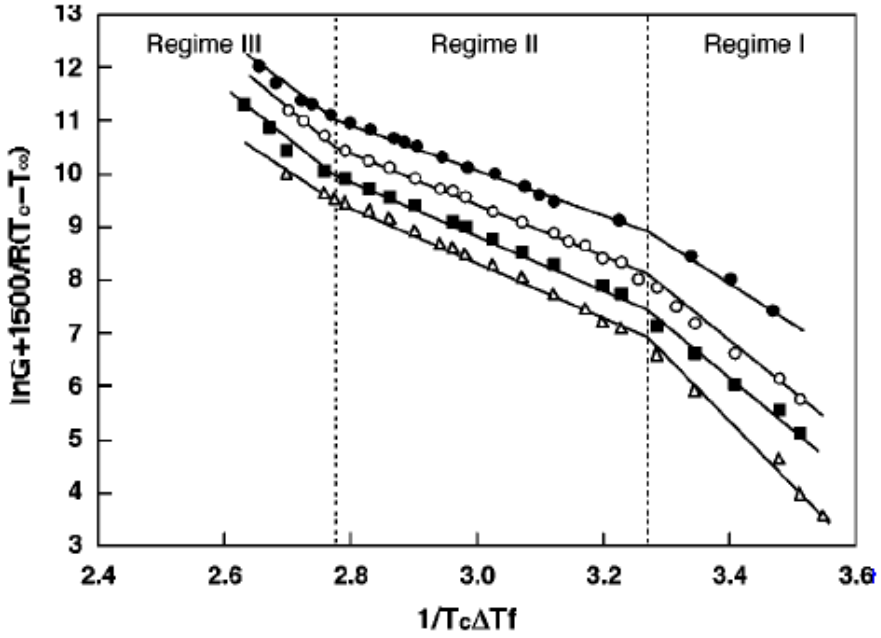

Figure 3. The Lauritzen–Hoffman PLA with different molecular weights [11].

2.4 PLA crystalline phases

PLLA crystals grow in three structural modifications, consisting in different helical conformations and cell symmetries developed upon different thermal and mechanical treatments [12]. The α form, the most stable type, forms upon melt or cold crystallization, and also from solution-spinning processes at low drawing temperatures [13]. Chain conformation of α phase is a left-handed 10_3 helix packing into an orthorhombic unit cell with parameters a = 1.06 nm, b = 1.737 nm, and c = 2.88 nm [14].

By stretching of α at high draw and high temperature ratios, another crystal structure, β, forms which has a unit cell with a = 1.031 nm, b = 1.821 nm, and c = 0.900 nm, and a chain conformation with left handed 3_1 helices [15]. The third crystal modification of PLLA, the γ form, has been reported to develop upon epitaxial crystallization on hexamethylbenzene substrate, with two antiparallel helices packed in an orthorhombic unit cell with a = 0.995 nm, b = 0.625 nm, and c = 0.88 nm [16]. **Table 1** summurizes Properties of PLA crystal forms.

Table 1. Properties of different PLA crystal forms.

Crystal type	**Dimensions**			**angles**		
-	a(nm)	b(nm)	c(nm)	α(°)	β(°)	ϒ(°)
α	1.06	1.737	2.88	90	90	90
β	1.031	1.82	0.9	90	90	90
ϒ	0.995	0.625	0.88	90	90	90

The crystallization kinetics of PLLA has been investigated by many research groups, and it has been found that it exhibits peculiar behavior [11,12,17,18]. The curve of the crystallization half-time ($t_{1/2}$) versus crystallization temperature (T_C) is basically continuous for most semi crystalline polymers, but for PLA it is discontinuous in the temperature range of 100-120 °C as can be seen in **Figure 4**. Besides, the profile of spherulite radius growth rate (G) versus T_C shows two maximums in **Figure 5** Two explanations exist for such an atypical behavior. Some studies have shown that this behavior can be ascribed to regime transition in crystalinity of PLA. Regime transitions of PLA crystal growth from the melt were investigated by Abe *et al.* using microscopic techniques [11]. Kinetic analysis demonstrated that regime transitions of PLA from regime III to regime II and from regime II to regime I took place at 120 °C and 147 °C, respectively. During transition from II to I, spherulitic crystals transformed to hexagonal

ones while no obvious morphology change was observed from II to III for spherulites. Di Lorenzo argues that the unusually high rate of crystallization below 120 °C cannot be attributed to the nucleation rate since no remarkable increment in the rate of nucleation was detected between 100 °C and 120 °C [19]. This phenomenon was ascribed to high radial growth rate of spherulites. No significant change in morphology of spherulites was observed as well. In addition, by using directly measured G values, a regime II-III transition was reported around 120 °C [19,20].

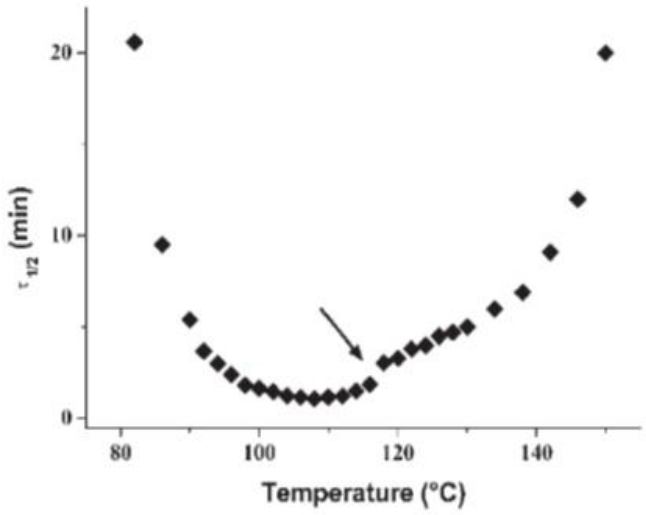

Figure 4. Crystallization half-time vs T_C for PLA [20].

Nevertheless, others have associated the unusually high rate of crystallization of PLA to polymorphic nature of PLA [17,21,22]. Ohtani [22] studied the crystallization behavior of amorphous PLA which was prepared by quenching from melt to ice-cold water. From the analysis of wide-angle X-ray diffraction, it was found that when amorphous PLA was crystallized below 120 °C, β crystals formed while annealed samples above 120 °C exhibited the α form of crystallites. Instead of $t_{1/2}$, Yasuniwa *et al.* [17] defined the peak of crystallization time, τp, as the time spent from the onset to the point where the exothermic crystallization peak appears. If the peak profile of isothermal crystallization is symmetric, then $\tau p = t_{1/2}$. They found that log τp against the isothermal crystallization temperature, Tc, changed discontinuously at 113 °C. Furthermore, the curve of spherulite growth rate, G vs. T_C, presented a discrete change at 113 °C. X-ray patterns proved that the crystal structure of samples crystallized below 113 °C and above 113 °C were trigonal (β form) and orthorhombic

(α form), respectively. They ascribed the discrete change of spherulite growth to a different growth mechanism of PLA crystalline phases.

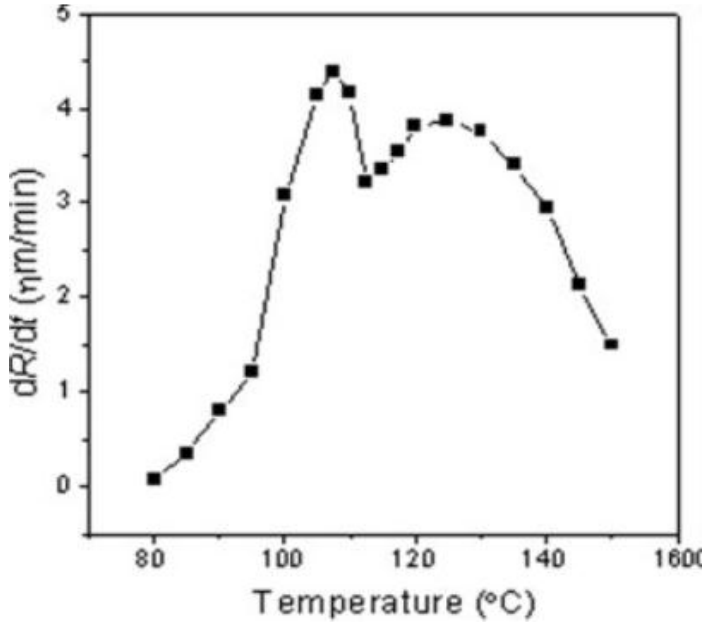

Figure 5. Spherulite radius growth rate of PLA as a function of T_C [18].

In recent years, a new crystalline structure designated as α', a disordered type of α, has been proposed for the PLLA samples which have been produced via melt or cold crystallization below 120 °C. This is different from the organized α form crystalized at higher temperatures [21,23,24].

For the first time, Zhang *et al.* [23,24,25] provided a comprehensive study on the effect of the isothermal crystallization temperature on the PLLA crystallization structure. They mentioned that the isothermal crystallization behavior of PLLA from the melt and glassy state by infrared spectroscopy was different [25]. The isothermal melt-crystallized PLLA sample was prepared at 150 °C after melting at 200 °C for 1 min whereas the isothermal cold-crystallized sample was prepared at 78 °C. No splitting band, induced by interaction of CH3 or C=O groups, was observed for the cold-crystallized sample while it was observed in the melt-crystallized sample.(When PLA is cooled from the melt we have the melt crystallization while when it is heated from solid state we have the cold crystallization). As a result, dissimilar chain packing was found during two different isothermal crystallization procedures. Additionally, WAXD patterns of the samples annealed at 80 °C and 140 °C were rather different. It, therefore, suggested the crystallization structure of PLLA samples prepared at different temperatures were dissimilar. Furthermore, in another attempt, they investigated the crystallization structure

of PLLA prepared between 80-150 °C [21]. Since there was no characteristic band at 908 cm^{-1} regarding β crystals of PLLA samples, it was concluded unequivocally there was no β form in the structure of prepared PLLAs crystalized at different temperatures. Moreover, in the region of 1810-1710 cm-1, the C=O stretching band area, a new band appeared at 1749 cm^{-1} with increasing the annealing temperature above 100 °C (**Figure 6**) [26]. The different electron diffraction patterns, ED, as well as TEM micrographs of samples taken from PLLA samples from 80 °C and 140 °C also confirmed the crystalline structure of PLLA was not similar at high and low isothermal crystallization temperatures. As previously mentioned above, IR analysis does not confirm the formation of the β structure at low temperatures. Consequently, based on this conclusion another type of crystalline structure for PLLA formed at low temperatures was defined. By means of IR spectroscopy, the α' form for PLLA was proposed. It has the 10_3 helix chain conformation and the different lateral packing of the helical chains, which is different from lateral packing of α crystalline phase.

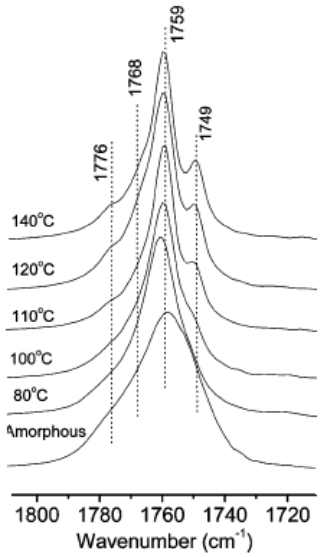

Figure 6. IR spectra of amorphous and crystalline PLLA crystallized at T_C =80-140 °C [26].

2.5 PLA multiple melting behavior

Multiple melting has been reported for many semi-crystalline polymers such as poly (ethylene terephthalate), PET [27], poly(butylene terephthalate), PBT [28], poly(ether ether ketone), PEEK, poly(butylene succinate), PBS [29], and poly (ethylene succinate), PES [30]. Thus far, three mechanisms have been suggested to explain the double melting behavior of semi-crystalline polymers; dual lamellae population, melt-recrystallization, and dual crystal structure [31].

Dual lamellae population has been reported mainly for PEEK [32,33]. This model is further divided into sub-models; the lamellae insertion model [34], and the lamellae stack model [35]. The absence of polymorphic transition thus excludes the possibility of two different crystal structures that could be assigned to the dual melting peaks often observed in PEEK thermographs. However, this is out of the scope of this research, which deals with PLLA, which is a polymorphous polymer.

The melt-recrystallization model explains the multiple melting. The low and high melting peaks can be assigned to the melting of some original crystals and to the melting of crystals formed during the crystallization process, respectively. The exothermic peak between these double endothermic peaks associates to the recrystallization. In other words, the melting progresses through the melting of the original crystals, their recrystallization, and finally the fusion of recrystallized crystals. Many researchers reported appearance of the double melting peaks in PLLA [31,36,37,38]. Jamshidi et al. studied the melting behavior of a series of PLLAs with different molecular weights [39]. The polymers with molecular weights lower than 3000 g/mol exhibited a weak and broad melting peak, slightly lower than that of the main endothermic peak. This peak disappeared by increasing the molecular weight. The broad peaks were attributed to an unstable crystalized region but further explanation was not given.

Figure 7 illustrates the DSC curves of melt-crystalized samples at a cooling rate of 1 °C/min from the melt [40]. There are two melting peaks designated low (L) and high (H). The H/L peak area ratio decreased with heating rate. According to the melt-recrystallization model, imperfect crystals transformed to more stable crystals through the melt-recrystallization mechanism [41,42]. When the rate of melting overcame the rate of recrystallization, an endothermic peak appeared while an exothermic peak appeared when the rate of recrystallization overwhelmed the rate of melting.

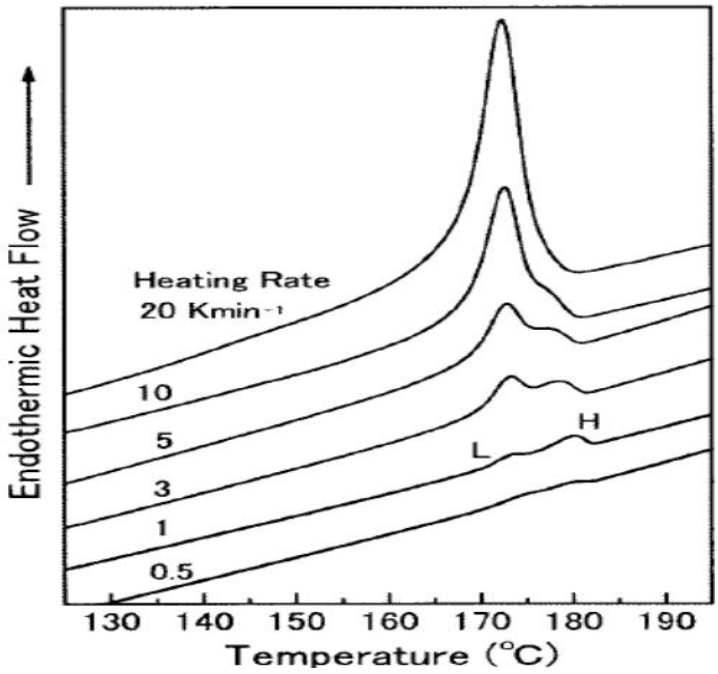

Figure 7. DSC curves of samples melt-crystalized at a cooling rate of 1 °C/min, being heated. The heating rates are indicated [40].

The double melting behavior, as well as an exothermic peak between two endotherms, for PLLA with the molecular weight of 18000 g/mol and higher ones, was also reported [43]. Some authors attributed this small exotherm to a cold crystallization [44]. It was then elucidated from the change in the X-ray diffraction patterns that the phase transition from the disordered crystal modification (α') to the organized form (α) occurred in a range of 155-165 °C for the samples isothermally crystallized at low temperatures, below 100 °C [38]. The lattice spacing calculated from the main diffraction peak, for isothermally crystallized samples at 80 °C and 100 °C, increased with temperature by thermal expansion. At 155 °C, a decrease in lattice space was observed and fitted to those of samples isothermally crystallized at 120 °C and 140 °C. This variation in lattice space corroborated the phase transition from α' to α. Kawai et al. [45] also confirmed this α' to α transform at 150 °C. They explained that this transition proceeded without melting in a very short time. Consequently, they considered this transition as a solid-solid phase transition.

2.6 Stereocomplex PLA

By a simple physical blending of PDLA and PLLA, stereocomplex PLA is formed. The PLA complexation occurs via the racemic crystallization process. This phenomenon was first introduced by Ikada *et al.* [46]. After that, many articles were published by Tsuji and coworkers about the other features of stereocomplex PLA [47,48,49,50,51,52,53,54,55]. **Figure 8** depicts the DSC curves of the pure PLLA and PDLA and their blend in different ratios. A single endothermic peak appeared in both pure enantiomers around 180 °C while a new melting peak was observed at 230 °C for the blends. When the blend ratio is 50/50, the peak around 180 °C disappeared and the peak around 230 °C was sharper. This outstanding rise in melting temperature was associated to a new crystalline structure due to co-crystallization of both enantiomers of PLA in their solution [46].

De Santis and Kovacs reported that the crystalline structure of PLLA and PDLA are left-handed and right-handed, respectively [56]. Stereocomplex crystal was formed through van der Waals forces as dipole-dipole interactions between two components. Okihara and his coworkers studied the crystalline structure of PLA stereocomplex using XRD [57]. The crystalline structure of the racemic crystal is triclinic with cell dimensions of a=0.916 nm, b=0.916 nm, c=0.87 nm and angles of α=109.2°, β=109.2° and γ=109.8°. In the unit cell, a PLLA segment and a PDLA segment are contained as a pair and packed laterally in parallel style. The *L*- and *D*- polylactides in the complex take a 3_1 helical conformation, which is a little extended from a 10 in the homopolymer crystal with the α form 3 helix.

According to Ikada *et al.* [46], the diffraction peaks for homopolymer appear at 2θ around 15°, 16°, 18.5° and 22.5° in WAXD patterns while PLLA50/PDLA50 exhibited the diffraction peaks at 2θ around 12°, 21° and 24°.

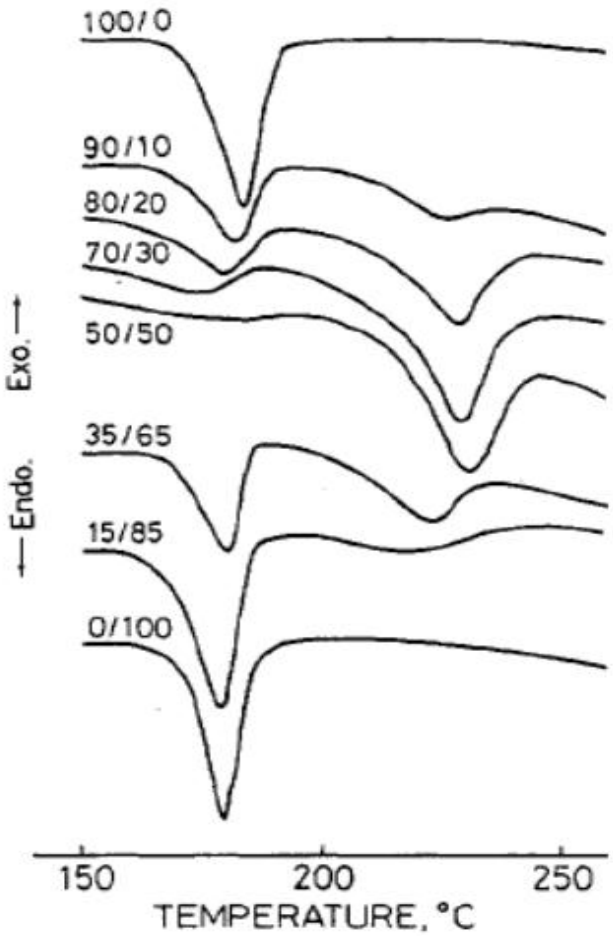

Figure 8. DSC thermograms of blend polymers from PLLA and PDLA. The ratios on the curves denote the blend ratios of PLLA to PDLA [46].

Various parameters including blending ratio [51,53,58,59,60], molecular weight [47,48,54,61], and optical purity [62,63,64] affect the racemic crystallization and homocrystallization of PLA.

2.6.1 Blending ratio

Equimolar ratio of PLLA and PDLA is the optimum ratio for the formation of PLA stereocomplex [46]. Changing this balance led to formation of homocrystals as well. According to Tsuji *et al.* [50], for PDLA mole fractions between 0.1 to 0.3 and 0.7 to 0.9, two melting peaks were observed regarding to homocrystals and stereocomplex crystals. For mole fractions between 0.4 and 0.6 only stereocomplex peak was observed [50,51].

2.6.2 Molecular weight

Crystallization of stereocomplex PLA from pairs of a low molecular weight PDLA, 4900 g/mol, and PLLA of various molecular weights was investigated by Tsuji *et al.*[50]. Mole fraction of PDLA was fixed at 0.5. By increasing the molecular weight of PLLA in the region above 60000 g/mol in the blend, the main melting peak of PLA stereocomplex decreased monotonically. The melting enthalpy, ΔH_m, calculated for PLLA with a molecular weight less than 60000 g/mol was approximately 70 J/(g-polymer) and was 50 J/(g-polymer) for PLLA with a molecular weight above 100000 g/mol. These results imply that when the molecular weight of at least one of the enantiomers is low enough, stereocomplex crystals form predominantly with almost no homopolymer crystals. To check this finding, further investigation was performed on the crystallization of PDLA having a high molecular weight, 360000 g/mol, and PLLA of various molecular weights. Analysis of DSC thermograms revealed that ΔH_m of homocrystals increased gradually with increasing molecular weight of PLLA, around 35-40 J/(g-polymer), whereas ΔH_m of stereocomplex crystals decreased monotonously with molecular weight of PLLA and at a molecular weight of 100000 g/mol it became virtually zero. These results confirm the postulation that racemic crystals form favourably to homopolymer crystals if the molecular weight of one of the components is sufficiently low. Other studies [51,65,66] also confirm this assumption.

2.6.3 Optical purity

Optical purity is associated to the ratio between *L*- and *D*- ratio units in PLA structures. Because the two repeating units are optically active, they rotate polarized light in opposite directions. Increasing the level of opposite enantiomeric monomer in a polymer causes the reduction of chain optical purity [67]. Optical purity of enantiomers affects the level of stereocomplexation. Tsuji *et al.* studied the crystallization of 50/50 blends of similar optical purity PLLAs and PDLAs prepared by solution casting and pure polymers as well as non-blended samples [64]. No spherulite structure was observed for non-blended samples with optical purity less than 76 %. By decreasing the isothermal crystallization temperature, the spherulite density increased. This effect was more pronounced for samples having lower optical purities. Furthermore, blended films had higher spherulite density than non-blended samples at any crystallization temperature and optical purity. DSC heating thermographs of melt quenched PLLA and PDLA samples displayed a cold crystallization temperature and

subsequent melting peaks. Increasing optical purity decreased the cold crystallization temperature and increased melting point. Whereas homopolymers with 83 % optical purity were not able to crystallize during heating in DSC, the blends of the homopolymers crystallized. Furthermore, at a constant crystallization temperature, increasing optical purity led to increasing the melting point.

2.7 Enhancing PLLA crystallization by nucleating agents

The most practical method to increase the nucleation density and the crystallization rate is the addition of heterogeneous nucleating agents. Even though the detailed mechanism of heterogeneous nucleation is not well understood, it is believed to arise from molecular interactions between the polymer and the surface of the nucleating agent [68]. This interaction results in a reduction in the interfacial free energy barrier for stable nucleus formation. Heterogeneous nucleation agents have been employed to reduce process cycle times, allow crystallization at a lower undercooling (high temperatures) and form smaller crystals to enhance material crystalinity.

Generally, nucleating agents are classified in two physical and chemical groups [69]. Through a chemical reaction, chemical nucleating agents can render the nucleation process such as organic salts of sodium used in crystallization of PET. Li and Huneault [70] examined the effect of sodium stearate on the crystallization of PLA. They reported that this nucleating agent showed no significant effect on the crystallization rate. They also measured the variation of viscosity of PLA with 0.5% of this substance and showed the viscosity of this compound was lower by a factor of 2.5 due to the chain scission.

Physical nucleating agents are mostly applied to promote PLA crystallization rate [71]. Henceforth, the effect of these nucleating agents on the crystallization of the PLA will be reviewed.

2.7.1 Talc

Kolstad [72] tested an assortment of nucleating agents and found that talc, a common nucleating agent for thermoplastics, was the most effective one. With 6 wt % of talc, the $t_{1/2}$ value of PLLA was found to be less than 1 min at crystallization temperatures between 90 and 120 °C. In addition, the nucleation density also increased by 500-fold. The epitaxial mechanism was used to explain the Talc nucleated crystallization of PLLA.

The well-known Avrami equation is often used to analyze the crystallization kinetics. It assumes that the relative degree of crystalinity develops with crystallization time, t, as:

$$1 - X(t) = \exp(-kt^n) \quad (1)$$

where $X(t)$ is the relative degree of crystalinity at time t; the exponent n is the Avrami exponent and k is a kinetic rate constant. The exponent is typically between 2 and 4 for polymer crystallization and is associated to the nucleation mechanism (homogeneous or heterogeneous and simultaneous or sporadicIf the nucleation sites are present at the early stage of the nucleation, then this is called simultaneous nucleation. However, when the nuclei form in the polymer matrix at a constant time rate, the nucleation is called sporadic. The higher n values are attributed to three dimensional spherulitic growth with a sporadic or a combination of sporadic and simultaneous nucleation type, whereas the lower amounts are related to two dimensional growth with instantaneous and some sporadic nucleation. Parameter k is a growth rate constant involving both nucleation and growth rate parameters. **Figure 9** depicts the degree of crystallization of PLLA versus time for different crystallization temperatures.

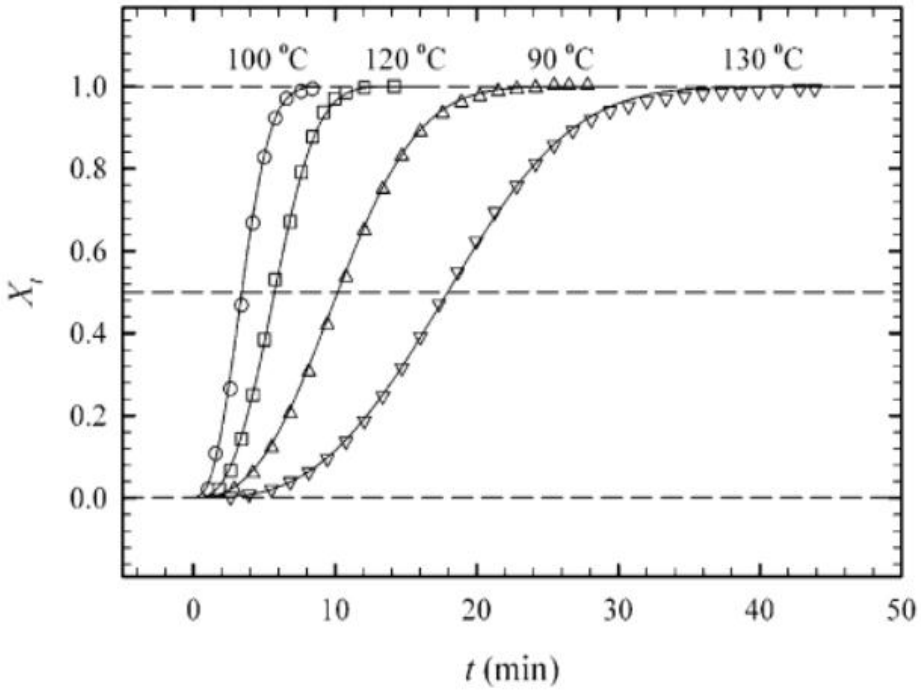

Figure 9. Degree of crystallization of PLLA vs. time for different crystallization temperatures [1].

Effect of talc as a nucleating agent to improve the crystallinity of PLLA in injection molding was also investigated [73]. Isothermal crystallization results illustrated that $t_{1/2}$ at 105 °C was 38.2 min for neat PLA that eventually reduced to 0.6 min for sample containing 2 % Talc corresponding to a 65-fold increment in crystallization rate. In non-isothermal crystallization with the cooling rate of 10 °C/min, neat PLA displayed no crystallization temperature while the sample containing 2 % Talc exhibited a crystallization temperature around 107 °C. The combination of nucleating agent and optimum processing conditions led to an increase in final crystallinity and a reduction of injection cycle time. Strength, modulus and heat distortion temperature of sample increased noticeably.

Nofar *et al.* also used Talc as a nucleating agent to promote the crystallization of both linear and branched PLA [74]. It was shown that Talc was an efficient nucleating agent, especially for linear PLA. It was reported that the addition of Talc to PLA enhanced the crystallinity of PLA samples with more linear structure, whereas for more branched PLA Talc had the least effect on crystallinity suggesting the branched structure dominated crystallization already regardless of the presence of Talc.

2.7.2 Clay

Particular interest has been recently paid to nanocomposites technology consisting of a polymer matrix and organoclay because they exhibit outstandingly improved mechanical and various other properties as compared to those of virgin polymers [75]. The detailed crystallization behavior and morphology of pure PLA and PLA/C18-MMT have been described by Young Nam *et al.* [76]. It was observed that ordering of spherulites was much higher in the case of pure PLA than that of PLA nanocomposites because the aggregation of MMT particles, which was not nucleated during crystallization, existed inside the spherulite and then the occurrence of the regular orientation of lamella stacks inside the spherulite could be disrupted. Moreover, the overall crystallization rate of neat PLA increased after nanocomposites preparation with MMT ; however, it had no influence on the linear growth rate of pure PLA. It should be mentioned that the overall 30% increase in crystallization rate in this case, was modest when compared with Talc.

Pluta [77] also investigated the effect of clay on the crystallization of PLA. It was reported that clay reduced slightly the crystallization rate of a PLA containing 4 % *D-LA* and shifted

the cold crystallization temperature to higher values in comparison with pure PLA. This phenomenon was attributed to reduced chain mobility.

The nonisothermal and isothermal crystallization behaviours of PLA and PLA-Organoclay nanocomposites in the presence of three different chain extenders Polycarbodiimide (PCDI), tris nonylphenyl phosphite (TNPP), and Joncryl ADR4368F were investigated [78]. Addition of PCDI increased the cold crystallization temperature and decreased the degree of crystallinity due to lower mobility of polymer chains reacted with chain extenders. In contrast, the degree of crystallinity and crystal growth rate increased as TNPP was added. Eventually, addition of Joncryl led to the formation of long-chain branching structure which disrupted the chain packing. The rate of crystallinity and level of crystallization decreased as well. According to these articles, it can be consequently concluded that organically modified layered silicates are less effective than Talc as a common nucleating agent.

2.7.3 Bio-based nucleating agents

Amid the different nucleating agents, bio-based ones are a specific subset of interest. Crystallization half-time of PLA decreased from 38 min to 1.8 min by incorporation of 2 % of a vegetable-based ethylene bis-stearamide, (EBS). In nonisothermal melt crystallization with the cooling rate of 10 °C/min a broad and weak crystallization peak was observed around 97 °C which was less effective than talc showing a sharp exothermic peak around 108 °C [73].

As a part of genetic molecule found in deoxyribonucleic, (DNA), and ribonucleic acid, (RNA), nucleobases are biocompatible and eco-friendly [79,80]. With addition of 1 % of uracil, one kind of nucleobases, PLLA could complete its crystallization upon cooling at 10 °C/min. Crystallization half -time decreased from 16.8 min for pure PLLA at 120 °C to 1.02 min with addition of 1 % of uracil. Moreover, the crystalline structure of PLLA was not affected by uracil [80].

A new study has shown that addition of polysaccharides such as chitin, chitosan, cellulose and starch from various plants had no significant effect on the overall PLLA crystallization [81]. Effect of various additives such as PDLA, talc, fullerene (C60), montmorillonite, and various polysaccharides on the non-isothermal crystallization of PLLA was investigated as well. The effect of additives in accelerating the overall PLLA crystallization during cooling from the melt, decreased in the following order: PDLA > Talc > C60 > montmorillonite >

polysaccharides. As a result, this finding indicates that polysaccharides are not suitable nucleating agents to enhance the PLA crystallization.

Starch is a biopolymer whose blends with PLA during last years have been under investigation [82,83]. The effect of starch on crystallization of PLA is smaller than that of talc. The blends containing 1-40 % starch, have crystallization half -time in the range of 14 min to 1.8-3.2 min whilst 1 % Talc is more efficient and has a $t_{1/2}$ around 0.4 min [84]. However, effect of starch becomes more remarkable when it is in its thermoplastic state [85]. By using interfacial modifier, the size of the dispersed phase in the blend of PLA/TPS decreased which had a significant effect on the crystallinity of PLA. In other words, unmodified sample did not show any exothermic peak at cooling rate of 10 °C/min while the compatibilized blend reached its maximum crystallinity level. Moreover, $t_{1/2}$ was around 1.25 min for the modified blend.

Polyglycolide, (PGA), and its copolymers are biodegradable aliphatic polyesters. PGA has a melting temperature of 220-230 °C which is much higher than that of PLA, 170-180°C. It could, therefore, act as a biodegradable nucleating agent for PLA. DSC studies indicated that the nucleation of PLLA was improved in the presence of PGA even at a PGA content as low as 0.1 wt.-% [86]. Increasing the amount of PGA above 3 % wt.-% led PLA and PGA to crystallize separately. A strong molecular interaction between PLA and PGA enhanced the growth of PLLA crystallites from the surface of PGA.

Thanks to its biocompatibility and high tensile properties, cellulose nanocrystals, CNC, have been examined to investigate their effect on the crystallinity of PLLA [87]. Having a 15nm diameter and 200-300nm length, the unmodified CNC exhibited no remarkable effect on the crystallinity of PLLA. However, when it was functionalized by partial silylation, SCNC, it presented a modest effect on the crystallinity. The crystallization half-time decreased 2-fold around 4 minutes with the incorporation of 1% of SCNC. Moreover, this surface treatment, improved the tensile strength and modulus of the nanocomposites. This enhancement attributed to reduction of the length of cellulose nano crystals leading to increase the efficiency of SCNC as a nucleating agent.

Cyclodextrin (CD) is a natural product of starch which has a cone shape and a hydrophobic cavity that is apolar relative to the outer surface. The penetration of polymer chains into the empty cavity of CD can lead to inclusive-complex (IC) [88]. The nucleation effect of IC has been demonstrated in several biodegradable polymers including poly (hydroxybutyrate), PHB,

poly(hydroxybutyrate valerate), PHBV, poly(butylene adipate), PBA, and poly(butylenesuccinate), PBS [89,90,91]. It is believed long polymer chains inside the CD cavity are crystallizable. Effect of IC of PLA on the crystallization of PLA has been investigated [92]. It was found α-CD had a modest effect on the crystallinity of PLA. At 118 °C, $t_{1/2}$ was 40 min for pure PLA while it was around 20 min for IC-PLA. For both pure PLA and IC-PLA composite, the Avrami exponent value n ranges from 1.8 to 2.3. It consequently implies that the addition of PLA-IC might not change the crystallization mechanism of PLA.

Orotic acid, OA, is also another green nucleating agent that was studied by Qiu *et al.* [93]. Addition of only 0.3 % of Orotic acid revealed a significant effect on the crystallinity of PLA. A sharp exothermic peak was observed by cooling the sample with the rate of 10 °C/min vicinity 124°C. The $t_{1/2}$ decreased to 38 seconds at temperature around 117 °C. The nucleation mechanism of this nucleator has not been understood; however, it was postulated that a good match between the b-spacing of PLLA and the a-spacing of OA could describe such a noticeable effect. Thus far, the most efficient reported nucleating agent for increasing the crystallization of PLA is OA.

Citric acid can form complex with many metal ions. Zinc citrate, Zncit, is a frequently used zinc supplement in foods, pharmaceutical and hygienic products. Effect of Zinc citrate complex, ZnCC, a nanoscale product of the reaction of zinc acetate and citric acid, as a nucleating agent on the crystallinity of PLLA has been studied. With the addition of 0.05 % wt % ZnCC, PLLA could complete the crystallization under cooling at 10 °C/min and the crystallization half-time dropped remarkably, with this effect being more prominent as increasing ZnCC content. Epitaxy is the possible mechanism offered by the authors to explicate the nucleation phenomenon of PLLA/ZnCC system [94]. On the basis of the data of k and n, Avrami parameters, and $t_{1/2}$, it was found that the nucleation ability of the three nucleating agents increased in the following order: Talc< Zncit< ZnCC. Based on WAXD patterns, an excellent matching existed between b-axis of PLLA and a-axis of ZnCC. Moreover, the hydrogen bond interaction between the hydroxyl groups of ZnCC and the carbonyl groups in PLLA chains could stabilize the nucleation process. Discrepancy between nucleation ability of Zncit and ZnCC was explained by the larger specific area of ZnCC.

PHB is one of the most famous biodegradable polyesters. Nevertheless, PHB has some weaknesses for example high crystallinity, brittleness and narrow processing window.

Blending with other polymers has been taken as an easy and profitable action to overcome the problems of this polymer [75,95,96,97]. PHB blended with PLA has drawn interests since both of them are biodegradable. Studies have shown the miscibility between these two polymers is dependent on the molecular weight of PHB [96,97]. DSC analysis results indicated that PLLA showed no miscibility with high molecular weight PHB, M_W = 650000 g/mol, in different range of blend ratios. On the contrary, some limited miscibility appeared with low molecular PHB, M_W=5000 g/mol, when the PHB content was below 25 %. Additionally, WAXD results showed that for all the samples, the disorder, α', phase of PLLA was produced in the nonisothermal crystallization process which was verified by an obvious transition related to the disorder to order transition, α'to α, around 160 °C [98].

There are many bio-based nucleants acting as a nucleating agent for PLA. For the sake of brevity, other studies have not been mentioned here. Most of these chemicals have not substantial effect on the crystallization kinetics of PLA, providing that we exclude the metal-citrate groups from this classification. For example, when these nucleants are compared to Talc as a most useful nucleating element in industry, it can be concluded that their effect is moderate. Therefore, application of these materials is limited in reality. Furthermore, the majority of these blends have been fashioned in the solution state which is far away the real processing techniques like extrusion and injection molding operating in molten state.

2.7.4 Organic nucleants

Organic materials can also nucleate the crystallization of PLA physically [1]. Providing organic nucleation sites, organic nucleants are low molecular weight substances that crystallize faster at a higher temperature than the polymer. N,N Ethylenebis (12-hydroxystearamide), commercial name of WX1, was employed as a nucleator for PLLA containing 0.8 % *D*- content. Upon heating at 5 °C/min, the cold crystallization temperature shifted to lower temperatures, from 100.7 °C to 79.7 °C, indicating WX1 is an effective nucleating agent. Optical micrographs showed a layer of trans -crystallites grown from WX1 surface , implying the epitaxial crystallization of PLA [99].

1,3,5-benzene tricarboxyamide (BTA) and its derivatives are the other types of organic compounds with benzene moiety that was investigated by Nakajima *et al.* [100]. Maximum crystallinity around 44 % was achieved by incorporation of 1 % of this compound at 100 °C for 300 seconds whereas pure PLA had 17 % of crystallinity in similar circumstances. In

another attempt, a comparison between talc, EBHSA, and hydrazide compound was made [101].The enthalpies of crystallization, ΔH_C, obtained upon cooling with the rate of 10 °C/min were: 26, 35 and 46 J/g for Talc, EBHSA and hydrazide, respectively. The crystallization peak exhibited a similar trend as well: 102, 110, and 131 °C for Talc, EBHSA and hydrazide, respectively. P-tert- butylcalix (TBC8-eb) also exhibited intriguing behavior [102]. Upon cooling at the rate of 5 °C/min, PLA containing 1% of this compound exhibited an exothermic peak around 134 °C. Kinetic analysis also demonstrated that TBC8-eb not only accelerated the rate of crystallization but also transformed spherulite crystals to sheaf-like crystals.

Neat dibenzylidene-D-sorbitol (DBS) has been utilized as a nucleating agent to change the crystalline rate and optical properties of some polymers such as PE, PP and PET [103,104]. Effect of 1,3:2,4 dibenzylidene-D-sorbitol on the crystallinity of PLLA was also investigated [105]. DSC and WAXD studies showed that by increasing the amount of DBS, regular α crystalline phase was favored. In other words, incorporation of DBS caused the α-form crystals to form at lower temperatures, lower than 120 °C. The DBS molecules are stacked through π-π interaction of the aromatic group to form a strand with the PLLA molecules by hydrogen bonding. In addition, changing the concentration of DBS from 0 to 4 % displayed no substantial effect on the cold crystallization of PLLA upon heating rate of 5 and 10 °C/min.

N,N'-Bis(benzoyl) suberic acid dihydrazide (NA), as nucleating agent for PLLA is synthesized from benzoyl hydrazine and suberoyl chloride, which was deprived from suberic acid via acylation [106]. The use of NA led to the shift of the melt crystallization to a higher temperature and crystallization peak became much sharper in the melting crystallization process. Upon cooling at 1 °C/min, with the addition of 0.8 % NA, T_C increased from 106 °C to 125.6 °C and ΔH_C increased from 1.38 to 31.63 J/g. In isothermal crystallization from melt, upon the addition of 0.8 % NA, $t_{1/2}$ of PLLA/NA decreased from 26.5 to 1.4 min at 115 °C. The hydrogen bonding interaction between C=O in the PLLA molecule and N-H in the nucleating agent was proposed as a possible mechanism of nucleation.

Recently, to accelerate the crystallization of PLLA and enhance its crystallization, a multiamide nucleator (TMC) contents from 0.25 to 1wt%, was introduced into the PLLA matrix [107]. The two melting points of TMC nucleated PLLA can be ascribed to the melt-recrystallization mechanism, suggesting that less stable crystals at lower crystallization

temperature transform through the melting–recrystallization process upon heating. At T=110 °C with addition of 1 % of TMC, $t_{1/2}$ decreased from 13.32 min to 1.28 min.

Organic nucleants often need a solvent to be blended with PLA. Most of these solvents are poisonous and not eco-friendly. It, therefore, limits application of these chemicals in real processing techniques.

2.7.5 Other nucleants

Due to their high aspect ratio, thermal, electrical and outstanding mechanical properties, carbon nanotubes, CNT, have established themselves as promising filler for thermoplastics. Furthermore, both modified and unmodified CNT have been studied as nucleating agent for PLA [108,109,110,111]. Xu *et al.* reported that a very low loading of multiwall carbon nanotube (MWCNT) <0.08 wt %, lowered the crystallization induction time and increased the density of nuclei. The highest amount of crystallinity, 44 %, was achievedby using a slow cooling rate and adding only 0.02 wt % of MWCNTs. Further increment of MWCNTs did not lead to a sensible improvement of final crystallinity, due to poor dispersion of filler at higher concentrations [111]. Additionally, a double melting peak was observed in both isothermal and non-isothermal characterizations. It was explained by the disorder-order crystal phase transition.

Grafting modification of CNT with PLLA enhances its disperion in the PLLA matrix. With 5% PLA-g-CNT, the minimum $t_{1/2}$ decreased from 4.2 min to 1.9 min. Moreover, upon cooling at 5 °C/min the level of crystallinity changed in the range of 12-14 % by increasing the PLA-g-CNT from 5 to 10 % [112]. In order to improve the dispersion of nanotube, functionalized multiwall carbon nanotube were introduced into PLLA. Thermal analysis revealed that CNT could not change dramatically the crystallinity of PLLA under rapid cooling or even at modest cooling rates as 10 °C/min. Further results also showed that in both pure PLLA and PLLA nanocomposites merely α crystalline phase formed during annealing [113]. Briefly, most studies imply that carbon nanotube cannot play a significant role in crystallization of PLA [1].

The crystallization behavior of PLA with carbon black, (CB), and modified carbon black, (MCB), was investigated [114]. Due to the small organic molecules grafted on the surface of CB, MCB had finer and more uniform particles than CB when dispersed into PLA. Both accelerated the crystallization of PLLA ; however, at cooling rate of 1 °C/min, MCB increased

the crystallization peak temperature of PLA more than CB. Furthermore, addition of CB increased the exotherm peak temperature from 101.9 °C to 115 °C, and to 122.3 °C with addition of MCB.

With a layered structure similar to clay, Metal phosphonate is another type of synthetic hybrid material used as a nucleating agent. Mechanical properties and thermal stability of polymers such as epoxy, PET, and polyacrylamide can be modified by incorporation of this material [115,116]. Crystallization of metal layered phosphonate, zinc phenylphosphonate(PPZn), reinforced PLLA composites were investigated [117]. Adding only 0.02 % of PPZn completed the crystallization upon cooling at 10°C/min. The rate of crystallization increased with the concentration of PPZn. Upon addition of 15% of this filler, crystallization half-time of composite decreased from 28 min to 0.33 min at 130 °C and from 60.2 min to 1.4min at 140 °C. The epitaxial nucleation was proposed as the possible nucleation mechanism of the PLLA/PPZn. The incorporation of PPZn had no appreciable influence on the polymorphism of PLLA. The effect of phenylphosphonic acid zinc (PPA-Zn) and talc, molding temperature and reinforcement by microfibrilated cellulose (MFC) on the injection molding of PLA was evaluated by Suryanegara *et al.* [118]. PPA-Zn was more effective than talc and MFC according to isothermal crystallization analysis. The mold temperature of 95 °C and incorporation of PPA-Zn increased the crystallization of PLA in injection molding; however, at this temperature, the molded PLA deformed during ejection. The addition of cellulose nanofibers led to increase the rigidity at elevated temperatures. Hence, the combination of faster crystallization kinetics and higher stiffness of the PLA/PPA-Zn/MFC composite injected at 95 °C led to the demolding of parts without distortion at a holding time of just 10 s. Wang also studied the effect of metal type on PLA/layered metal phosphonate by comparing zinc, calcium and Barium phosphate [119]. The nucleating ability of PLLA incorporating PPZn, PPCa and PPBa decreased in the following order: PPZn > PPCa > PPBa. This difference was attributed to the different dispersion and interfacial interaction of nucleating agents with PLA.

Polyhedral oligomeric silsesquioxane, POSS, is another member of the class of inorganic/organic hybrid materials. Through covalent bonds the organic and inorganic elements of this material are connected to one another unlike organoclays in which the components are connected via electrovalence bonds. The core of this material is comprised of a silicon and oxygen nanocage grafted with organic arms. In a series of articles, effect of this

compound on the crystallization of PLA has been evaluated [120,121,122,123]. Depending on the concentration of POSS and the type of arm, cold crystallization temperatures shifted to lower temperatures between 10 and 22°C upon the heating at 20 °C/min. Maximum amount of crystallinity around 44 % was obtained. Upon cooling at 5 °C/min, the melt crystallization peak increased between 10-15 °C with respect to neat PLA. By increasing the cooling scanning rate to 15°C/min, a small exothermic peak appeared at 92 °C for PLA containing 2 % POSS. Isothermal crystallization analysis revealed that the crystallization half-time decreased to 72 s for nanocomposites containing POSS with vinyl arms.

The isothermal and cold crystallization of PLA/nucleating agents ($CaCO_3$, TiO_2 and $BaSO_4$, content from 0.05 % to 2.5 %) was studied [124]. The maximum crystallinity was 14.9 % when 0.5 % $BaSO_4$ was added into PLA. Additionally, $BaSO_4$ and TiO_2 demonstrated better efficiency on the crystallinity. Even though the diameters of all nucleating agents were almost the same, about 100 nm, and the surface was treated by aliphatic acid, the difference in crystallinity was associated to different shape and property. The shape of $CaCO_3$ is cubic whilst the other two were spherical. When the content of nucleating agent was 1 %, at T=120 °C, the system showed the higher crystallinity and the highest crystallization rate.

The melting and crystallization behavior of PLA with two nucleating agents, Talc and Bamboo fiber (BF) was investigated [125]. DSC curves revealed that BF had a minor effect on the crystallization while Talc had a great effect on the crystallization of PLA. In both pure PLA and PLA containing 1% Talc and 1% BF a double melting peak was observed after slow cooling rates; however, for PLA containing 1 % Talc and PLA containing 1% BF just a single endothermic peak appeared. The defects of BF structure promoted the recrystallization in the melting process and the Talc promoted formation of small crystals. The double melting behavior was explained by melt-recrystallization mechanism.

PLA exhibits poor melt strength. Therefore, its application is limited in processes like foam processing. In order to overcome this problem, some amounts of long chain branched PLA, LCB-PLA, is added to PLA to increase the elasticity. Cold crystallization and melt crystallization of linear PLA and LCB-PLA were investigated [74]. Non-isothermal cold crystallization experimental results revealed that PLA samples with a higher branching degree exhibited higher crystallizability than the linear PLA samples. The non-isothermal crystallization during cooling presented that the branching increased the crystallinity of the

PLA samples because of its crystal nucleation effect. In addition, according to the Avrami analysis, it was shown that homogeneous nucleation and 2-D spherulitic growth were more likely to occur for PLAs with higher branching degree. For isothermal temperatures in which the crystallization growth rate was faster, the crystal growth had higher tendency to have 3-D and heterogeneous crystallization because of higher chain regularity.

2.8 Enhancing PLLA crystallization by plasticizers

Compared to the nucleating agents, fewer studies have been performed so far to enhance the crystallinity of PLA by plasticizers. The main effect of plasticizer on a polymer is the reduction of the glass transition temperature, T_g, of the polymer. Decrease in T_g extends the window of crystallization. Addition of plasticizer facilitates the chain mobility of polymer molecules as well and can help them to put themselves into crystalline structures. This effect becomes more prominent when crystallization occurs at low temperatures where the diffusion of polymer chains is very sluggish. Ironically, incorporation of a plasticizer might have an unfavorable effect on the crystallization of a semicrystalline polymer. The presence of a plasticizer results in decrease of melting point and, therefore, reduces the degree of undercooling, T°_m-T_C, promoting the crystallization and primary nucleation process. Hence, the improvement in chain mobility might be slightly compensated for by reduced primary and secondary nucleation [1,126].

Among the numerous plasticizers, polyethylene glycol, PEG, has been extensively. Adding PEG reduced the T_g nearly 2 °C per plasticizer percentage whereas it did not change the melting point considerably which was desirable for crystallization. Secondly, in comparison to the other available plasticizers as citrate ester, fatty acid ester, dibutyl sebacate, PEG demonstrated the highest efficiency regarding the decraese of T_g and cold crystallization temperature [83,127]. The effect of end group of PEG on crystallization was examined [128,129,130]. Low molecular weight PEGs, M_W between 400 g/mol and 750 g/mol, did not show any remarkable effect on the crystallization and growth rate of spherulits [130]. Terminated group of plasticizer displayed a key effect on the miscibility of PLA and plasticizer as it was found the miscibility declined following the order according the ending group: 2NH2> 2CH3> OH-CH3> 2OH. Melting point reduction also obeyed the miscibility order as well. The highest miscibility between amine-terminated PEG and PLA was ascribed to the ionic interaction of amine groups with carboxylic acid groups of PLA ends.

Furthermore, compared to the other end-group types, the amine-terminated one exhibited the lowest $t_{1/2}$ and this phenomenon became more considerable when more plasticizer was added into the blend.

Aside PEG, the effect of polypropylene glycol, PPG, on the crystallization and plasticization of PLA has been studied as well [131,132]. PPG displayed a comparable effect on the reduction of T_g like PEG. PLA blended with 12.5 % PEG showed a second T_g around -77 °C due to phase separation. It consequently indicates that PPG is less compatible with PLA in comparison with PEG. Crystalline growth and nuclei density of PLA/PPG were less than those of PLA/PEG system. This also implies that PPG is less telling than PEG to enhance the crystallization of PLA.

Effect of citrate esters and their derivatives on the plasticization and crystallinity of PLA have been reported in papers [133,134,135]. It has been found that these low molecular weight compound decreased the melting point more than PEG. Addition of 20-25 % of tributyl citrate decreased the cold crystallization temperature, T_{CC}, from 95 °C to around 68 °C; however, its effect on the melt crystallization was not significant.

Other low molecular weight chemicals triphenyl phosphate (TPP) and dioctyl phthalate not only decreased the glass transition temperature but also enhanced the crystalline growth rate of PLA. Incorporation of 30% of TPP reduced T_g by 40°C. The maximum growth rate for PLA containing 30% was reported around 52.8 μm/min while that of neat PLA was 16.8 μm/min. Also the optimum temperature reduced to 102 °C while the optimum temperature for pure PLA was 132 °C [136,137]. For the neat and plasticized PLA, the spherulites displayed the characteristic Maltese Cross extinction pattern in low temperature, but the Maltese Cross disappeared, became irregular and distorted with temperature. Moreover, such changes were shifted to lower temperature with the addition of TPP. The Avrami exponent, n, almost remained unchanged despite the changing the crystallization temperature as well as the amount of TPP. This indicated that PLA plasticized with TPP almost did not change the crystallization mechanism of PLA. The crystal structure of PLA was not changed by the plasticizer as well.

While highly volatile, unlike conventional plasticizers, CO_2 is regarded as a plasticizer to investigate its effect on the crystallization of PLA [138,139,140,141,142]. CO_2 dissolves into PLA well and is widely applied in foam extrusion process as a physical blowing agent.

Reduction of T_g in the presence of 15 % CO_2 is by 58 °C. Takada *et al.* found that the crystallization rate followed the Avrami equation. However, the crystallization kinetic constant was changed depending upon the crystallization temperature and concentration of CO_2 dissolved in the PLLA. The crystallization rate was accelerated by CO_2 at the temperature in the crystal-growth rate controlled region (self-diffusion controlled region), and decreased in the nucleation-controlled region. WAXD patterns also exhibited that the crystalline structure of PLA remained unchanged with incorporation of CO_2 [138]. Yu *et al.* reported that the enthalpy of cold crystallization decreased with pressure, indicating that the final crystallinity of samples was lower after cold crystallization under pressure. It was also found that the crystallization half-time at 70 °C reduced sharply from 360 min under atmospheric pressure to about 10 min by increasing CO_2 pressure to 2 MPa. [140]. While in static conditions $t_{1/2}$ was 40 min for pure PLA, a very rapid crystallization development happened in the presence of 6-7% CO_2. According to the authors, such a drastic effect could not be explained exclusively by the plasticization effect of the gas. A kind of nucleation effects, like carbon dioxide clusters, might provide an explanation of this behavior [142].

2.9 Enhancing PLA crystallization by combination of a nucleating agent and a plasticizer

Combining nucleating agents and plasticizers could have a synergistic effect on PLA crystallization kinetics, due to the improved chain mobility and the enhanced nucleating ability [70]. Pluta studied the combination of 20 % PEG and 5 % clay, either unmodified or organically modified, on the crystallization of PLA [143]. While neat PLA and its composite with 3 and 5% clay did not show any exothermic peak upon low cooling rate at 2 °C/min, PLA containing both nucleating agent and plasticizer revealed a crystallization peak with the enthalpy equal to 22 J/g. This value dropped to l3 J/g upon the cooling rate at 15 °C/min. Li and Huneault examined the synergistic combination of talc and PEG or acetyl triethyl citrate (ATC) on the PLA crystallization [70]. Upon cooling at 10 °C and 20 °C/min, the samples showed a sharp crystallization peak around 105 °C. The obtained ΔH_C was more than 40 J/g. However, PLA/ Talc 1% had a T_C around 94 °C and reached at 50 % of crystallinity. A similar study was performed by Li *et al.* but a higher amount of plasticizer, 20 % PEG, was employed [144]. The addition of PEG into PLA/talc led to a decrease in the concentration and an

increase in the sizes of spherulites, and the effect was more significant with increasing the content of PEG. This was ascribed to the plasticization effect of PEG.

Figure 10 displays the developed crystallinity as a function of cooling rate for neat PLA, PLA/talc, and PLA/plasticizer [1]. ΔH_C of pure PLA reduced drastically from 35 J/g to nearly 1 J/g when the cooling rate was increased from 1.5 to 10 °C/min. PLA/talc also showed a similar trend at higher cooling rates, around 40 °C/min while the composite containing both nucleating agent and plasticizer still crystallized even at higher cooling rates like 80°C/min. Formulation encompassing PEG and Talc exhibited a higher crystallinity than the one containing ATC and talc.

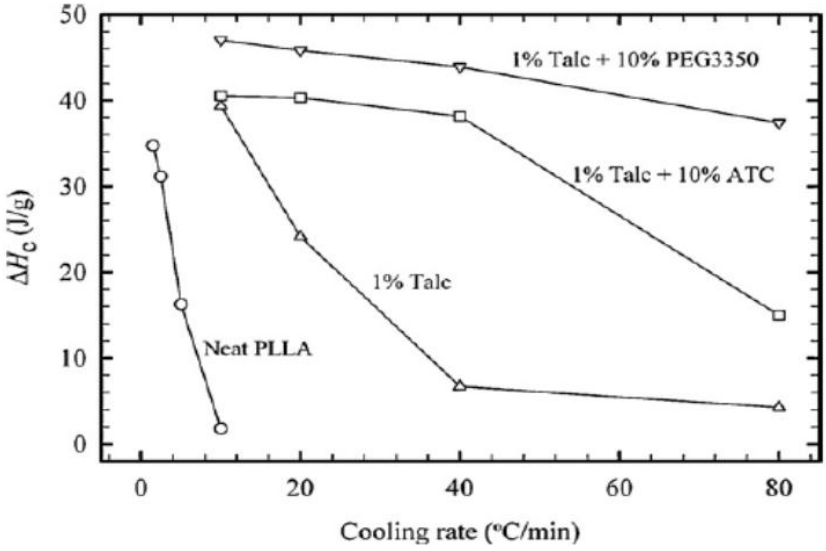

Figure 10. Crystallization enthalpy as a function of cooling rate for difference formulation [1].

In another attempt, TPP was employed as a plasticizer to improve the crystallization of PLA [145,146]. Wide angle X-ray diffraction (WAXD) confirmed that pure PLA and its blends with TPP and/or Talc isothermally crystallized in the temperature range of 113–128 °C, and all revealed the α phase. PLA/Talc 1.2/TPP 15 exhibited the fastest kinetics. Half –time crystallization temperature reduced from 3.6 min for the neat PLA to 42 and 54 seconds for PLA/1.2 Talc and PLA/1.2 Talc/TPP15, respectively.

Effect of mold temperature on the crystallinity development of PLA/Talc 1 %/5 % ATC composites in injection molding was investigated [70]. A cycle time of 30 s was enough to obtain fine parts without distortion during ejection in the 20-40 °C mold temperature but the crystallinity level of specimen were too low, almost amorphous. The quality of samples

molded at 50-60 °C was not proper since this range of temperature was very close to the Tg of PLA causing the distortion of the samples. However, at high temperatures, 70-100 °C, the crystallinity of materials increased. Fine parts were obtained without distortion but higher amounts of time, 60 s, was needed.

All the mentioned avenues, containing different nucleating agents and plasticizers or combination of these methods, have been mostly carried out in quiescent conditions and the effect of processing conditions like flow field, time and temperature have been rarely taken into account. Moreover, in order to evaluate the efficiency of these methods the reference is always pure PLA and the highest limit of efficiency has not been introduced.

2.10 Self-nucleation

The efficiency of nucleating agents is basically considered in two different ways: either in an anisothermal experiment by measuring the increase in T_C in cooling (or reduction of T_{CC} upon heating) or in an isothermal test by assessing the reduction of crystallization half-time. In both cases, the reference is always the pristine polymer; the polymer without any ingredients but undergone the equal processing conditions performed to add the nucleating agents. Despite giving valuable information through analysis of data, the previously mentioned techniques have an inherent weak point because they exclusively use a single reference, the virgin polymer, which is usually the lower limit regarding the crystalline nuclei density. A more comprehensive evaluation requires defining an upper limit of crystalline nuclei density. Fillon *et al.* introduced the upper limit obtained with an ideally nucleated polymer achievable via self-nucleation[147]. This term first was used by Blundell *et al.* to explain the nucleation of chain folded crystals by fragments of high molecular mass present in the same solution [148]. The self-nucleation procedure is known to promote numerous nuclei via this protocol, crystal fragments performing as ideal nuclei in terms of both their interactions, chemical and crystallographic, and their state of dispersion could be achieved. This procedure occurs with partial melting of the original crystalline lamellae. Normally, a four-step procedure is required to perform the self-nucleation:

- The sample should be at first melted 20 or 30 degrees above its melting temperature to erase all previous thermal history.

- Then, it will be cooled with the determined scanning rate to a certain temperature in order to create a standard thermal history.
- Afterwards, the sample is heated with the same ramp up to a temperature in partial melt zone, T_S or self-nucleation temperature. Normally, the sample is held at this temperature for a specific period of time, for 5 minutes.
- Finally, a cooling scan is performed by cooling the sample from T_S to the certain temperature to detect the crystallization peak.

According to Fillon *et al.* the nucleation efficiency scale, NES can be defined:

$$NES = \frac{T_{C-}T_{Cmin}}{T_{Cmax-}T_{Cmin}} \times 100 \quad (2)$$

T_{Cmax} and T_{Cmin} are the crystallization temperatures of optimum self-nucleated and neat polymer melt, respectively. T_C is the crystallization temperature of the heterogeneously nucleated system. **Figure 11** illustrates the typical melting behavior of a semi crystalline polymer. In Domain I, all the polymer crystals have completely melted. In Domain II, crystals undergo the self-nucleation process. In this domain, by decreasing T_S, the crystallization temperature shifts to higher degrees. However, in Domain III crystals are large enough that combination of self-nucleation and annealing takes place. In Domain I all thermal history of the polymer has been erased and it is completely in molten state. In the second domain, there are some small crystal fragments that can act as a nucleating agent. In Domain III, like Domain II crystals can be found but there are larger than those of Domain II, therefore, annealing can take place [149,150,151,152,153] . Consequently, Domain II is favorable for the self-nucleation. Although many articles have been published on the self-nucleation behavior of PP and other polymers like PET, PC and poly(p-dioxane), only a few ones reported the self-nucleation behavior of PLA [154,155].

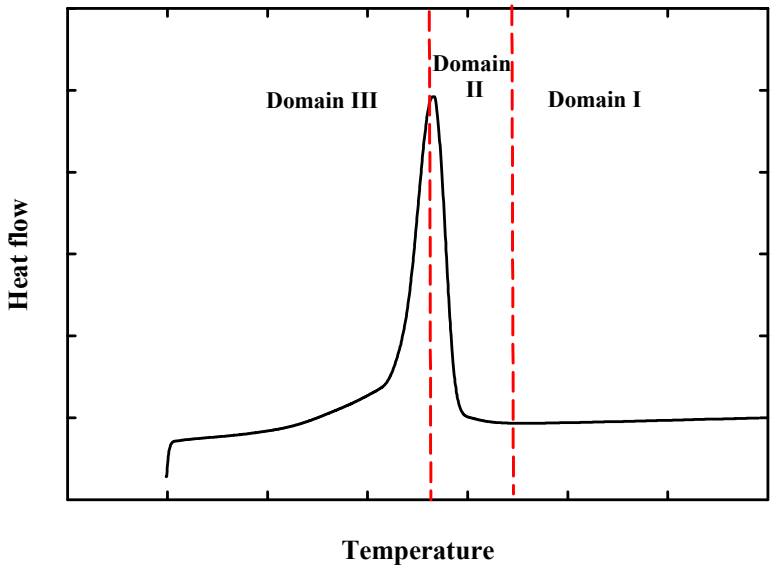

Figure 11. Partial or complete melting domains of a semi crystalline polymer.

Schmidt *et al.* studied the self-nucleation behavior of PLLA in solution media. Under the cooling rate at 5°C/min, T_{Cmin} =106 °C, and T_{Cmax} =157 °C were obtained, respectively. Efficiency of stereocomplex by adding some amounts of PDLA into PLLA also were assessed by this technique. PLLA/Talc 6 % revealed a NES equal to 32 %, while PLLA/PDLA 6 % exhibited a NES equal to 56 %. Interestingly, crystallization kinetics analysis demonstrated that the increment of nucleation density did not necessarily lead to increase of overall crystallization rate due to reduction of chain mobility of PLLA molecules by tethering effect of stereocomplex crystals[155]. Nucleation efficiency of stereocomplex were measured again but this time in the molten state with different molecular weights of PDLA, M_n = 5.8, 14, and 48 kg/mol, and concentration, range from 0.5 to 3 %. Upon the cooling rate at 5°C/min, T_{Cmin} =104.3°C, and T_{Cmax} =142.9°C, and under the cooling rate at 2°C/min T_{Cmin} and T_{Cmax} were 111 and 146 °C, respectively. The highest NES value was 107 % for PLLA and PDLA with molecular weight of 14000 g/mol. This result indicates the stereocomplex crystallites were more actually efficient than even the PLLA crystallites coming from the self-nucleation experiment. For comparison, NES of Talc in the molten state was also investigated. NES of PLLA/Talc 6 % was 50 %, thanks to better dispersion of Talc in the melt blends [154]. The samples were cooled from 240 °C at which no racemic crystals existed. Yamane *et al.* [58] have studied the effect of molecular weight of PDLA on the efficiency of stereocomplex

crystals as a nucleating agent in solution state. It was found that when the samples were cooled from 200 °C, below the melting temperature of the stereocomplex, high molecular weight PDLA was more efficient. Nevertheless, when samples were cooled from 240 °C, above the melting temperature of stereocomplex, lower molecular weight PDLA was more efficient. When the blend was cooled from lower temperatures, stereocomplex crystals were already in the system and stereocomplex blends generated by higher molecular weights could provide a larger surface area for crystallization of PLLA. However, when samples were cooled from higher temperatures, lower molecular weight PDLAs demonstrated higher chain mobility than higher molecular weight PDLAs. As a result, they can form stereocomplex more easily.

Nevertheless, studies in our research group indicated that the efficiency of the stereocomplexed PLA was not that high as claimed in the articles [156]. For example, our studies revealed that there is no significant difference between the efficiency of Talc and that of stereocomplex crystallites. This might refer to the different molecular weight used in our work and the others. In addition, the effect of the heating and cooling rate and the effect of α and α'phases on the self-nucleation of PLA have not been clarified yet.

2.11 Shear-induced crystallization of PLA

Even though the quiescent crystallization phenomenon is not completely understood, several attempts have been made to study the effect of shear and elongational flow on the crystallization of polymers [103,157,158,159]. Most of polymers are subjected to intense flow fields during common processing operations such as injection molding, extrusion or blow molding. The crystallization kinetics and the morphology of the semicrystalline polymer in the final product depend on the orientation of the melt by the flow field. Therefore, study the polymer melt crystallization under dynamic conditions would be interesting.

Different crystal morphologies can be generated depending the flow conditions. Spherulites form under no flow conditions or when the deformation rate is very low. When the deformation rate increases shish-kebab structures can form. Pennings first proposed a model consisting of a combination of an extended chain crystal (Shish) and folded chain crystals (kebabs). In Pennings' model the "shish" forms first during a crystallization process under stress and then later the "kebabs" overgrow this "shish" structure epitaxially[160]. A schematic of shish-kebab structure is shown in **Figure 12**.

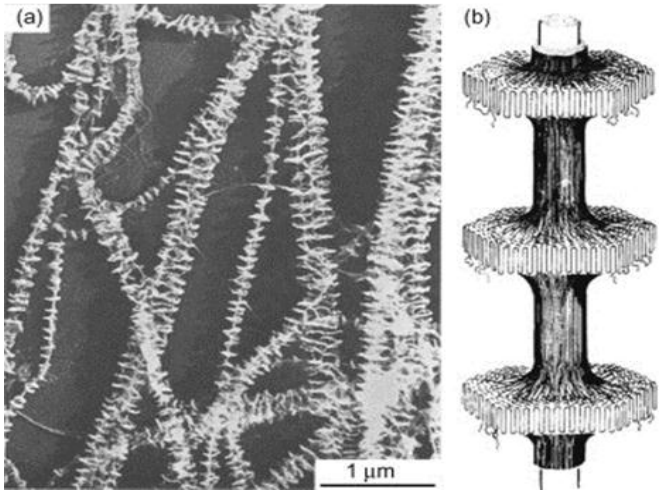

Figure 12. Schematic of shish-kebab structure [161].

Many articles have been published so far on the microstructure, morphology and enhancement of the crystallization of PLA in quiescent conditions, whereas the effect of shear on the crystallization of PLA has attracted limited attention.

Juan *et al.* investigated the nonisothermal crystallization behavior of PLA under static and dynamic conditions in a hot shear stage device [161]. In quiescent conditions, the typical morphology of PLA samples was spherulitic. The onset crystallization temperature, T_{onset}, was reduced by increasing the cooling rate. It particularly declined from 122 °C at 0.5 °C/min to 107 °C at 2 °C/min. When the cooling rate is low, polymer molecules have enough time to place themselves in crystalline structures while they do not have enough time to form nuclei. The results also showed that above the shear rate of 5 s^{-1} for 1 minute, cylindrite structures were formed. Upon high shear rate, the polymer chains have to orientate along the shear flow to form cylindrite structure. On the other hand, under low shear rates, the possibility exists for polymer chains to relax and thereby stable nuclei cannot be formed. T_{onset} was raised by shear rate from 104 °C at 4 s^{-1} to 133 °C at 6 s^{-1}.

The crystallization behavior of PLA under isothermal crystallization was studied by Xu-Juan Li [162]. At 120 °C, under the shear rate of 5 s^{-1}, the cylindrite structure was observed which was closely similar to the shish-kebab structure reported in PP. At lower shear rates, 1s^{-1}, when crystallization temperature was above 120 °C, the cylindrite structure appeared. Micrographs also exhibited some spherulites formed as well. The formation of these isotropic structures stemmed from the non-sheared parts or low-molecular weight polymer chains relaxed before crystallization.

Effect of temperature was also intriguing. At temperatures below 120 °C, only aligned spherulites were observed. However, at higher temperatures, cylindrite structures apparently appeared. It is well understood that orientation and relaxation of molecular chains are temperature and molecular weight dependent, respectively. High T_C facilitates the chain mobility and causes the chain alignment more easily. On the contrary, a high temperature shortens the relaxation time of junction points which would be shorter than shearing time. As a result, these two elements contest one another during crystallization. In static state, high T_C does not lead to crystallization whereas shear effectively increases the difference energy between nuclei and the surrounding melt. Based on these reasons, it is believed at higher temperatures, shear exhibits a dominant role to make polymer chains align along the shear flow to form cylindrite structures despite of shorten relaxation time of junctions.

Effect of shear on crystal structure, morphology and melting behavior of PLA was investigated by Huang *et al.* [163]. The PLA samples were melted at 200 °C for 1 min to erase the thermal history. Then the samples were cooled down to 96.5 °C, 106 °C, 115.5 °C and 130 °C at which α', mixture of α' and α, and only α crystals exist, respectively. As temperature reached at T_C, the samples were sheared for 5s. After held for 60 min at T_C, the samples were quenched to 30 °C. It was found that crystal structures of PLA were temperature and shear dependent. In absence of the shear, for the sample annealed at 96.5 °C, a small exothermic peak was observed prior to the melting peak which was already explained, due to disorder to order transition, α' to α. However, in samples annealed at 106 °C and 115.5 °C this transition vanished and a multiple melting peak appeared. For the sample isothermally crystallized at 130 °C, there was only a sharp endothermic peak while when shear was exposed on the sample, a crystallization peak appeared which implied the plenty of nuclei were in samples. For higher shear rate, 20 s^{-1}, an exothermic peak prior to melting was also detected due to crystal transition. XRD patterns verified that only α-crystals formed at 130 °C. Consequently, these exothermic peaks were attributed to the crystal structures formed during the heating process. The crystal structure formed during the heating was deficient because of the relatively low PLLA chain segment mobility. Hence, when temperature jumped, phase transition and recrystallization of their imperfect crystal structure took place at high temperature range. Increasing the shear rate also directed to increment of crystallization enthalpy change, $\Delta H_{\alpha-\alpha'}$. Presence of the shear shortened the inducement time, and oriented the polymer chains, and the

pre-oriented molecules crystallized easily and acted as nucleating agent. Under weak shear effect, the surfaces of polymer films were influenced, and under strong shear effect, the surfaces and inside of polymer films were affected. Consequently, more nuclei could be formed inside polymer film under high shear rate. A small exothermic peak also appeared before the melting peak in each shear rate, which indicates the α' to α transition.

Thus far, it is well understood that nucleating agent and shear flow have remarkable effect individually in the enhancement of the crystallinity of polymers. Recently, researchers have attempted to investigate the combined effect of shear and nucleating agent on the crystallinity of polymers. Legasse and Maxwell [164] found that shear-induced crystallization of PP was unaffected by the presence of nucleating agents. Naudy [165] *et al.* and also recently D'Haese *et al.* [166] corroborated this result that the acceleration of the crystallization of polymers with shear rate was less outstanding for polymers containing nucleating agents. Conversely, synergistic effect was reported for other group of polymers containing nucleating agents [167,168,169,170]. These articles investigated the combination of shear and nucleating agent on PP and polybutylene (PB) with aramide fibers, graphene nanosheet and CNT. For example, Tang *et al.* argued that the flow- induced crystallization of PP in the presence of the shear was 40 times higher than that of static conditions. Surprisingly, there are a few articles to address this question whether this synergistic effect exists for PLA containing nucleating agents or not. Shear-induced nonisothermal crystallization of PLA with the presence of CNT at high cooling rate was investigated by Tang *et al.* [171]. The crystallinity and the onset of crystallization of PLA increased remarkably by extra nucleating sites created by interplay of shear and nucleating agents. It was also reported that the shear flow helped formation of more ordered crystalline α phase during nonisothermal crystallization upon high cooling rates.

Rotational rheometry along with optical microscopy was also applied to investigate the isothermal and non-isothermal crystallization of PLA [172]. It was found that the shear flow essentially promoted the crystallization kinetics of PLA. Additionally, higher level of shear rate and shearing time enhanced the crystallization kinetics of PLA as well as increasing the nuclei density. Optical microscopy also revealed that upon shear at a given temperature, the spherulite growth rate was almost unchanged. Effect of long chain branching on the shear-induced crystallization of PLA was also studied [173]. Under similar shearing conditions, the long chain branched PLA exhibited faster crystallization kinetics, higher nuclei density and

formation of shish-kebab structure compared to linear PLA. In another study, this research group examined the shear-induced crystallization kinetics at 160 °C for asymmetric (PLLA)/ (PDLA) blends [174]. The rheological measurements exhibited the formation of stereocomplex crystallite networks in the blends, which could act as a heterogeneous nucleating agent, accelerating the crystallization kinetics of PLLA. Recently, formation of the shish-kebab structure has been studied by Huan *et al.* [175].They succeeded to develop the shish structure by a unique transient intensive shear flow with the duration of 1s and a shear rate to 100 s^{-1}. By increasing the isothermal crystallization temperature in 130-140 °C range, the oriented shish-kebabs were formed. This finding was in obvious contrast with the existing data in the literature revealing that a high amount of shear and long shearing time can generate the shish precursor.

CHAPTER 3 Effect of Thermal History on Nucleation and Crystallization of PLA

Avant-propos

Auteurs et affiliation:

Amirjalal Jalali: *Département de génie chimique et de génie biotechnologique, Faculté de génie, Université de Sherbrooke.*

Michel.A.Huneault: *Département de génie chimique et de génie biotechnologique, Faculté de génie, Université de Sherbrooke.*

Saïd Elkoun: *Département de génie mécanique, Faculté de génie, Université de Sherbrooke.*

Date d'acceptation: 10 mai 2016

État de l'acceptation: version finale publiée.

Revue: Journal of Materials Science

Référence: *Journal of Materials Science,* Volume 51, Issue 16, pp 7768-7779.

Titre français: Effet de l'histoire thermique sur la nucléation et la cristallisation du poly (acide lactique)

Contribution au document: Présenter l'étude de l'auto-nucléation du PLA et l'leffet des phases cristallines sur l'auto-nucléation.

Résumé français

Dans cet article, un protocole de chauffage et de refroidissement successif a été conçu pour étudier le comportement d'auto-nucléation du poly (acide lactique), PLA. L'objectif principal de cette étude était d'étudier l'efficacité des phases cristallines du PLA, α et α' quant à la

nucléation cristalline du PLA. Ceci a été réalisé en comparant les témperatures de cristallisation lors du refroidissement après l'auto-nucléation des échantillons préalablement cristallisés isothermiquement à différentes températures allant de 80 à 130 °C. Au cours du chauffage dans la plage de fusion partielle, trois différents mécanismes ont été observés pour les échantillons cristallisés. Les échantillons cristallisés en dessous de 100°C, ont affiché un pic exothermique avant le pic principal de fusion qui est attribué à une transition à l'état solide α'- α. Pour les échantillons cristallisés entre 100 et 120 °C, un mécanisme de fusion - recristallisation a été observée. Les échantillons cristallisés au-dessus de 120 °C ont exhibé seulement la fusion de la phase α. Lors du refroidissement après la fusion partielle, on a trouvé que des échantillons comprenant un mélange de phases α et α' présentent la plus haute température de cristallisation, la densité de noyaux la plus haute et la plus petite taille de sphérolites. En outre, on a observé que les échantillons qui ont été cristallisés isothermiquement entre 100 et 120 °C puis chauffés dans la zone de fusion partielle et finalement refroidis à la température ambiante présentaient ainsi deux pics de cristallisation propres à 100 et 120 °C. Ce phénomène a été attribué à la formation des phases cristallines, α et α', comme révélé par diffraction des rayons X. De plus, en modifiant légèrement la température dans la plage de température d'auto-nucléation, un changement de la proportion de chaque pic a été observé.

Mots-clés : Cristallisation du PLA, auto-nucléation, phases cristallines.

3.1 Abstract

In this paper, a successive heating and cooling protocol was designed to investigate the self-nucleation behavior of poly(lactic acid), PLA**.** The main objective of this investigation was to study the efficiency of the α and α' crystalline modifications of PLA**.** This was carried out by comparing crystallization temperatures upon cooling after self-nucleation of samples previously crystallized at various isothermal temperatures ranging from 80 to 130 °C. During heating to the partial melting range, three different mechanisms were observed for crystallized samples. For samples crystallized below 100 °C, an exothermic peak was detected prior the main melting peak which is ascribed to the α'- α solid state transition. For samples crystallized between 100 and 120 °C, a melt recrystallization mechanism was observed. Finally, for samples crystallized above 120 °C only melting of the α phase was detected. Upon cooling after partial melting, it was found that samples comprising a mixture of α and α' exhibited the highest crystallization temperature, the highest nuclei density and the smallest spherulite size. Moreover, it was observed that samples isothermally crystallized between 100 and 120 °C, heated up to partial melting and cooled back to room temperature exhibited two peculiar crystallization peaks at 100 and 120 °C. This phenomenon was ascribed to the formation of α and α' crystalline phases as revealed by X-Ray diffraction. In addition, by slightly changing the temperature within the self-nucleation temperature range, a change of the proportion of each peak was observed.

Keywords: PLA crystallization, self-nucleation, crystalline phases.

3.2 Introduction

Poly(lactic acid) or PLA, is a biodegradable and biocompatible polymer that can be produced from renewable resources. It has raised particular attention as a potential replacement for petroleum-based polymers. Commercially available biobased PLA grades are generally made from a monomer mix containing mainly the *L*-enantiomer with small concentrations of *D-LA* impurities that can act as crystal defects. PLA exhibits high tensile modulus and strength, along with high transparency. Accordingly, this biobased polymer is a promising material for various applications such as textiles, bottles, thermoformed containers, paper and cardboard coating. Due to its low glass transition temperature (T_g ~ 60-65 °C), PLA has a low heat resistance unless it can be fully crystallized and therefore PLA crystallization has been a subject of great interest in the past decade [1]. Crystallization of this polymer is strongly dependent on *D*- content and is hindered as *D*- concentration increases. Furthermore, it suffers from low crystallization kinetics unless it is subjected to high orientations. Hence, increasing the crystallization rate in processing techniques, such as injection molding where orientation levels are relatively low, is required to improve its thermal resistance [82,118,142,176,177,178,179,180].

It is well understood that PLA is a polymorphous polymer. During the last decade, the crystal structure of PLA has attracted particular attention of researchers. It has been shown that PLA exhibits two different crystalline phases termed α and α'. By means of FTIR and WAXD analysis, α' was described as a disordered form of the stable α phase [18,21,23,26,181,182]. Differences between the crystalline structures were associated to chain conformation and chain packing mode between the disordered and ordered forms. It was found that crystallization at temperatures below 100 °C lead predominately to the α' crystalline form whereas at temperatures above 120 °C the α phase was the main form [23,45]. Within the 100-120 °C crystallization temperature range, a mixture of these crystalline phases was present. Different thermal properties for α' and α phases stem from the structural difference and interchain interactions. Equilibrium melting enthalpy, ΔH_m°, of α' crystals is 57 J/g which is 40 J/g lower than that of α, 96 J/g [183,184].

The crystallization of PLA can be enhanced by the addition of nucleating agents and plasticizers or combination of both to increase nucleation density and chain mobility [1,70]. From a crystallographic and chemical point of view, the self-seeded nuclei can be regarded as

ideal nucleating agents for improving the crystallization of semi-crystalline polymers. Based on this assumption, Fillon *et al.* developed a nucleation efficiency scale to measure the efficiency of heterogeneous nucleating agents for polypropylene [147,150,151,185,186]. In this technique, the crystallization temperature of the investigated polymer formulation was compared to those obtained with the pure polymer and to the pure polymer subjected to a procedure known as self-nucleation. Self-nucleation was produced by first heating to the partial melting region, where the temperature is in the vicinity of the melting peak temperature. Then, by cooling down with a controlled cooling rate, the exothermal crystallization peak can be recorded. The highest crystallization temperature T_C^{max} found is taken as the upper limit for the nucleation efficiency scale.

Self-nucleation can also be employed as a convenient procedure to establish a relationship between crystallization and the microstructure of polymers. Nucleation behavior of poly (vinylidene fluoride), PVDF, in its α phase has been studied by Schneider *et al.* [187]. It was observed that the sample containing the highest number of defects after the self-nucleation exhibited the lowest crystallization temperature on subsequent cooling.

The Successive and Self-nucleation and Annealing, (SSA), thermal fractionation has also been introduced by Müller *et al.* [188,189,190]. This technique involved successive self-nucleation and annealing steps and was used to characterize copolymers. SSA gives information on the distribution of short chain branching and lamellar thickness. In random copolymers, the second component disturbs the crystallization of the major element and materials are sensitive to thermal fractionation.

A nucleation efficiency scale for PLA has been developed in the solution state by Schmidt and Hillmyer [155]. Upon cooling at 2 °C/min, T_C^{min} and T_C^{max} were 106 °C and 157 °C, respectively. In another study, Anderson and Hillmyer used the same procedure for the melt processed PLA [154]. By using a cooling rate of 5 °C/min, T_C^{min} and T_C^{max} were 104.3 °C and 142.9 °C, respectively. However, by changing the cooling rate to 2 °C/min, T_C^{max} shifted to 149 °C.

Isothermal and non-isothermal crystallization of PLA were examined from the molten and glassy state by De Santis *et al.* [191]. Nucleation and growth rate of the formed crystals were calculated. Crystallization kinetics from the glassy state exhibited a faster rate than from the molten state. The kinetics of crystal formation of PLA at non-isothermal condition was

examined at different cooling rates [192]. Although the crystallization of PLA took place on cooling the melt at rates lower than $0.5Ks^{-1}$, crystal nuclei shaped even at cooling rates up to $50Ks^{-1}$. Additionally, decreasing the cooling rate led to increase the nuclei density.

In this contribution, a thermal protocol was designed to characterize and understand the self-nucleation mechanism of PLA. The work first aimed at better understanding the crystallization temperature on the formation of α and α' crystals. Secondly, the α' to α transition upon heating to self-nucleation range was investigated. Finally, the effect of these induced crystalline phases on self-nucleation was assessed. For this purpose, calorimetric, x-ray diffraction as well as optical microscopy was employed to investigate the crystallization behavior of PLA.

3.3 Experimental

3.3.1 Materials

A commercial PLA, grade 4032D supplied by NatureWorks, was used. This PLA is a semi-crystalline grade that contains 2 % *D-LA*. The measured weight-averaged molecular weight (M_w) and polydispersity index (M_w /M_n) of PLA were 109 kg/mol and 1.57, respectively [193].

3.3.2 Sample preparation

The main reason of this study was to find out the optimum crystallization kinetics for the crystallization of PLA in realistic condition in which PLA is processed in molten state. For this reason, the samples were extruded. Samples were prepared using a HAAKE Minilab conical twin screw micro compounder (Thermo Scientific). PLA was vacuum dried at 50°C for 2 days prior to melt mixing. Mixing was carried out at 180 °C for 5 minutes at a rotation speed of 100rpm. The extruded samples were also dried in the same conditions and prepared in a twin screw extruder at 180 °C at a mass flow rate of 20 kg/h.

3.3.3 Characterization

(i) Thermal behavior: Differential scanning calorimetry

The thermal behavior of PLA samples was studied using a DSC Q2000 from TA Instruments. Temperature was calibrated before measurements by using Indium as a standard material. Samples weight was kept constant in the range of 10-15mg. The typical variation on crystallization and melting temperatures was assessed at ± 0.2 °C while the accuracy of crystallization and melting enthalpies was estimated at ± 1.5 J/g.

(ii) Microstructure analysis: Wide-Angle X-ray Diffraction Analysis (WAXD)

Wide-angle X-ray Diffraction (WAXD) patterns were obtained by means of an X-ray diffractometer (D-8, Bruker) to detect the crystalline phases at different crystallization temperatures. The samples were exposed to an X-ray beam with the X-ray generators running at 40 kV and 40 mA. The copper Kα radiation (λ=1.542Å) was selected and the scanning was carried out at 0.03 °/s in the angular region (2θ) of 5-40°.

(iii) Isothermal crystallization: Hot-stage and Optical Microscopy

Isothermal crystallization experiments were performed by means of optical microscopy, Leica MDRX polarized, to observe the effect of isothermal crystallization on PLA crystalline morphology, and to measure nuclei density and growth rate. The samples were melted between two glass slides at 200 °C and then the glasses were gently pressed to squeeze the melt into a very thin film. The prepared slides were moved onto a Mettler Toledo FP82HT hot-stage (UNITRON Bi-9691), kept at 200°C for 3 minutes, then quenched to 130 °C, and finally held at that temperature to monitor the spherulite growth rate in isothermal condition.

3.4 Results and discussion

3.4.1 PLA self-nucleation: cooling rate and thermal protocol effect

For most semi-crystalline polymers the heating and cooling rates in calorimetric experiments is around 10 °C/min. Due to slow crystallization kinetics of PLA, a cooling rate of 10 °C/min is too high to detect any crystallization peak. Hence, selecting the appropriate scanning rate for PLA is a crucial parameter in a study on the self-nucleation behavior of PLA. **Figure 13** presents the cooling curves after maintaining PLA sample at 200 °C for 5 minutes and subsequently cooling down at 20, 10, 5 and 2 °C/min, respectively. Upon cooling at 20 and 10 °C/min no peak can be observed. At the cooling rate of 5 °C/min, a broad and weak crystallization peak was detected around 91 °C but the crystallization enthalpy is only 2.3 J/g. However, by decreasing the cooling rate to 2 °C/min, a clear and well defined crystallization peak at approximately 98 °C was observed with a crystallization enthalpy of 25 J/g. Based on these results, a cooling rate of 2 °C/min was selected for the study of self-nucleation of PLA and, accordingly, to detect crystallization upon cooling within a reasonable time frame.

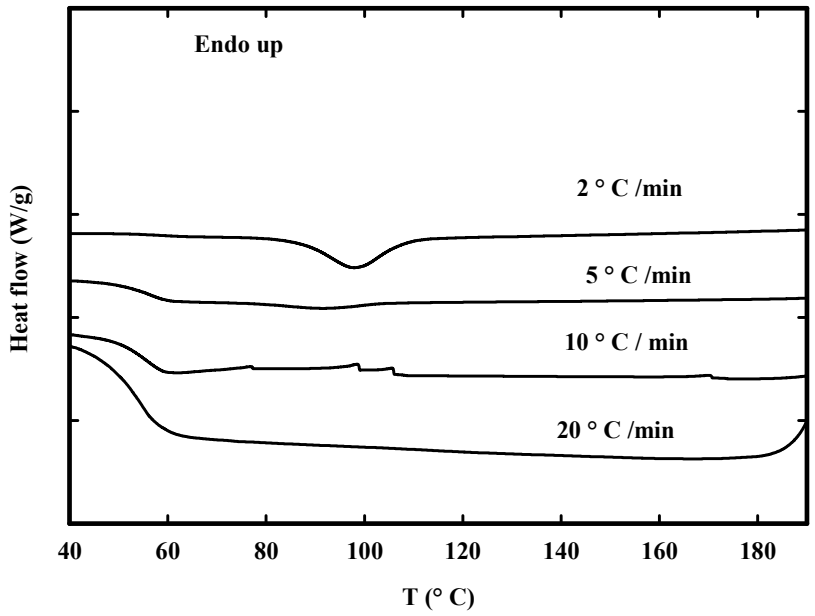

Figure 13 . DSC curves for PLA at different cooling rates after holding at 200 °C for 5 minutes.

Figure 14 presents the protocol used to investigate the self-seeding of PLA. The sample was first heated up to 200 °C and held for 5 minutes to erase thermal history. This is referred to as Segment **A** in the figure. The sample was then quenched to a determined annealing temperature, T_{iC}, and held for a period, ranging from 1 to 4 hours, until completion of crystallization. This is referred to as Segment **B** in **Figure 14**. Afterwards, the sample was heated up to the self-seeding range under the heating rate of 2 °C/min. Once at the self-nucleation or, (self-seeding), the temperature was held constant for 5 minutes. This is referred to as Segment **C** in the figure and has been used to assess the partial melting endotherm. To measure the crystallization temperature of the self-nucleated sample, the sample was cooled down to room temperature at 2 °C/min to detect the crystallization exotherm in what is referred to as Segment **D** in the figure. Finally, to assess the melting behavior and type of the crystal modification, the sample was reheated again in Segment **E** at 2 °C/min up to complete melting.

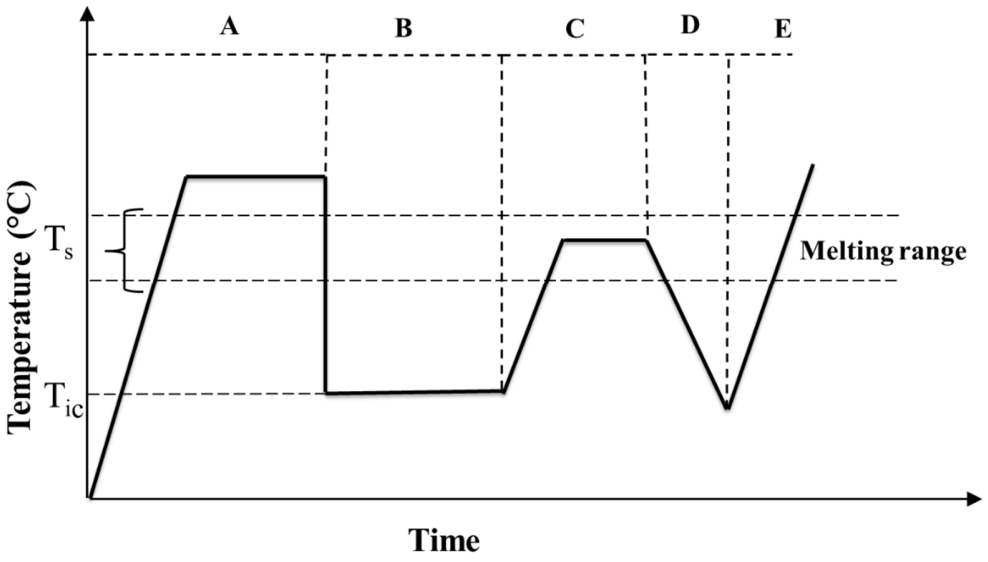

Figure 14. Schematic representation of temperature protocol for the self-nucleation of PLA.
A: Erasing thermal history, **B:** Isothermal crystallization,**C:** Partial melting , **D:** Cooling down, **E:** Final heating, $\mathbf{T_{iC}}$ **:** Isothermal crystallization temperature, $\mathbf{T_S}$**:** Self-nucleation temperature.

3.4.2 Isothermal crystallization at 80 °C

At first, self-nucleation of samples crystallized at 80 °C was examined. In these conditions, it took 4 hours to complete the crystallization and only the formation of α' phase was expected. **Figure 15** displays the DSC thermographs under cooling at 2 °C/min after self-nucleation at different temperatures, T_s. This corresponds to segment **D** in the thermal protocol presented previously (c.f. **Figure 14**). **Table 2** summarizes the transition temperatures and enthalpies obtained for T_s between 167 and 174 °C. For the samples molten at T_s equal to 174 °C or higher, the obtained crystallization temperature after cooling remained constant at approximately 100 °C. The above 174 °C is called Domain **I**. In this region, nearly all crystal fragments were molten down and since there was no self-nucleation, crystallization temperature was independent of T_s. In the $170\ °C \leq Ts \leq 174\ °C$ region, the self-nucleation occurred and the crystallization temperature increased as T_s decreased. This domain, known as Domain **II**, is characterized by the presence of very small crystal fragments whose concentrations vary with T_s. The presence of these very small crystals largely favors self-nucleation over annealing. This noticeable increase in crystallization temperature with decreasing T_s can be ascribed to a significant increase in nucleation density associated with the

higher concentration of residual crystal fragments. In addition, the enthalpy of crystallization, ΔH_C, increased as T_s decreased from 174 °C to 170 °C. A similar increase in ΔH_C upon decreasing T_s has been reported for PET and poly(p-dioxanone), PPDX, within Domain **II** [147,152,153]. The range of self-nucleation temperatures below 170 °C is called Domain **III**. In this region, although self-nucleation takes place, the annealing effect of existing crystals is the predominant mechanism.

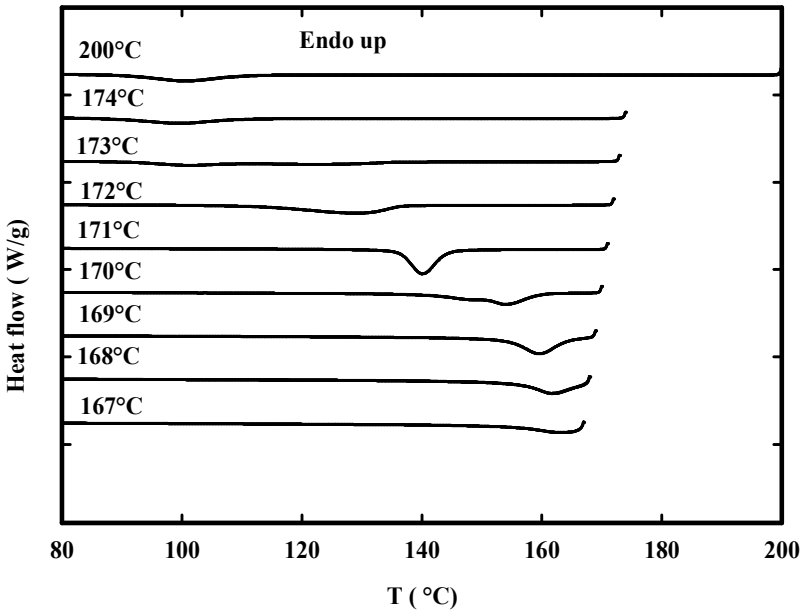

Figure 15 . DSC cooling scans at 2 °C/min for sample previously crystallized at TiC=80 °C then self-nucleated for 5 minutes at the indicated self-nucleation temperature, Ts. (Segment D in Figure 14).

Table 2. Crystallization temperature, enthalpies of crystallization and melting as a function of self-nucleation temperatures.

T_s (°C)	T_{C1} (°C)	T_{C2} (°C)	ΔH_C (J/g)	T_{m1} (°C)	T_{m2} (°C)	ΔH_m (J/g)
167	163.5	-	-*	-	169	42
168	161.8	-	-*	167	170.3	44
169	159.4	-	37.3	168	170.5	45.2
170	153.9	148	48.7	-	169	47.8
171	140	-	42.7	-	170.6	53.5
172	129.2	-	39.7	173	175	52.6
173	122	101	34.2	173.3	175.2	59.5
174	99.9	-	24.2	-	175	58.4

Figure 16 depicts the larger scale of DSC cooling curves for T_s in Domain **II**. After self-nucleation at 170 °C, two crystallization peaks can be observed upon cooling. The first one is at 153.9 °C and the next small one is around 148.1 °C. Moreover, when temperature increased within this domain, a double exothermic crystallization peak was detected again after cooling from T_s =173 °C. The first crystallization peak was observed at around 120 °C and the second one was around 100 °C. The double crystallization peak can be ascribed to crystalline phases of PLA. This will be discussed in next sections.

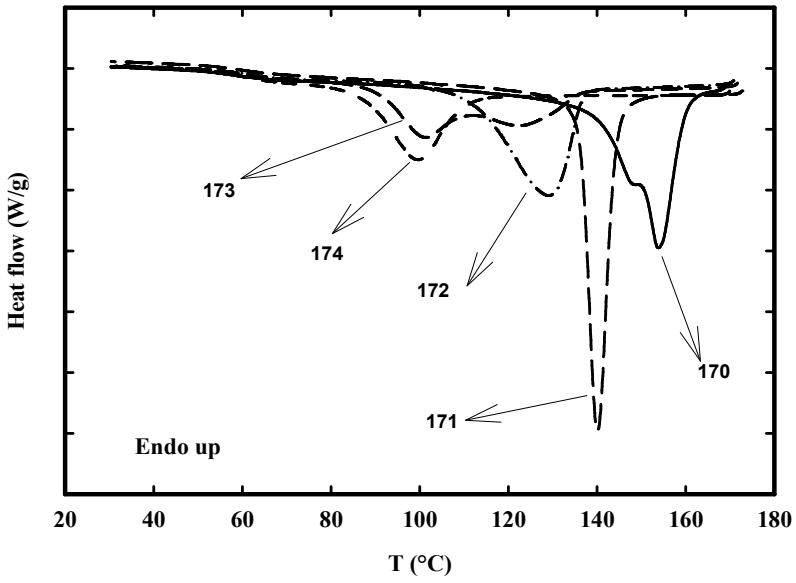

Figure 16. DSC enlarged cooling scans at 2 °C/min for sample previously crystallized at T_{iC}=80 °C then self-nucleated for 5 minutes at the indicated self-nucleation temperature, T_s. (Segment D in Figure 14).

In order to determine the frontiers of each domain, a subsequent heating scan after self-nucleation is required. Hence, a final heating at the rate of 2 °C/min was also carried out to further probe the structure developed upon cooling after self-seeding. This corresponds to segment **E** in the thermal protocol presented (c.f. **Figure 14**). **Figure 17** illustrates these heating scans. For most samples in Domain **II,** there were two melting peaks. The lower melting peak, changed with T_s whereas the higher one was independent of T_s .The lower melting peak could be associated to the melting of crystals formed upon cooling from T_s while the second endothermic peak could be ascribed to melt-recrystallization of crystals taking

place upon the heating process. For T_s in Domain **III** (i.e. T_s < 170 °C), two melting peaks were also observed. However, in this domain, crystal fragments are larger and annealing competes with self-nucleation and is more likely to happen as T_s decreases. Accordingly, the higher melting peak is ascribed to the annealing process during heating and the lower endothermic peak corresponds to melting of crystals that formed during cooling and recrystallizing upon heating.

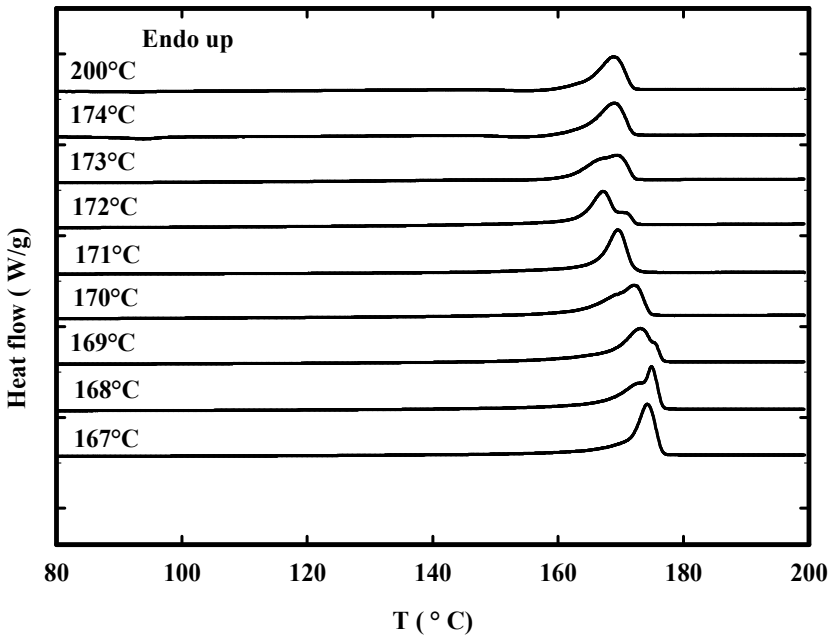

Figure 17. DSC heating scans at 2 °C/min after the cooling shown in Figure 14. T_s values are indicated above each curve. (Segment E in Figure 14).

3.5 Effect of crystalline phase on self-nucleation

3.5.1 Crystalline structure

Figure 18 presents the XRD patterns of PLA isothermally crystallized at 80, 115 and 130 °C, respectively. The XRD patterns of PLA crystallized at these temperatures were rather similar. For sample crystallized at 80 °C, where only the α' phase was expected, two strong diffraction peaks were observed at 16.6 ° and 18.9° , corresponding to (110)/ (200) and (203) planes [38]. These peaks shifted slightly to higher 2θ with crystallization temperature, T_{iC}, due to a decrease in lattice spacing. Additionally, for samples crystallized at 115 °C, where a mixture of α and α' phases is expected, and at 130 °C, where only the α phase should be present, three small diffraction peaks at 12.5°, 15° and 22° associated to the α phase appeared. Thus, these

XRD patterns confirmed the gradual shift from the α' to the α form with increasing isothermal crystallization temperature.

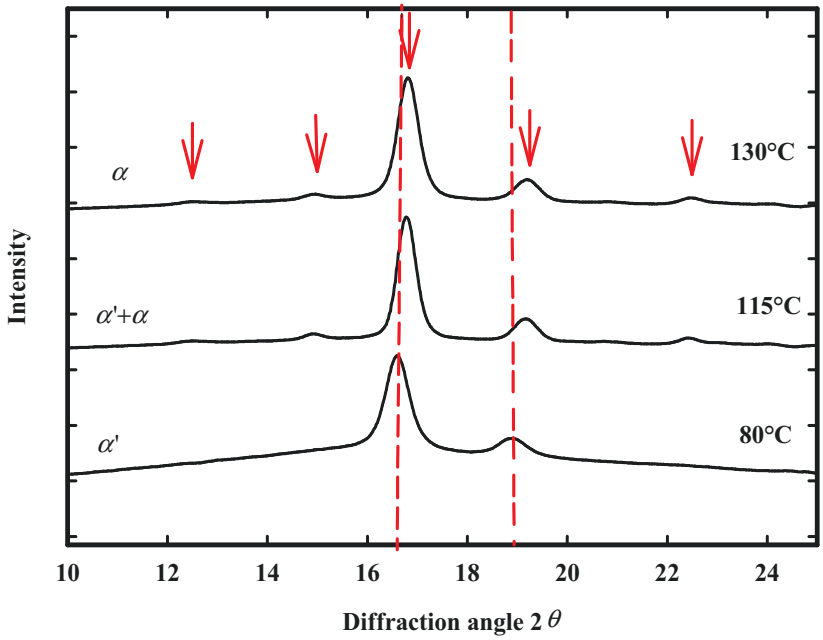

Figure 18. XRD patterns of PLA at indicated isothermal crystallization temperatures.

3.5.2 Self-nucleation of (α'+ α) and α phases

In order to investigate the effect of the crystalline phases developed upon the isothermal crystallization step on the subsequent self-nucleation experiments were repeated following isothermal crystallization at different temperatures, T_{ic}. As explained in the experimental section, the samples were quenched from the melt state to the desired isothermal crystallization temperature, held for sufficient time to complete the crystallization and subsequently reheated to the self-seeding range.

The DSC heating scans from the isothermal crystallization temperature to the self-seeding temperature were carried out and are shown in **Figure 19**. This corresponds to segment **C** in the thermal protocol presented in **Figure 14**. For T_{iC} = 80 and 100 °C, a small exotherm appeared prior to the main melting peak. However, for temperature inclusively between 105 °C and 120 °C, this exotherm was replaced by an endothermic peak. For PLA crystallized at 130 °C, no peak can be seen before the main melting peak. Three different mechanisms may be invoked. Indeed for samples crystallized at 100 °C or below, the observed exothermic peak

is associated to a solid state transition where disordered α' phase transforms into the ordered α-phase [23]. For samples crystallized between 100 and 120 °C, α'-α transformation takes place through a melt recrystallization mechanism. Finally for sample crystallized above 120° C, no phase transition occurs [45].

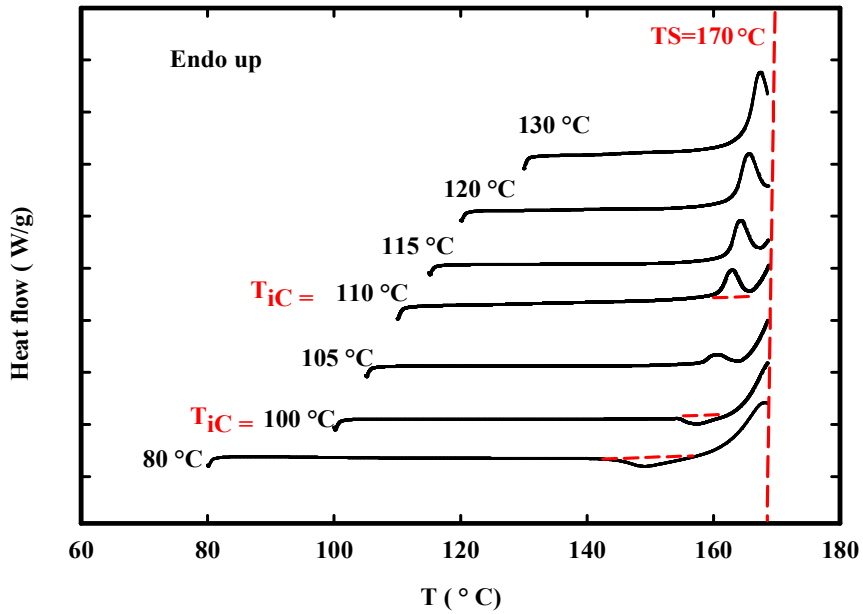

Figure 19. Heating scans obtained from various isothermal crystallization temperatures ranging from 80-140 °C to Ts = 170°C at 2 °C/min. (Segment C in Figure 14).

For all the investigated isothermal crystallization temperatures, Domain II was found to be located in the 170 °C≤T_s≤174 °C temperatures range. Moreover, a significant effect of the initial crystallization temperature was obtained. **Figure 20** exemplifies these effects by depicting T_C^{max} as a function of annealing temperature, Tic for samples that were self-seeded at 170 °C. It was found that T_C^{max} displayed a clear maximum at Tic =110 °C. It is of immense surprise that Tic revealed a large effect on the crystallization process since all crystals present at the end of self-seeding step are supposedly of α modification. One potential reason explaining this result might come from the nuclei density, N, and/or spherulite size, D, prior to self-nucleation. Isothermal crystallization experiments were, therefore, performed by optical microscopy and DSC to assess N and D.

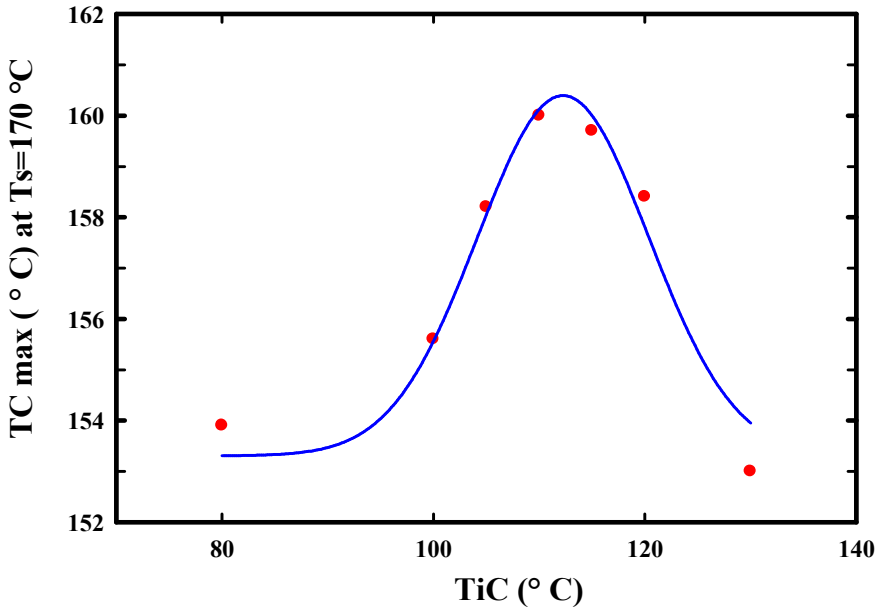

Figure 20. Maximum nonisothermal crystallization temperature, $T_{C\,max}$, obtained after self-nucleation at T_s=170 °C as a function of the crystallization temperatures, T_{iC}.

3.6 Effect of T_{ic} on the nuclei density

To compare nuclei density of PLA crystallized at different isothermal crystallization temperatures (T_{ic}), the self-nucleated PLA specimens were quenched from T_s to 130 °C. Under isothermal conditions, nuclei density, N, can be derived by the well-known Avrami Equation [47] which assumes that the relative crystallinity, $X(t)$, changes with the time t, according to the following equation:

$$1 - X(t) = exp(-kt^n) \tag{3}$$

where n is the Avrami exponent and k is the crystallization rate constant. $X(t)$ can be calculated according to Equation 4:

$$X(t) = \frac{\Delta H_t}{\Delta H_\infty} = \frac{\int_0^t \frac{dH}{dt} dt}{\int_0^\infty \frac{dH}{dt} dt} \tag{4}$$

where ΔH_t and ΔH_∞ are the amounts of enthalpy generated at time t and infinite time, respectively, and $\frac{dH}{dt}$ is the enthalpy evolution rate. In order to graphically determine n and K, the Avrami Equation is often written in the following form:

$$\ln[-\ln(1-X(t)] = nlnt + lnk \quad (5)$$

The crystalline fraction $X(t)$ is plotted in the form of $\ln[-\ln(1-X(t)]$ vs. $ln\, t$ to yield the characteristic Avrami plot. The slope of this plot gives the Avrami constant n. The value of k is obtained by using the value of $X(t)$ at $t=t_{1/2}$, crystallization half-time. The crystallization half-time is defined as the time spent from the onset of the crystallization to the point where the crystallization is 50% complete. The bulk crystallization rate can be deduced through the following equation:

$$k = \frac{ln2}{t_{1/2}^n} \quad (6)$$

In the case of predetermined nucleation and three dimensional growth, the crystallization rate k is directly proportional to the total concentration of the number of nuclei, N, through the equation 7:

$$N \approx \frac{3K}{4\pi G^3} \quad (7)$$

where G is the spherulite growth rate measured by optical microscopy. As the value of N is obtained, the average spherulite size can also be determined according to the following equation[194]:

$$D = (\frac{6}{\pi N})^{1/3} \quad (8)$$

At first, an attempt was made to measure the Avrami parameters of the samples self-nucleated from T_s= 170 °C. The Avrami parameters for the sample self-nucleated at 170 °C and 171 °C could not be determined, because crystallization took place too fast and occurred during quenching. As a result, a value of T_s = 172 °C was selected. **Figure 21** depicts the plot of $\ln[-\ln(1-X(t)]$ vs lnt for some samples self-nucleated at 172 °C. In all cases, the Avrami plots were linear confirming the applicability of the Avrami equation. **Table 3** summarizes the

effect of crystallization temperature T_{iC} on crystallization half-time, $t_{1/2}$ and Avrami parameters**, (**n and k). For all T_{ic} , the Avrami constant was very close to 2. The literature on PLA isothermal crystallization generally reports indexes between 2.5 and 4 [1].

Unfortunately, the morphology of the self-nucleated samples after cooling down to 130 °C could not be observed by optical microscopy due to the small crystal size (and high nucleation density). The different Avrami exponent may be due to the different nature of the crystal nuclei (i.e. Self-nucleation vs homogeneous and heterogeneous) and will deserve further investigation. As T_{iC} increased from 80 °C to 105 °C, the $t_{1/2}$ decreased from 8.8 to 4.4 min. These values then remained relatively constant up to 115 °C indicating that T_{iC} of 105 to 115 °C is optimal in terms of crystallization. The half-time increased again (and K decreased) for higher T_{iC} showing slower crystallization. It is important to insist here that these results do not represent the crystallization rate as a function of crystallization temperature as often found in literature. Indeed, they present the effect of a prior crystallization prior to self-nucleation and further cooling. Nonetheless, the behavior is strikingly similar to that found when examining the effect of crystallization temperature on crystallization kinetics with an optimal crystallization temperature range in the 105-115 °C.

Table 3. Effect of isothermal crystallization temperatures, T_{ic}, on crystallization half-time,$t_{1/2}$, Avrami values, n and k, Nuclei density N, and average spherulite diameter D.

T_{ic} (°C)	n	K (min^{-n})	$t_{1/2}$ (min)
80	2.15	0.00654	8.75
100	2.3	0.017	6.04
105	2	0.042	4.4
110	2.2	0.035	3.9
115	2.2	0.035	3.9
120	2.2	0.012	6.7
130	2.5	0.00045	17.7

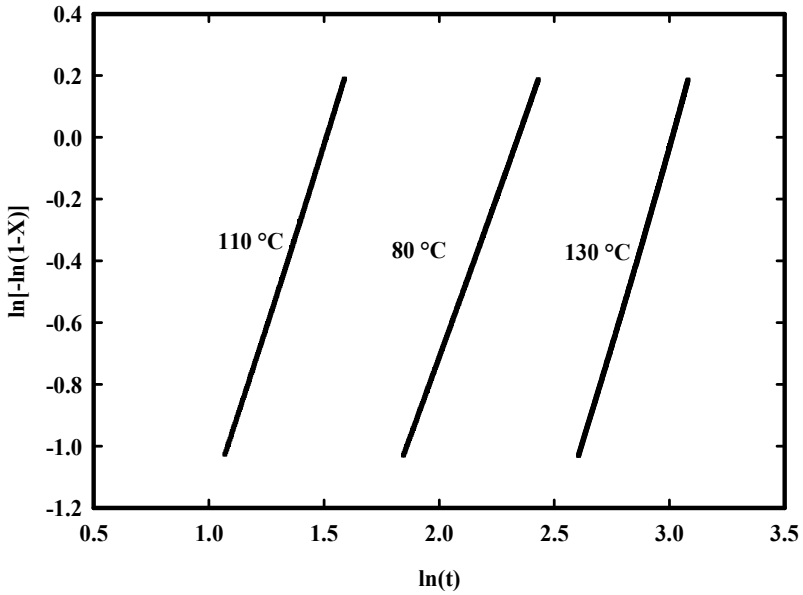

Figure 21. Plot of ln[−ln(1−X)] versus ln t under crystallization at 130 °C for PLA that was first crystallized at the indicated T_{ic} , next self-nucleated at T_s= 172 °C, and finally cooled back to 130.

Figure 22 illustrates the variation of the average spherulite diameter, D, and nuclei density, N, versus the isothermal crystallization temperatures, T_{ic}, again for PLA being crystallized at 130 °C**.** The nuclei density exhibited a maximum at 110°C that was about one order of magnitude higher than the value measured at 80°C. The spherulite size was relatively constant at almost 50 microns between 105 to 115 °C and then increased rapidly to 220 microns at 130 °C.

Moreover, another intriguing phenomenon was found for samples that were initially crystallized at T_{ic} of 100-120 °C. When the samples were heated up to 173 °C for self-nucleation and then cooled down to check their crystallization (c.f. segment **D** in the thermal protocol, **Figure 14**), two crystallization peaks upon cooling were found. This DSC cooling scan is shown in **Figure 23**. Clear crystallization peaks at around 100 °C and 120 °C were found. So far, this peculiar behavior had not been reported for pure PLA containing heterogeneous nucleating agents. It might suggest that the crystallization mechanism is affected by the nature of nuclei (i.e. self- nucleated vs heterogeneous nuclei). Additionally, when the self-nucleation temperature was minutely changed increases inside the self-seeding range from 173 °C to 173.8 °C, the 100 °C was favored over the 120 °C. These crystallization peaks could be associated to the formation of the α' and α crystalline phases and shows how a

minute change within self-nucleation temperature can result in significant changes in the mix of the α and α' phases.

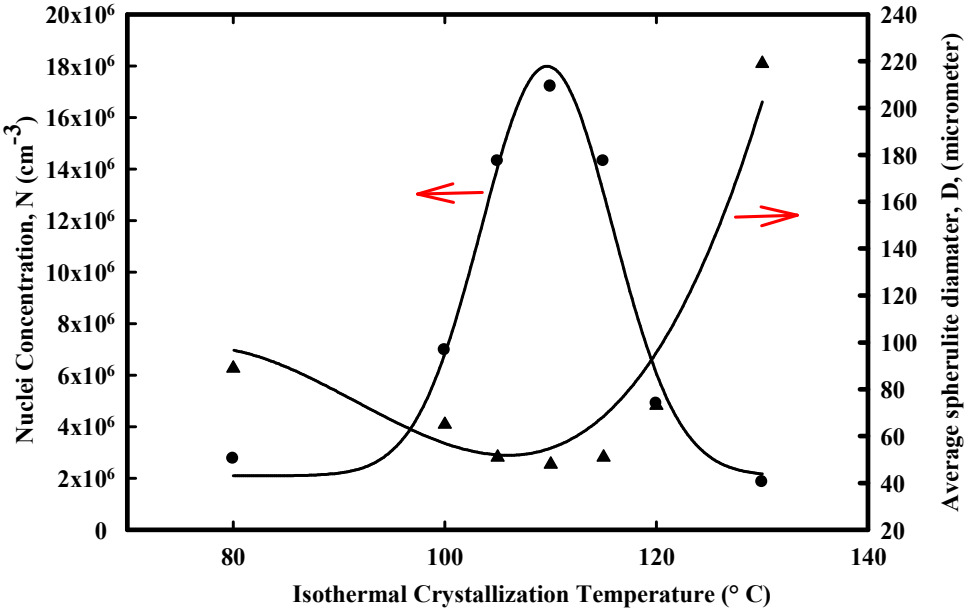

Figure 22. Variation of the Nuclei density (black circle) and the average spherulite size (black triangle) of self-nucleated samples at T_s= 172 °C versus T_{ic}.

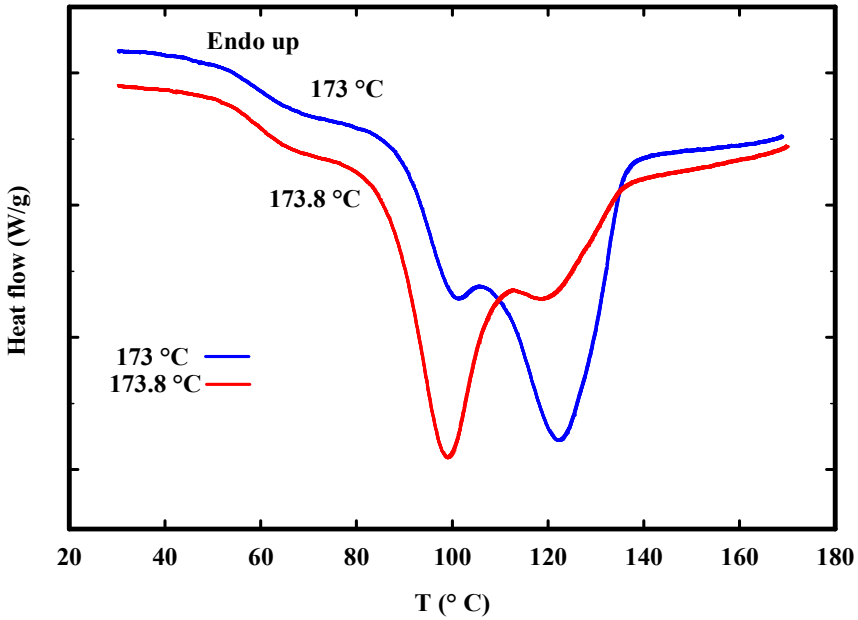

Figure 23. DSC cooling scans (Segment D in thermal protocol (c.f. Figure 13) after self-nucleation at the indicated temperatures, T_s, for the samples were previously isothermally crystallized at 115 °C in the isothermal crystallization step.

3.7 Microstructure analysis by WAXD

In order to characterize the structure during cooling when the double crystallization peaks were observed, XRD experiments were carried out. During cooling in the DSC chamber, samples were taken out of the chamber and immediately quenched in cold water right after the first and second crystallization peaks**Figure 24**(a, b) depicts the WAXD patterns of the samples after self-nucleation at 173 and 173.8°C after the first (23a) and second (23b) crystallization peaks, respectively. As can be seen in **Figure 24**a, after the first crystallization exotherm, both samples exhibited the characteristic diffraction peaks of the α phase. For the sample self-seeded at 173.8 °C, the level of crystallinity was smaller in agreement with the DSC results (c.f. **Figure 23**). **Figure 24**b displays similar results but for the samples quenched after the second crystallization peak. The microstructures of all samples were rather similar and differentiation between the α and α' phases was difficult. Therefore, thermal behavior of these mixed α and α' samples upon heating was investigated.

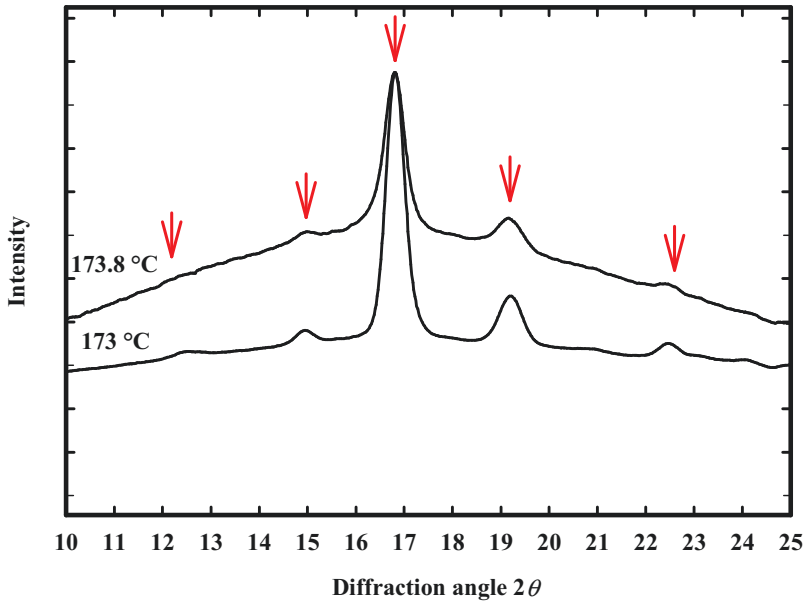

a)

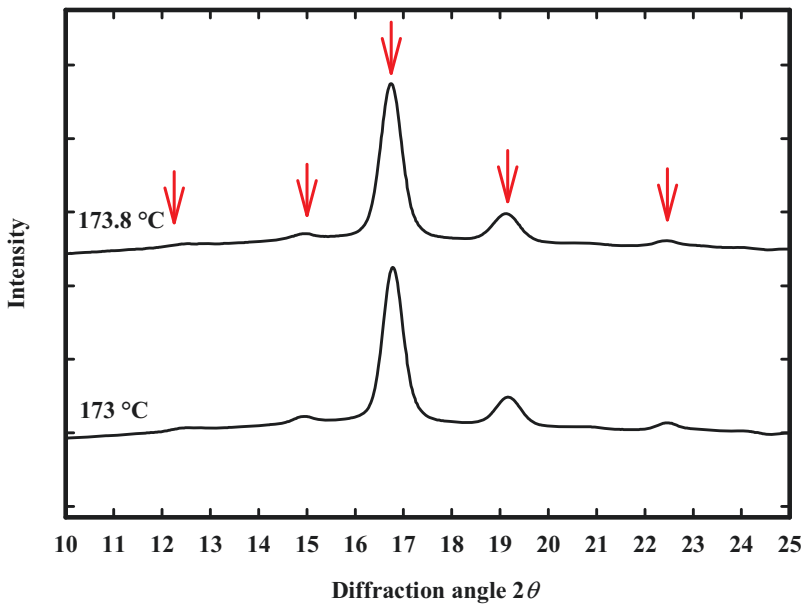

b)

Figure 24. XRD patterns of samples self-nucleated at indicated T_s , cooled at 2 °C/min and then quenched: a) after the first crystallization peak b) after the second crystallization peak . Note that the arrows indicates five characteristic peaks of the α phase.

3.8 DSC heating curves

In this section, we discuss about results obtained in segment E of the thermal protocol (c.f. **Figure 14**) for the samples self-nucleated at 173 and 173.8 °C. It was observed in **Figure 25**, upon heating at 2 °C/min, that the sample self-nucleated at 173.8 °C exhibited an exothermic peak prior to the single melting peak. As previously mentioned, this peak is associated to the α'-α solid state transition. It indicates that in this sample, the fraction of the α' phase was higher than that of α phase. Conversely, for the self-seeded sample at 173 °C, no exothermic peak was observed which implies that it possessed a higher α phase content. The later sample also exhibited a double- melting peak. The first melting peak, T_{mI}, is ascribed to melting of original α phase whereas the second melting peak T_{mII} belongs to α'crystals transformed to α phase through melt-recrystallization. It was also observed that for the sample self-nucleated at 173 °C, the height of T_{mI} was higher than that of T_{mII}. It implies that more α phase was present. Structural evolution of the melt and cold crystallization of PLA has been investigated using FTIR, WAXD and SAXS patterns by Wasanasuk *et al.* [195]. According to these

authors, crystallization from the melt state does not lead directly to the α or α' phases but instead to the formation of a mesomorphic phase prior to the formation of α or α' phases. Mesophase or mesomorphic phase is regarded as a state of matter between liquid and solid. In self-nucleation experiments, a self-nucleated polymer can be taken more or less as the mesophase. The conclusion that can be drawn from the double crystallization behavior is that the crystallization mechanism of self-nucleated PLA might differ from melt-crystallized sample. It could also explain why PLA exhibited two peculiar crystallization peaks upon subsequent cooling whereas this peculiarity has not been observed for samples directly cooled from the melt state.

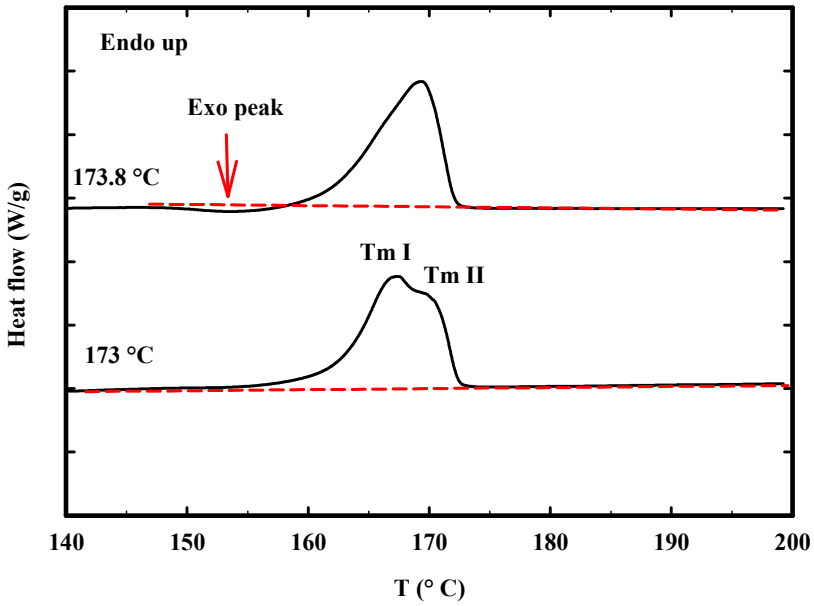

Figure 25. DSC heating scans at 2°C/min in Segment E of the thermal protocol (c.f. Figure 13) after cooling from the indicated self-nucleated temperatures, T_s.

3.9 Conclusions

A thermal procedure was designed to examine the self-nucleation behavior of PLA. Fully crystallized samples, previously isothermally crystallized between 80 to 130°C, were self-nucleated near the melting temperature. Based on the non-isothermal crystallization temperature obtained upon cooling, three temperature domains were distinguished. In Domains **I**, the crystalline structure is completely destroyed. In Domain **II**, crystallization is nucleated by remaining crystals and finally in Domain **III**, crystallization proceeds by

annealing of existing crystals. Domains **I**, **II** and **III** were found for PLA as Ts $>$ 174 °C, $170 \leq Ts \leq 174$ and Ts $<$ 174 °C respectively where T_s is the self-nucleation temperature. Effect of crystalline modification on the self-nucleation of PLA was also investigated. It was observed that samples where a mixture of α and α' crystal phases were generated, exhibited the highest nucleation efficiency compared to samples iso-thermally crystallized at temperatures leading to a single type of crystals. These samples also displayed the highest nuclei density and the smallest spherulite size. Furthermore, the samples crystallized between 100-120 °C, exhibited two crystallization temperatures, around 100 °C and 120 °C, upon cooling after self-nucleation. In addition, by slightly changing the temperature within the self-nucleation temperature range, a change of the proportion of each peak was observed. It is for the first time that two exothermic peaks are reported for PLA upon cooling. These peaks were ascribed to α and α' crystalline phases explaining the peculiar crystallization behavior of PLA.

CHAPTER 4 Effect of molecular weight on the nucleation efficiency of poly(lactic acid) crystalline phases

Avant-propos

Auteurs et affiliation:

Amirjalal Jalali: *Département de génie chimique et de génie biotechnologique, Faculté de génie, Université de Sherbrooke.*

Michel.A.Huneault: *Département de génie chimique et de génie biotechnologique, Faculté de génie, Université de Sherbrooke.*

Saïd Elkoun: *Département de génie mécanique, Faculté de génie, Université de Sherbrooke.*

Date de soumission: 30 septembre 2016

Revue: Journal of Materials Science

Titre français: Effet de la masse molaire sur l'efficacité de la nucléation des phases cristallines de poly (acide lactique)

Contribution au document: Présenter l'étude de l'auto-nucléation du PLA et effet des phases cristallines sur l'auto-nucléation compte tenu de l'effet des paramètres cinétiques et de la masse molaire.

Résumé français

Le PLA est bien connu pour souffrir d'un degré de cristallinité faible et d'une cinétique de cristallisation lente. Il présente deux phases cristallines légèrement différentes généralement appelées comme α et α'. Ce travail vise à étudier l'effet des phases cristallines sur la cinétique de cristallisation, au moyen d'une technique simple, appelée auto-nucléation. Pour accomplir cet objectif, le PLA a été cristallisé à différentes températures afin de produire des échantillons avec différentes proportions de cristaux α et α'. Les échantillons ont ensuite été chauffés

jusqu'à la plage de fusion partielle puis cristallisés à nouveau pour évaluer l'effet des cristaux résiduels de α et α' sur la cristallisation non-isotherme.Un double pic de cristallisation a été clairement observé démontrant des capacités de nucléation différentes pour les deux phases. L'analyse thermique, la diffraction des rayons X et la microscopie optique ont été combinées pour examiner l'effet de la vitesse de refroidissement et du temps de maintien à une température de fusion partielle donnée sur le rapport entre les deux pics de cristallisation observés et les formes cristallines induites. En outre, on a étudié l'effet de la masse molaire du PLA sur la cinétique de cristallisation et l'auto-nucléation du PLA. Les expériences d'auto-nucléation ont révélé que les PLA de faible et de haute masse molaire montraient températures maximals non-isotherme similaire, T_{cmax}, égale à 160 °C pour des échantillons préalablement isothermique cristallisés dans la plage de températures comprises entre 80-130 °C. Pour le PLA de masse molaire élevée, T_{cmax} était une fonction de la température de cristallisation isotherme préalable alors que pour le PLA de faible masse, T_{cmax} était indépendant de la température de cristallisation isotherme peu importe le ratio initial entre les phases. En se basant sur les enthalpies de cristallisation et de fusion, la proportion des phases α and α' a été quantifiée par déconvolution.

Mots-clés : cinétique de cristallisation, PLA, masse molaire.

4.1 Abstract

PLA is well known to exhibit a low degree of crystallinity and slow crystallization kinetics. It is also a polymorphic material with two slightly different crystalline phases named α and α'. This work aimed at investigating the effect of PLA crystalline phases on the kinetics of crystallization, by means of a simple, telling and expedient technique, known as self-nucleation. To achieve this purpose, PLA samples were first crystallized at various temperatures to change the mix in the α and α' phases. The samples were then partially melted by increasing the temperature near the melting temperature and then crystallized again upon cooling to examine the effect of the α and α' crystal remnants on the non-isothermal crystallization behavior. A double crystallization peak was clearly evidenced for self-nucleated PLA samples indicative of the different crystallization efficiency of the two PLA phases using a specific thermal protocol. Thermal analysis, XRD and optical microscopy were combined to examine the effect of cooling rate and holding time at a given partial melting temperature on the ratio between the two observed crystallization peaks. Moreover, effect of molecular weight of PLA on the crystallization kinetics and the self-nucleation of PLA was investigated. The self-nucleation experiments revealed that the low and high-molecular weight PLA exhibited the highest nonisothermal crystallization temperature, T_{cmax}, equal to 160 °C for the samples isothermally crystallized in the range of temperature between 80-130 °C. Although for the high-molecular weight PLA T_{cmax} was a function of the original crystalline phase as well as the phase transition mechanism, for the low-molecular weight PLA, it was constant regardless of what the initial crystalline phase was. Based on crystallization and melting enthalpies, the proportion of the α and α' phases was quantified using deconvolution analysis.

Keywords : Crystallization kinetics, PLA, molecular weight.

4.2 Introduction

Poly (lactic acid) or PLA is a biobased polyester that boasts a high modulus and strength, biodegradability and high transparency. Because of these characteristics, PLA stands out as an appropriate candidate in miscellaneous applications such as carrier materials for drug delivery, packaging films, non-woven fibers as well as bottles for fresh products such as milk and water [1,196,197]. However, PLA is well known for its slow crystallization kinetics as well as its low level of crystallinity and it is often used in its amorphous form. Crystallizing PLA, however, is an effective means to improve its thermal resistance and hydrolytic stability and therefore it is important to understand PLA's crystallization behavior. PLA crystallization is highly affected by the enantiomeric purity of the lactic acid monomer. The poly(L-lactic acid), PLLA, is the most common form where the presence of the *D*-lactide acid units play the role of crystal defects and must be minimized to enable full crystallization of PLA. PLA exhibits two crystalline phases, namely α and α', depending on the isothermal crystallization temperature. The α phase develops at temperatures above 120 °C while the α' forms at temperatures below 100 °C. A mixture of α and α' coexists in range of temperature between 100 and 120 °C [18,21,198]. In our previous contribution, a specific thermal procedure was designed to elucidate the nucleation efficiency of PLA's crystalline phases [199]. This was carried out by comparing crystallization temperatures upon cooling after partial melting of samples previously crystallized at various isothermal temperatures, $T_{iC,}$ ranging from 80 to130 °C. The self-nucleated samples crystallized at T_{iC} =110 °C exhibited the highest nuclei density and the smallest spherulite size upon cooling. It was also found that the highest crystallization temperature upon cooling, 160 °C, was achieved where a mixture of the α and α' was present. It should be mentioned that 160 °C is the highest reported crystallization temperature in literature for PLA. Additionally, it was observed that samples isothermally crystallized between 100 and 120 °C and then heated up to 173 °C, exhibited, upon cooling, two peculiar crystallization peaks at 100 and 120 °C, respectively. This phenomenon was ascribed to the formation of the α and α' crystalline phases as revealed by X-Ray diffraction and Differential Scanning Calorimetry. Furthermore, by slightly changing the temperature within the partial melting range, T_s, from 173 °C to 173.8 °C, a change of the proportion of each peak was observed.

A double exothermic peak has also been observed for Poly (ethylene terephthalate), PET, but in this case, it was observed upon heating during the so-called cold crystallization [200,201]. This double cold crystallization peak was ascribed to two different amorphous regions (i.e. interlamellar amorphous regions and complete amorphous regions between spherulites). Moreover, semi-crystalline polymers containing heterogeneous nucleating agents also display double crystallization peak upon cooling [70]. The peak at higher temperature is related to heterogeneous nucleation, whereas the one at lower temperature is attributed to homogenous nucleation. Biaxially oriented Polypropylene, BOPP, also reveals a double crystallization peak upon cooling [202,203]. Thermal analysis of the oriented samples revealed that the higher crystallization peak refers to the crystallization of the oriented structures. However, in the case of PLA, this double crystallization was observed for self-nucleated PLA, containing no heterogeneous nucleating agent, in quiescent conditions. In this paper, effect of molecular weight on the crystallization kinetics and on the self-nucleation of PLA was examined. Moreover, the effect of cooling rate and holding time at a given partial melting temperature on the ratio between the induced crystalline forms was investigated. Thermal analysis, XRD and optical microscopy were employed for this purpose.

4.3 Experimental

4.3.1 Materials

A commercial PLA, grade 4032D was used. This PLA is a semi-crystalline grade supplied by Nature Works that contains 2 % *D-LA*. It will be referred to as our higher molecular weight PLA. In order to obtain a lower molecular weight PLA with the same *D-LA* content, a hydrolysis reaction in an aqueous media was conducted. It is well recognized that degradation of PLA chains due to hydrolyze leads to decrease of the molecular weight [204,205]. Preparation of the low-molecular weight samples and the molecular weight distribution measurements are described by Rodriguez *et.al* [206]. The low and the high molecular weight PLA will be referred to as L-PLA and H-PLA, respectively Number-average molecular weight (M_n), weight-average molecular weight (M_w) and molecular polydispersity index of the original and the hydrolyzed PLA sample are presented in **Table 4**.

Table 4. Number-average molecular weight (M_n), weight-average molecular weight (M_w) and polydispersity index (PDI) of the low and high molecular weight PLA samples.

Sample code	M_n (kg/mol)	M_w (kg/mol)	PDI
H-PLA	98.1	164	1.68
L-PLA	19.4	35.5	1.83

4.3.2 Characterization

(1) Differential Scanning Calorimetry (DSC)

The thermal behavior of PLA was studied using a DSC Q2000 from TA Instruments. Temperature was calibrated before measurements using Indium as a standard material. Samples' weights were kept in the range of 10-15mg. The typical variation on crystallization and melting temperatures was assessed at ± 0.2 °C while the accuracy of crystallization and melting enthalpies was estimated at ± 1.5 J/g. For the non-isothermal crystallization, the samples were heated to 200 °C and kept in the molten state for 5 min to erase the prior thermal history. The samples were then cooled at cooling rates of 10 °C/min down to 0 °C. Subsequently, the samples were heated back to 200 °C at a rate of 10 °C/min.

For the isothermal crystallization, the sample was first completely melted by heating from 20 to 200 °C at 100 °C /min and maintaining at 200 °C for 5 min to erase the thermal history. Subsequently, it was rapidly cooled (100 °C/min) to the isothermal crystallization temperature and held there until completion of crystallization. Once crystallized, the samples were reheated to 200 °C at 2°C /min in order to measure the melting behavior.

For deconvolution of overlapping peaks, a non-linear fitting software (PeakFit v4) was employed. An asymmetric logistic peak function with standard least-squares minimization was used to find the optimum.

(2) Self-nucleation thermal protocol

Figure 26 presents the protocol used to investigate the self-nucleation of PLA [199]. The sample was first heated up to 200 °C and held for 5 minutes to erase thermal history. This is referred to as Segment **A** in the figure. The sample was then quenched to a determined annealing temperature, T_{iC}, and held for a period, ranging from 1 to 4 hours, until completion of crystallization. This is referred to as Segment **B** in **Figure 26**. Afterwards, the sample was

heated up to the self-seeding range under the heating rate of 2 °C/min. Once at the self-nucleation or, (self-seeding), the temperature was held constant for 5 minutes. This is referred to as Segment **C** in the figure and has been used to assess the partial melting endotherm. To measure the crystallization temperature of the self-nucleated sample, the sample was cooled down to room temperature at 2 °C/min to detect the crystallization exotherm in what is referred to as Segment **D** in the figure. Finally, to assess the melting behavior and type of the crystal phase, the sample was reheated again in Segment **E** at 2 °C/min up to complete melting.

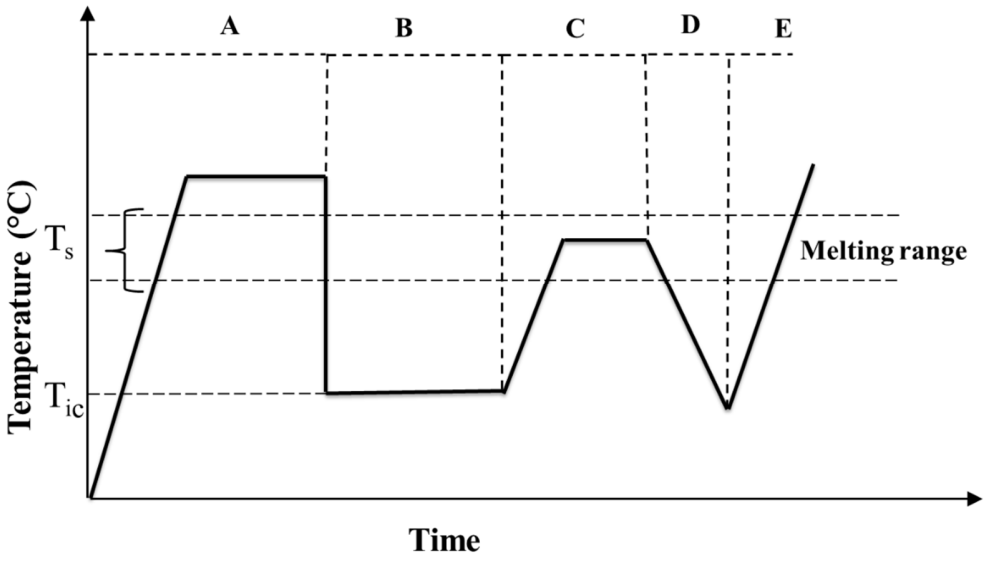

Figure 26. Schematic representation of temperature protocol for the self-nucleation of PLA.
A: Erasing thermal history, **B:** Isothermal crystallization, **C:** Partial melting , **D:** Cooling down, **E:** Final heating, T_{iC} **:** Isothermal crystallization temperature, T_S**:** Self-nucleation temperature

(3) Wide-Angle X-ray Diffraction analysis (WAXD)

Wide-angle X-ray Diffraction (WAXD) patterns were obtained by means of an X-ray diffractometer (D-8, Bruker) to detect the crystalline phases at different crystallization temperatures. The samples were exposed to an X-ray beam with an X-ray generators running at 40 kV and 40 mA. The copper Kα radiation (λ=1.542Å) was selected and the scanning was carried out at 0.03 °/s in the angular region (2θ) of 5-40°.

(4) Hot-Stage and Optical Microscopy

Isothermal crystallization experiments were performed by means of optical microscopy, Leica MDRX polarized, to observe the morphology of spherulites. The samples were melted between two glass slides at 200 °C and then were gently pressed to squeeze the melt into a very thin film. The prepared slides were moved onto a Mettler Toledo FP82HT hot-stage and kept at 200 °C for 3 min prior any thermal protocol.

4.4 Results and discussion

4.4.1 Effect of molecular weight on the microstructure and crystallization kinetics

Figure 27 presents the WAXD patterns of the crystalline structure for L-PLA and H-PLA, crystallized at 80, 115 and 130 °C. Both the low and high-molecular weight samples presented similar patterns. For samples crystallized at 80 °C, two characteristic XRD peaks of the α' phase were observed while for PLA crystallized above 120 °C, only the full XRD pattern expected for the α phase was present. For the samples crystallized at 115 °C, in the known range of mixed crystals formation (i.e. approximately between 100 and 120 °C) intermediate weak patterns with 15 and 22.5 ° peaks were observed.

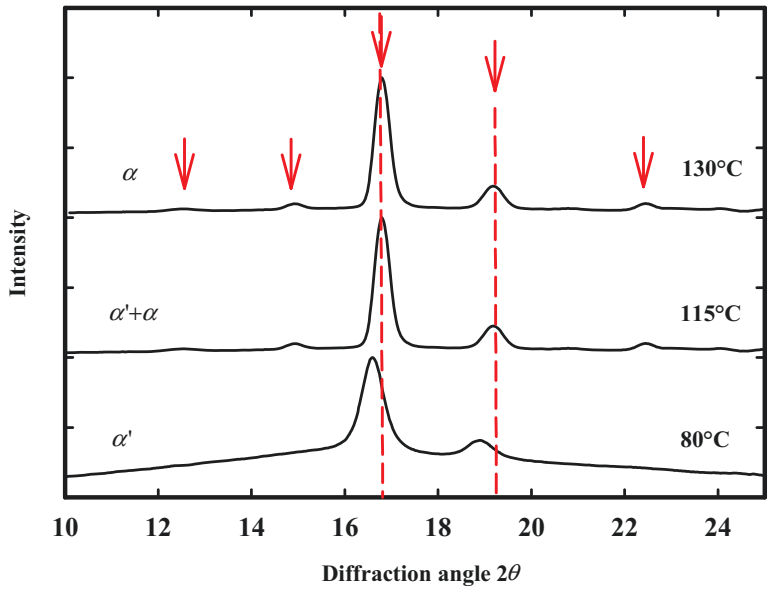

a)

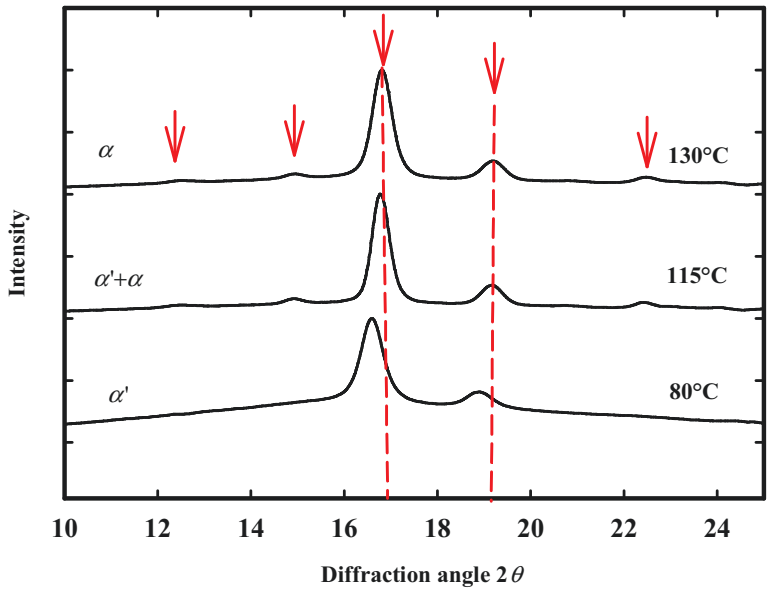

b)

Figure 27. XRD patterns of a) L-PLA b) H-PLA.

Non-isothermal characterization is worthwhile because most of polymer processing operations take place in the melt state and type, extent and dimension of the generated crystals upon cooling play a key role on the final properties of the material. The DSC thermograms obtained for the cooling rate at 10 °C/min (after first heating to erase thermal history) and second heating at 10 °C/min are shown in **Figure 28**. The cooling scans revealed no crystallization peak for both PLAs. This was expected for H-PLA based on our previous work [199] but it suggests that even for low molecular weight PLA crystallization upon cooling at 10 °C/min cannot take place. Compared to H-PLA, L-PLA revealed lower glass transition temperature (T_g) and melting temperature (T_m) and similar cold crystallization temperature (T_{cc}). **Table 5**. summarizes the obtained T_g, T_{cc} and T_m for L-PLA and H-PLA.

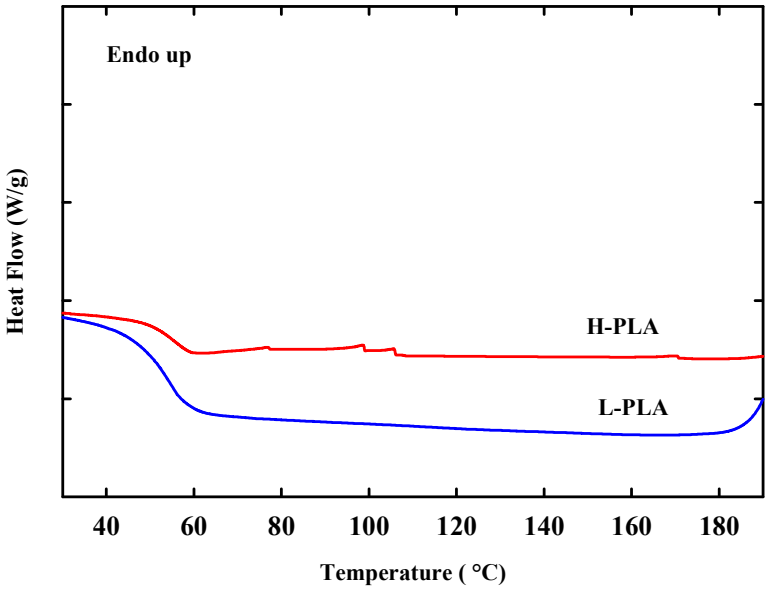

a)

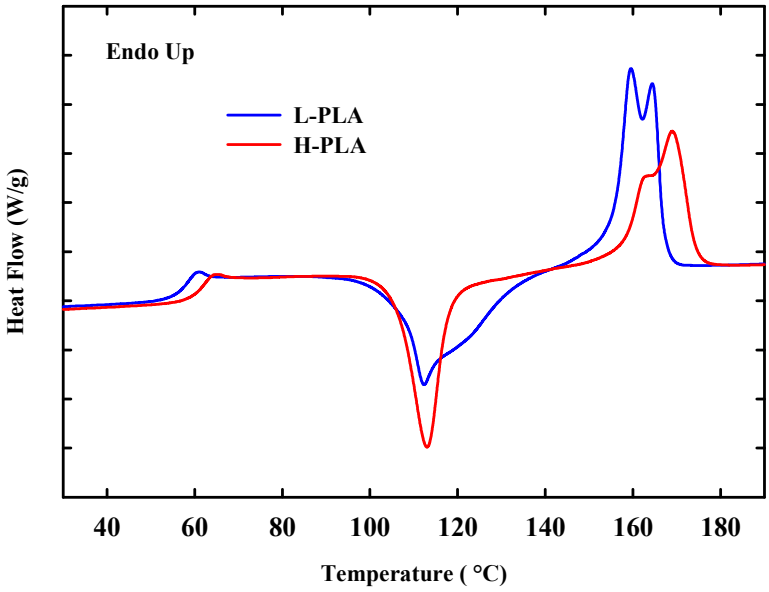

b)

Figure 28. a) cooling and b) second heating DSC scans at 10 °C/min for L-PLA and H-PLA.

Table 5. Characteristics of the low and high- molecular weight PLAs.

Sample	T_g (°C)	T_{cc} (°C)	T_m(°C)
L-PLA	58	112	164
H-PLA	62.5	113	170

Isothermal crystallization experiments can be used to determine the crystallization kinetics at a selected crystallization temperature. A convenient way to evaluate the effect of temperature on the crystallization rate is to plot the crystallization half-time, $t_{1/2}$, as a function of the isothermal crystallization temperature as depicted in **Figure 29**. The crystallization half-time is defined as the time required reaching half of the maximum achievable crystallinity. H-PLA displayed a minimum crystallization half-time of 20 minutes at 110 °C. On the other hand, L-PLA showed a faster crystallization with a minimum crystallization half-time of 6 minutes at 110 °C. The curve of the crystallization half-time versus crystallization temperature is typically continuous for most semi crystalline polymers ; however, for L-PLA and H-PLA a discontinuity was observed in the range of temperature between 100 and120 °C. There is no consensus on underlying causes of this peculiarity but it has been ascribed to crystallization regime change [11] and to the polymorphic nature of PLA [17,21,22].

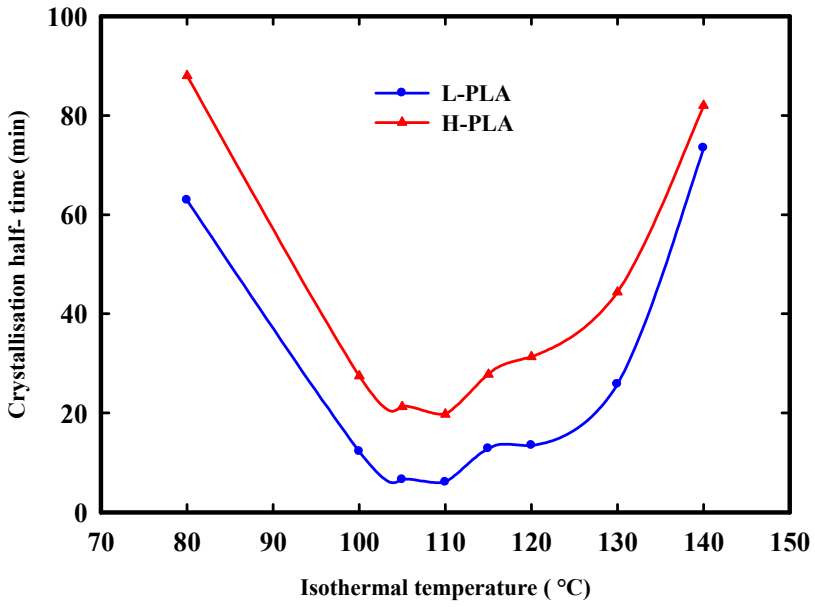

Figure 29. Crystallization half-time vs isothermal crystallization temperature for L-PLA and H-PLA.

Isothermal crystallization kinetics generally depends on the nucleation rate and spherulite growth rate. One way to pinpoint the direct effect of temperature on spherulite growth rate is to directly record the spherulite growth rate under an optical microscope. **Figure 30** presents the spherulite growth rate, G, as a function of the isothermal crystallization temperature between 120-135 °C. The low-molecular weight PLA exhibited a faster spherulite growth rate, with the maximum rate of 20 μm/min at 125 °C, whereas a slower spherulite growth rate with the maximum rate of 9 μm/min at 125 °C was observed for the high-molecular weight PLA. The presented crystallization half-time data along with the results of spherulite growth rate indicated that decreasing the molecular weight of PLA significantly influenced crystallization kinetics, which was anticipated. Compared to L-PLA, H-PLA had low chain mobility, due to longer chains, which made it difficult for the polymer chains to move into crystalline structures. It is, therefore, expected that with increasing the PLA molecular weight the overall crystallization becomes slower.

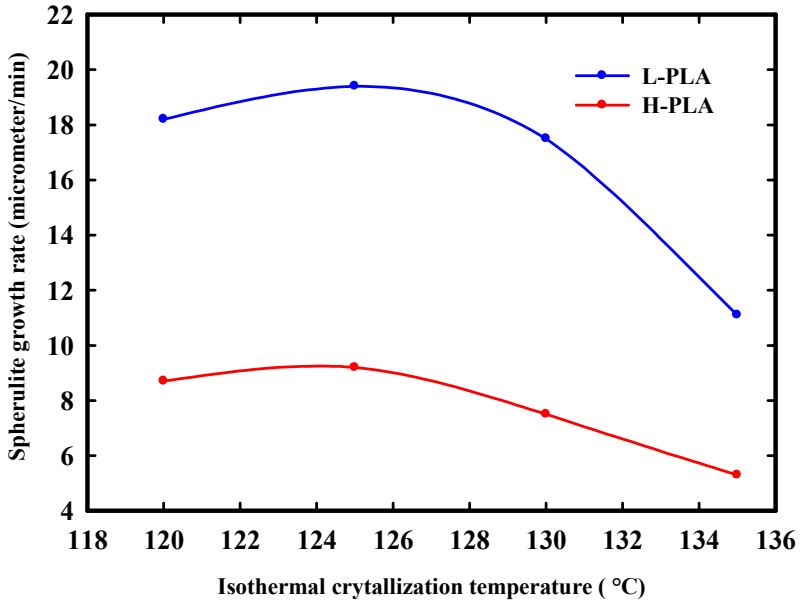

Figure 30. Spherulite growth rate, G, as a function of isothermal crystallization temperature for L-PLA and H-PLA.

4.4.2 Effect of molecular weight on the self-nucleation of PLA

In this section, the focus will be brought on the self-nucleation experiments described in the experimental section. **Figure 31** presents the DSC heating scans at 2 °C/ min for L-PLA and H-PLA isothermally crystallized at T_{iC} between 80 and140 °C. This corresponds to segment C

in **Figure 26**. At the higher crystallization temperature (130 140 °C), the low and high molecular weight PLA exhibited a single melting peak. At intermediate crystallization temperatures, two peaks appeared with the lower temperature peak becoming predominant as T_{iC} was increased. It is only at low T_{iC} that the behavior of L and H-PLA differed radically. For high-molecular weight PLA crystallized at T_{iC} of 80 and 100 °C, an exothermic peak was observed prior the main melting peak. In contrast, for the low molecular weight samples, an endothermic peak was observed prior the main melting peak. The explanation for this behavior can be interpreted in view of formation and transition between the α and α' phases. At high crystallization temperature, the α phase formation is favored and this results in a single α crystal population and correspondingly to the single melting peak. At intermediate crystallization temperature, namely in the 100-120 °C range, a mixture of the α and α' are formed. The melting curve is indicative of the relative proportion since the α crystals will melt first and the higher melting peak is associated to the melt-recrystallization of the α' phase. At T_{iC} such as 80 and 100 °C, the α' phase formation is favored. For the high molecular weight PLA crystallized at low temperature, the exothermic peak seems to indicate that an α'-α solid phase transition takes place prior the main melting peak. For low molecular weight PLA in contrast, the same melt-recrystallization mechanism described for intermediate T_{iC} continues to hold, leading still to the double melting peaks. Using DSC and time resolved FTIR spectroscopy, Pan et al. found that the melting mechanism of PLA changed drastically with molecular weight at T_{ic} below 100 °C [26]. At $T_{ic} < 100$ °C, both high and low-molecular weight samples share the α' crystalline phase. According to Pan et.al [26]; however, due to higher chain mobility and lower undercooling, ($T^{\circ}_{m} - T$), some amounts of the α' crystals of the L-PLA melt down directly and the rest of them transform partially into the α phase. A similar melting behavior was reported for the β-form crystals of isotactic polypropylene, iPP [207]. It was revealed that before the final melting, the temporary melting of the β crystals and recrystallization into the α phase took place simultaneously.

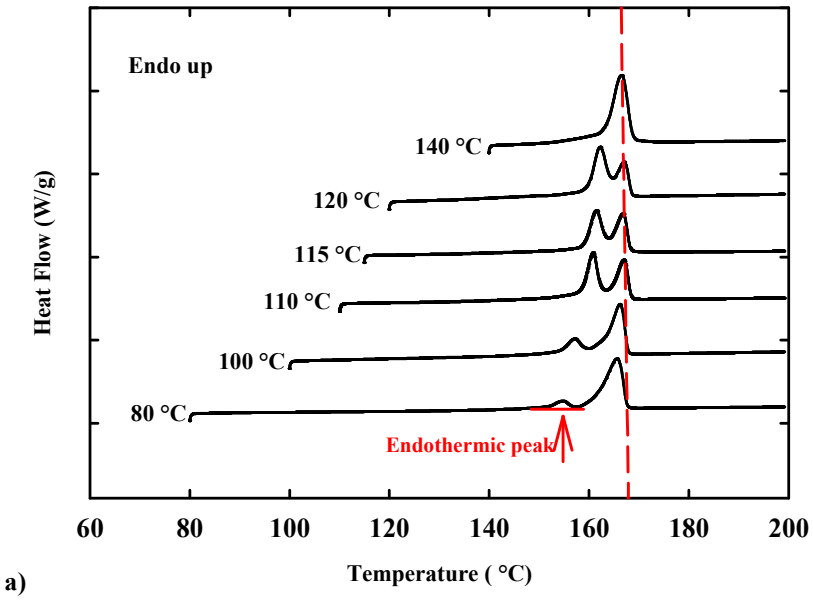

a)

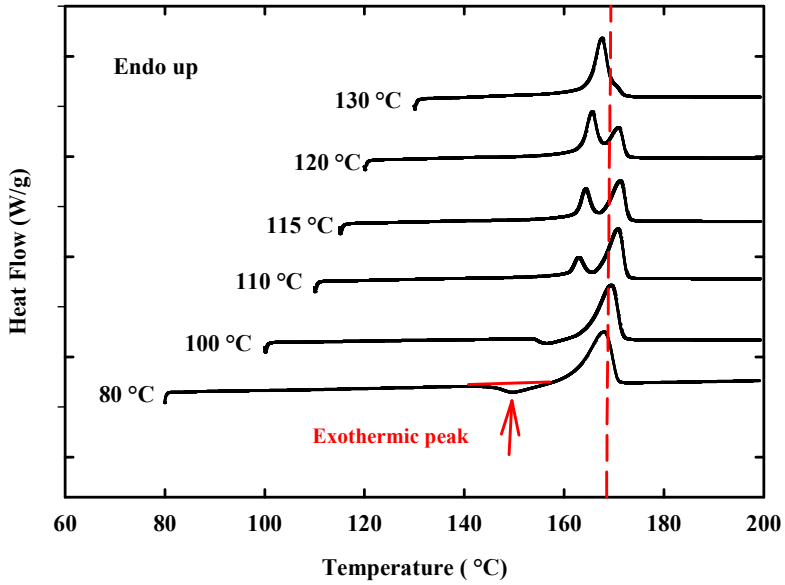

b)

Figure 31. DSC heating curves of a) L-PLA b) H-PLA to 200 °C after isothermal crystallization (segment C in thermal protocol of Figure 1) at the indicated different isothermal crystallization temperatures. Dashed line represents the T_s.

An attempt was made to understand the relationship between the role of PLA crystalline phases and their nucleation efficiency. **Figure 32** illustrates the variation of the maximum obtained crystallization peak temperature upon cooling (after self-nucleation),T_C^{max}, as a function of the prior isothermal crystallization temperature, TiC. The T_C^{max} is obtained upon cooling in segment D of the thermal protocol illustrated in Figure 26. The maximum T_C^{max} was 160 °C for both low and high molecular weight PLA. Surprisingly it was independent of the prior crystallization temperature for L-PLA while for H-PLA in contrast T_C^{max} exhibited a clear maximum centered at TiC of 110 °C. To the authors' knowledge, 160 °C is the highest reported non-isothermal crystallization temperature for PLA. The crystallization occurs at an undercooling of undercooling of around 4 °C for L-PLA and of around 10 °C for H-PLA. Hence, it might imply that the lower molecular weight sample displayed higher nucleation efficiency, compared to the higher molecular weight. The lower T_C^{max} at Tic < 100 °C for H-PLA indicates that crystals formed through the solid α'-α phase transition might not be as efficient nucleants as the one formed by the melt-recrystallization mechanism. As previously stated when the molecular weight decreases, apart from the solid phase transition, an additional mechanism, which was the direct melting of the α'crystals, played an important role. In other words, the direct melting of some α'crystals remarkably promoted the nucleation efficiency of L-PLA. In the range of temperature between 100-120 °C, the nucleation efficiency of L-PLA and H-PLA were rather comparable. Despite the fact that at Tic > 120 °C, for both L-PLA and H-PLA the direct melting of the α phase took place, L-PLA's nucleation efficiency seemingly exceeded that of H-PLA. Possibly, thanks to its lower undercooling and chain mobility, the L-PLA α crystals exhibited higher efficiency.

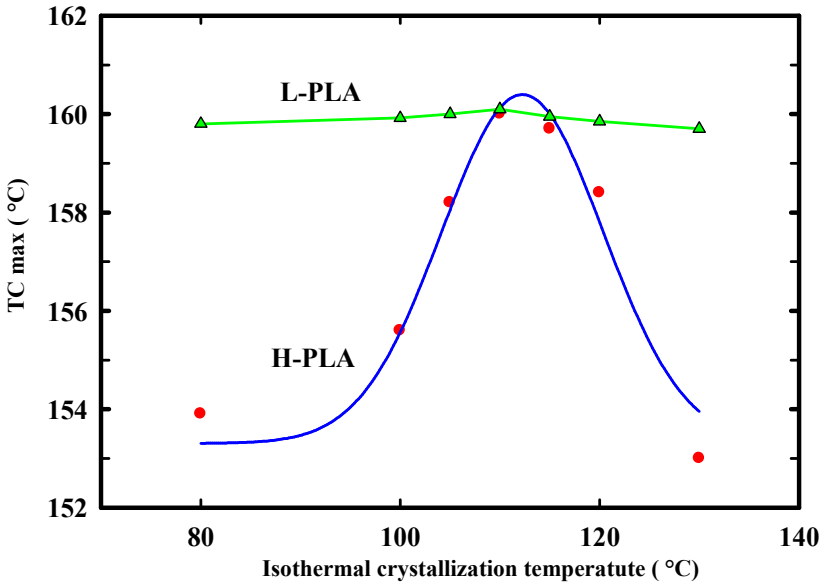

Figure 32. Variation of T_{cmax} as a function of isothermal crystallization temperature for L-PLA (triangle) and H-PLA (circle).

4.4.3 Double crystallization peak

In this section, the effect of cooling rate and holding time at a given partial melting temperature on the self-nucleation of PLA will be presented. This would enhance our understanding how the cooling rate and the time spent at the partial melting range can influence on the nucleation of PLA regarding the role of the α and α'phases. **Figure 33** depicts the cooling curves after partial melting at different indicated partial melting temperatures, T_S. This corresponds to segment D in **Figure 26**. All samples were previously isothermally crystallized at T_{iC}=115 °C and thus have a similar thermal history except for the partial melting temperature. At 2 °C/min, a double crystallization peak upon cooling around 120 and 100 °C was observed marked by T_{CI} and T_{CII} on the figure. In our previous work, these peaks were respectively attributed to the α and α' phases by means of XRD and DSC analysis [199]. In this work, we further investigate the role of a very slight change of partial melting temperature from 173 to 174 °C. At 173 °C, the higher temperature peak was stronger. At 173.5 °C, the peaks shared virtually the same size and at 174 °C, almost all crystallization took place around 100 °C along with only a very weak peak at 120 °C. This result is quite striking considering the minute changes in partial melting temperature. It can be interpreted as a sign of rapid transition in the 173-174 °C range from a mixture of α and α' phases gradually to an

α' rich phase. With reducing the cooling rate to 1 °C/min, the T_{CI} and T_{CII} shifted to higher temperatures, near 135 °C and 110 °C, respectively. At lower cooling rates, there is more time for the self-nucleated sample to crystallize. Accordingly, the observed crystallization peaks shifted to higher temperatures. By increasing the self-nucleation temperature, T_S, at the lower cooling rate, the same shift in peak area from the high to the low temperature peak was observed. The cooling curves for L-PLA were quite similar with the dual peak behavior and peak area shift with increasing T_S. This suggests that both the low and high-molecular weight samples comprised the α and α' phases upon cooling after self-nucleation.

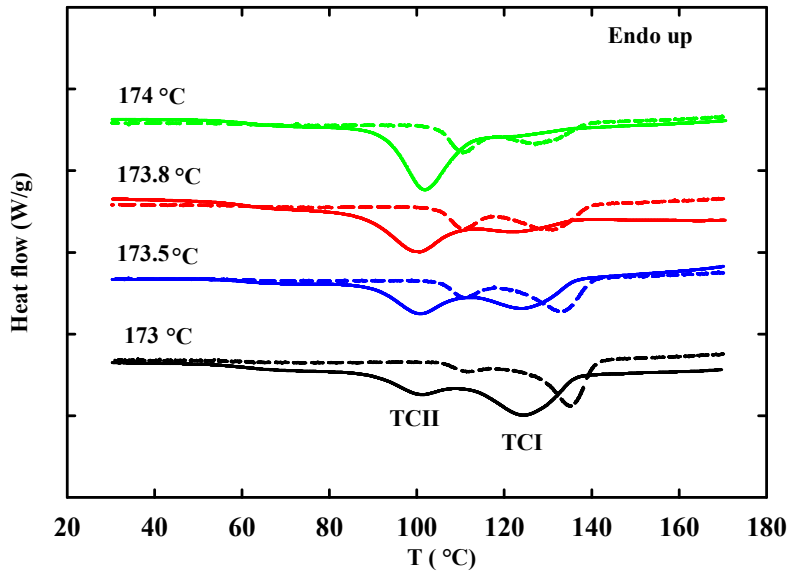

a)

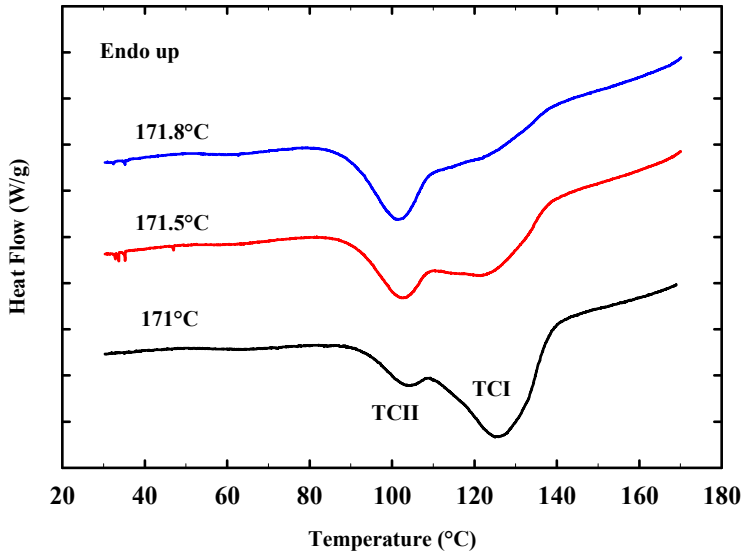

b)

Figure 33. DSC cooling scans after self-nucleation at different T_s for samples previously isothermally crystallized at 115 °C a) H-PLA at 1(dashed line) and 2 °C/min (solid line) for b) L-PLA at 2 °C/min. (Segment D in Figure 26).

4.4.4 Morphology of the self-nucleated

The remarkable effect of a 1 °C change in the partial melting range, T_S, discussed above led to the investigation of the spherulitic morphology by optical microscopy. **Figure 34** compared the morphology of H-PLA samples partially melted at 173 and 173.8 °C. This small difference in thermal history led to an important morphology change. The spherulites for T_s =173 °C were rather large, while the spherulites for T_s =173.8 °C were generally much smaller with only a few large spherulites dispersed among the small ones. As the self-nucleated sample is cooled down, at firs α crystals are nucleated and grow into large spherulites. At lower temperature, a high density of α'crystals are nucleated leading to smaller spherulites. As previously mentioned, the α phase develops at high temperatures, whereas the α' forms at low temperatures. Due to high thermal agitation at the elevated temperatures, the rate of nucleation is expected to be lower and thus larger spherulites can form. [19,208]. The optical micrographs therefore further support the α and α' lead to selective crystallization at different temperatures. At T_s=173 °C, the sample comprise a higher α fraction leading to more crystallization at the higher crystallization temperature while the opposite is true at T_s =173.8 °C.

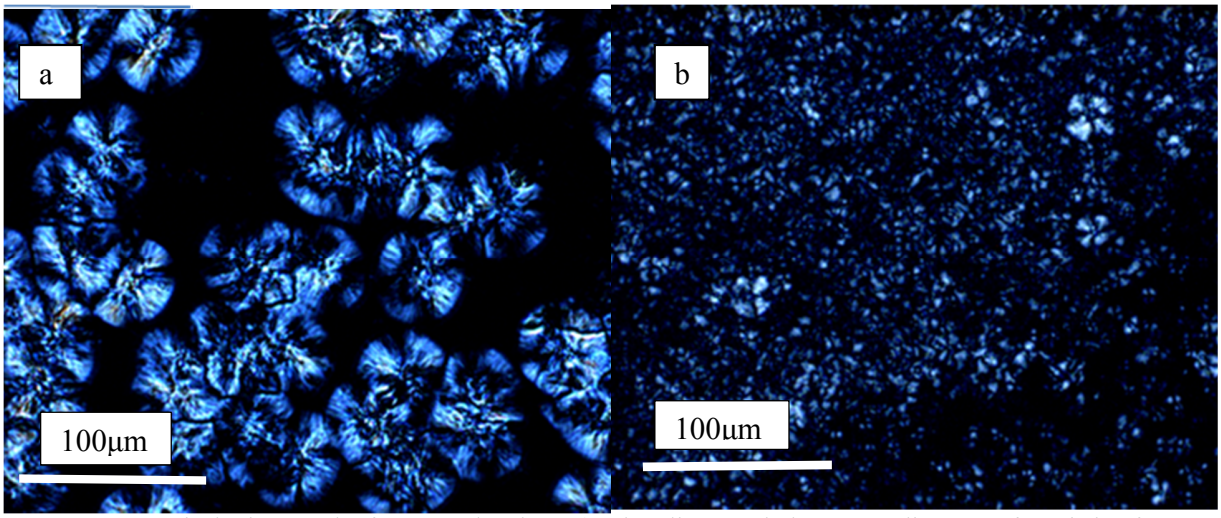

Figure 34. Optical micrograph of H-PLA showing : a) spherulite morphology at cooling rate of 2°C/min after holding for 5 minutes at T_s =173 °C b) spherulite morphology at cooling rate of 2°C/min after holding for 5 minutes at T_s =173.8 °C.

4.4.5 Final heating curves

The final heating in the self-nucleation thermal protocol (segment E in **Figure 26**) can be used to further probe the low temperature transition between two crystalline phases. **Figure 35** displays these final heating curves. The self-nucleated H-PLA at 173.8 °C exhibited a cold-crystallization exotherm around 93 °C (**Figure 35a**). The size of the exotherm increased as T_s was increased from 173 to 173.8 °C. This exothermic peak can be ascribed to reorganization of imperfect crystals [31]. This result should be put in perspective with the cooling results of **Figure 33**. The sample partially melted at 173.8 °C exhibited a much larger low-temperature crystallization peak and thus has formed a larger amount of the α' phase which is prone to reorganize upon re-heating. The same material and the one partially melted at 174 °C exhibited a second thermal exothermal peak right before the main melting (**Figure 35b**). This exothermic peak indicated that the α'-α phase transition took place [23,181]. The one partially melted at lower temperatures did not show any exothermic peak prior the melting peak but ended up showing the dual peak signature marked by the T_{mI} and T_{mII} lables. These samples had exhibited stronger high-temperature crystallization peak upon cooling thus leading to greater α phase fraction. From the results, we can draw in this case no solid state reorganization took place at low temperature. However, when reaching the melting, the melt-recrystallization phenomenon occurred. Using this interpretation, the first melting endotherm could be ascribed to melting of the original α crystalline phase whereas T_{mII} could be attributed

to melting of the α' phase transferred to the α phase through the melt-recrystallization mechanism. Again, it was also observed that the slight change in the partial melting temperature led to a change in the ratio between peaks.

For L-PLA a double melting peak was observed for the samples partially melted at 171, 171.5 and 171.8 °C, which are marked by T_{mI} and T_{mII} in **Figure 35c** A similar interpretation can be given for the two peaks and this showed that the melt-recrystallization mechanism could be applicable for the low molecular weight material as well.

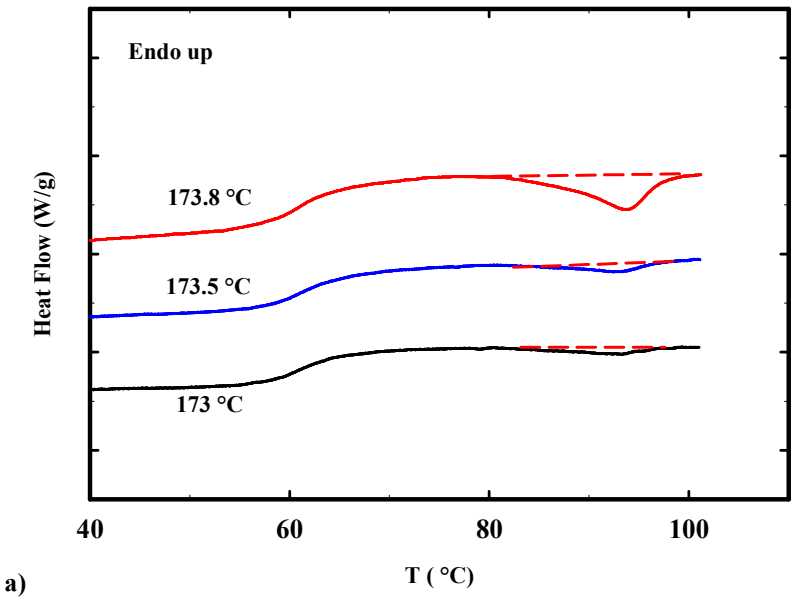

a)

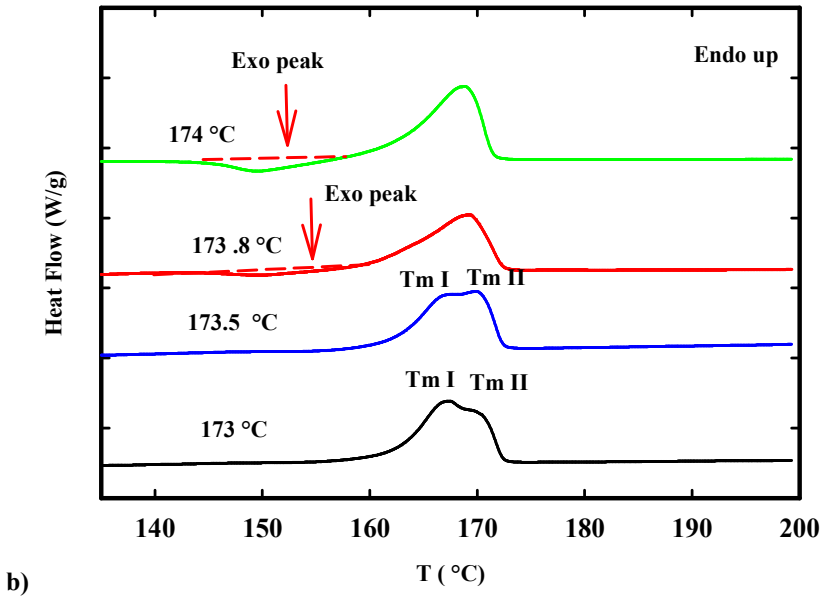

b)

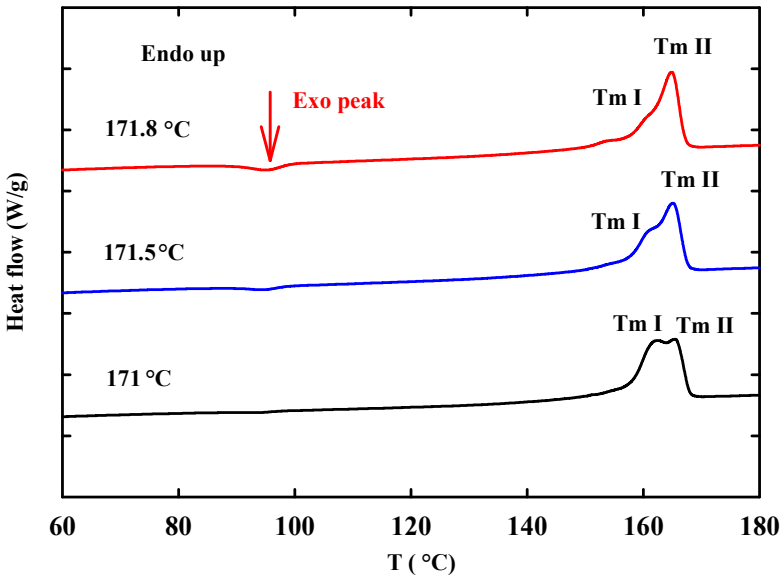

c)

Figure 35. Final DSC heating scans at 2 °C/min after cooling from different T_S: a) HPLA between 40 and 100 °C b) HPLA between 140 and 180 °C and c) L-PLA.

4.4.6 Quantification of the α and α' phase fractions

In order to quantify the fraction of the α and α' phases, deconvolution of the crystallization (**Figure 33**) and melting peaks (**Figure 35.b**) was carried out. **Table 6** summarizes the crystallization and melting enthalpies as well as the proportion of the α' phase for the self-nucleated H-PLA samples at different T_S. The proportion of the α' phase calculated on the basis of the crystallization enthalpies increased from 29 to 54% when T_S was raised from 173 to 173.8 °C. It is noteworthy that the sum of the crystallization enthalpies for the two peaks remained constant, around 38J/g, for the self-nucleated sample at 173 and 173.5 °C. However, it dropped to 28 J/g for the sample partially melted at 173.8°C. It can be argued that the sample self-nucleated at 173.8 °C is closer to the temperature at which complete crystal melt down occurs. Interestingly, the proportion of the α' phase derived from crystallization and melting peaks are in close agreement. Based on the melting enthalpies, the α' fraction increased from 25 to 41% for T_s increasing from 173 to 173.5 °C. For the higher T_S, only one melting peak was observed and therefore the α' fraction could not be determined.

Table 6. Crystallization and melting enthalpies as well as the proportion of α' phase according to the indicated T_s.

T_S (°C)	Crystallization			Melting		
	$\Delta H_{c\alpha}$ (J/g)	$\Delta H_{c\alpha'}$ (J/g)	α' phase (%)	$\Delta H_{m\alpha}$ (J/g)	$\Delta H_{m\alpha'}$ (J/g)	α' phase (%)
173	27	11	29	14	14.6	25
173.5	23.6	14.3	38	10.7	7.5	41
173.8	13	15.5	54	-	-	-

4.4.7 Effect of holding time at the partial melting range

Near the melting temperature of a semi-crystalline polymer, there are some crystal fragments that can act as potential nucleating agent upon cooling. These crystal fragments are not thermodynamically stable and with the spent time in the partial melting range, their concentration will change [151,186,199]. To ascertain how the holding time in the partial melting zone influences the self-nucleation efficiency, the effect of holding time was examined. **Figure 36** presents the effect of holding time at the partial melting range for H-PLA isothermally crystallized at 110 °C and then partially melted at 173 °C. Without a holding delay (t=0) at the partial melting range, the sample revealed a significant peak above

120 °C and a small one nearby 100 °C, respectively. However, when the sample was held at T_s for longer times, for example: 5, 10, 20 and 60 minutes, the peak ratio remained almost unchanged. It might be concluded that the α -α' phase transition occurring during the partial melting range step takes place rapidly, within around one minute. From a thermodynamical point of view, the condition for the formation of the stable α phase is expected with the holding time. Surprisingly, the opposite took place and the less stable α' phase was favored. It could be argued that the formation of the α and α' is kinetically controlled. It should be mentioned that Lorenzo *et al.* [209] investigated the effect of annealing time on the self-nucleation behavior of semicrystalline polymers, in particular PP. It was reported that crystallization temperature shifted to lower temperatures as annealing time, in the partial melting range, increased at a given T_S. However, in our case, no significant shift in the double crystallization peaks was observed.

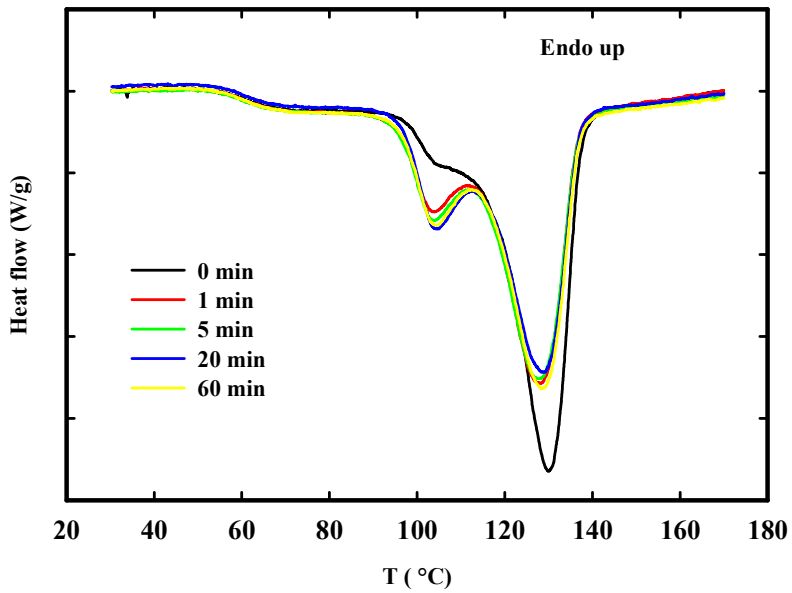

Figure 36. DSC cooling curves at 2 ° C/min for the self-nucleated H-PLA samples at 173 °C at different holding times.

4.5 Conclusions

Effect of molecular weight of PLA on the crystallization kinetics and on the self-nucleation of PLA was investigated. Although the low- and high-molecular weight PLA shared comparable microstructure, isothermal crystallization characterization showed that the low-molecular weight PLA exhibited faster crystallization kinetics and spherulite growth rate. In the self-

nucleation experiments, it was found that the both low and high-molecular weight PLA presented the similar maximum crystallization temperature, T_{cmax}, which was equal to 160 °C. This is the highest reported nonisothermal crystallization temperature for PLA. For the high-molecular weight PLA, T_{cmax} was a dependent function of the initial crystalline phase; however, for the low-molecular weight PLA, it was constant and independent of the original crystalline form. It was also found that the molecular weight significantly influenced the transformation of the PLA's crystalline phases upon heating. For the high-molecular weight PLA it was found that the crystals formed through the solid α'-α phase transition were not as efficient nucleants as the one formed by the melt-recrystallization mechanism. However, for the low-molecular weight PLA, a combination of the direct melting crystals and the solid phase transition of the α' led to a higher efficiency. Moreover, both the low and high-molecular weight PLA exhibited a double crystallization peak indicative of the presence of the α and α' phases. Deconvolution analysis revealed that the α'phase fraction was increased as the partial melting temperature was increased. In addition, it was shown that after heating the high-molecular weight PLA to the partial melting range, the formation of the α' phase took place rapidly, within around one minute.

CHAPTER 5 Effect of molecular weight on the shear-induced crystallization of poly(lactic acid)

Avant-propos

Auteurs et affiliation:

Amirjalal Jalali: *Département de génie chimique et de génie biotechnologique, Faculté de génie, Université de Sherbrooke.*

Shant Shahbikian*: Département de génie chimique et de génie biotechnologique, Faculté de génie, Université de Sherbrooke*

Michel .A. Huneault: *Département de génie chimique et de génie biotechnologique, Faculté de génie, Université de Sherbrooke.*

Saïd Elkoun: *Département de génie mécanique, Faculté de génie, Université de Sherbrooke.*

Date de soumission: 23 septembre 2016

Revue: Polymer

Titre français: Effet de la masse molaire sur la cristallisation induite par cisaillement du poly (acide lactique)

Contribution au document : étude de la cristallisation induite par cisaillement du PLA et de l'effet de la masse molaire sur celle-ci.

Résumé français : L'étude de l'effet de contraintes de cisaillement sur l'écoulement et la cristallisation du PLA a été réalisée par des mesures rhéologiques sur des matériaux de trois différentes masses molaires. Afin d'étudier l'effet d'un faible écoulement, des échantillons de PLA ont été chauffés jusqu'à 190 °C pour effacer l'histoire thermique avant d'être refroidis rapidement jusqu'à 130 °C. Enfin, ils ont été soumis aux différentes vitesses de cisaillement comprises entre 0.01 et 0.1 s^{-1}. L'effet du taux de cisaillement et de la déformation totale sur la cristallisation du PLA a été examiné. Il a été observé que la masse molaire a un grand

impact sur la cristallisation induite par cisaillement du PLA. Il a également été mis en évidence que des niveaux de déformation plus élevés sont nécessaires pour amorcer la cristallisation lorsque le taux de déformation a augmenté. L'effet d'un pre-cisaillement fort sur la cinétique de cristallisation du PLA a également été examiné. À cet effet, des échantillons des masses molaires différentes ont été pré-cisaillés puis cristallisés à la même température pendant une période déterminée. L'évolution de la cristallisation a été contrôlée par la variation du module de conservation (G ') en fonction du temps (t). Le comportement thermique et la microstructure des échantillons cisaillés ont été étudiés par calorimétrie différentielle à balayage (DSC) et par diffraction des rayons X aux grands angles (WAXD).

Mots-clés: cristallisation induite par cisaillement, poly(acide lactique), cristallisation, rhéologie.

5.1 Abstract

Effect of weak and strong shear flow on the crystallization of poly(lactic acid), PLA, with different molecular weights, (M_w), was investigated by rheological measurements. To study the effect of the weak flow, PLA samples were heated up to 190 °C to erase thermal history, then rapidly cooled down to 130 °C and finally subjected to a shear flow with shear rates ranging between 0.01 to 0.1 s^{-1}. Effect of shear rate and strain on the shear-induced crystallization of PLA was examined. A remarkable effect of M_w on the shear-induced crystallization of PLA was observed. It was also found that higher levels of strain were required to initiate crystallization with increasing deformation rates. The effect of the strong shear flow on the crystallization kinetics of PLA was also examined. For this, different molecular weight samples were pre-sheared and then crystallized at the same temperature for a specific period of time. Evolution of crystallization was monitored by the variation of storage modulus, G', versus time, t. Thermal behavior and the microstructure of the sheared samples were studied by Differential Scanning Calorimetry, DSC, and Wide-Angle X-ray Diffraction, WAXD**.**

Key words: shear-induced crystallization, poly(lactic acid), crystallization, rheology.

5.2 Introduction

With the increasing interest for biobased polymers in medical and engineering applications, research concerning poly(lactic acid), PLA, has drastically increased over the last decade. PLA is a high modulus and high tensile strength material but its use is limited to low temperature applications unless it can be fully crystallized. For this reason, PLA crystallization has been the focus of numerous investigations and it is well understood that PLA exhibits slow crystallization kinetics. Despite the fact that an extensive body of literature exists on quiescent crystallization kinetics of PLA [1,70,196,199,210], little attention has been paid to its flow-induced crystallization.

Practically all thermoplastic products are fabricated by melt processing techniques (e.g. injection molding, extrusion, and film blowing). These operations are performed in dynamic conditions and crystallization of polymer melts can be noticeably accelerated by flow. It is assumed that shear flow can orient polymer chains in the melt, which significantly improves the crystallization kinetics. Orientation of polymer chains reduces the entropy and therefore increases the melting temperature [211]. Furthermore, the morphology of crystalline structures formed in dynamic conditions differs from the one formed under quiescent ones. In the quiescent conditions, polymer crystals tend to form spherulites while under shear flow row-like structures, so-called “shish-kebabs” are developed [212]. Shish consists of long central fiber core that is surrounded by lamellar crystalline structure, kebabs, periodically attached along it.

In order to study the effect of temperature and shear flow on the crystallization of semi-crystalline polymers, different techniques have been employed including shearing under optical microscope [213,214] , fiber pull-out [215,216], rheo-X-ray [217,218], rheo-Raman [219], and rotational rheometry [220,221,222,223]. Compared to the other techniques, rheometry is not only convenient and fast but also can provide an online monitoring of the rheological properties (e.g. viscosity and storage modulus) of the system during the crystallization process [224].

A great deal of experimental and modeling investigations has been dedicated to flow-induced crystallization of conventional thermoplastics like polyethylene (PE), and polypropylene (PP) [157,221,222,225,226,227]. Comparatively, very few studies have addressed the shear-induced crystallization of PLA. Rotational rheometry along with optical microscopy was

applied to investigate the isothermal and non-isothermal crystallization of PLA [172]. It was found that the shear flow essentially promoted the crystallization kinetics of PLA. Additionally, higher level of shear rate and shearing time enhanced the crystallization kinetics of PLA as well as increasing the nuclei density. Optical microscopy also revealed that upon shear at a given temperature, the spherulite growth rate was almost unchanged. Xu-Juan *et al.* [162] accentuated the role that crystallization temperature played during the steady shear induced isothermal crystallization of PLA. It was found that 120 °C was a critical temperature above which cylindrical structure was evidenced whereas below, shear-induced nuclei were developed. Impact of shear on crystalline structure, morphology and melting behavior of PLA was also studied by means of a Linkam shear stage device [163]. It was reported that at low crystallization temperature equal to 96.5 °C, combined with pre-shearing for 5 seconds and then isothermal crystallization for 1 hour yielded the stable α crystalline structure. At crystallization temperature of 130 °C, a mix cylindrical morphology with a size of hundred microns along with spherulites was observed. Effect of long chain branching on the shear-induced crystallization of PLA was also studied [173]. Under similar shearing conditions, the long chain branched PLA exhibited faster crystallization kinetics, higher nuclei density and formation of shish-kebab structure compared to linear PLA. In another study, this research group examined the shear-induced crystallization kinetics at 160 °C for asymmetric (PLLA)/(PDLA) blends [174]. The rheological measurements exhibited the formation of stereocomplex crystallite networks in the blends, which could act as a heterogeneous nucleating agent and accelerating the crystallization kinetics of PLLA. Recently, formation of the shish-kebab structure has been studied by Huan *et al*. [175]. They succeeded in developing the shish structure by a unique transient intensive shear flow with the duration of 1 s and a shear rate to 100 s^{-1}. By increasing the isothermal crystallization temperature in the 130-140 °C range, the oriented shish-kebabs were formed. This finding was in contrast with the existing data in the literature revealing that a high amount of shear and long shearing time can generate the shish precursor.

Under quiescent condition, it was found that molecular weight had a pronounced effect on crystallization kinetics of PLA [1,26,191,228] . Compared to high-molecular weight PLA, low molecular weight PLA exhibited a shorter crystallization half-time as well as a higher spherulite growth rate. Literature abounds on the effect of molecular weight, M_w, and

molecular weight distribution on flow-induced crystallization of polymers [158,215,216,229,230,231,232,233,234,235,236,237,238,239,240]. In the case of a polydisperse polymer, under the identical flow conditions, longer polymer chains are better aligned than shorter chains because they exhibit longer relaxation time. Therefore, the high molecular weight fraction plays an important role upon shear flow that promotes the crystallization kinetics. Acierno *et al.* [240] investigated the role of molecular weight on the crystallization of poly (1-butene), iPB. An increase of molecular weight enhanced crystallization rate and nucleation density in sheared materials. A series of fiber-pulling experiments on PP samples of varying molecular weight also showed that the nucleation density and crystal growth rate exhibited an exponential relationship with M_w at a given shear rate. Moreover, under static and shear conditions, α phase was developed ; however, after cessation of flow β phase was formed due to relaxation of the oriented chains [215,216].

Despite the above reported efforts, the literature is meager regarding the effect of molecular weight of PLA on shear-induced crystallization. To our best knowledge, it is the first time that the effect of molecular weight on the shear induced crystallization of PLA using rotational rheometry is reported. In this contribution, the effect of shear rate and strain on crystallization kinetics is discussed and on the morphology and microstructure of the shear-induced PLA crystals is investigated.

5.3 Experimental

5.3.1 Materials

A commercial PLA, grade 4032D supplied by NatureWorks, was used. This PLA is a semi-crystalline grade that contains 2 % *D-LA*. It will be referred to as our higher molecular weight PLA. In order to obtain medium and low molecular weight PLAs and keeping the *L*- and *D*-content constant, hydrolysis of the high molecular weight PLA was performed. Preparation of the low-molecular weight samples and the molecular weight distribution measurements are described by Rodriguez *et.al* [206]. The low, medium and the high molecular weight PLA will be referred to as L-PLA, M-PLA and H-PLA, respectively. Number-average molecular weight (M_n), weight-average molecular weight (M_w) and molecular polydispersity index of the original and the hydrolyzed PLA samples are presented in **Table 7**.

Table 7. Number-average molecular weight (M_n), weight-average molecular weight (M_w) and polydispersity index (PDI) of the PLA samples.

Sample	M_n (kg/mol)	M_w (kg/mol)	PDI (M_w/ M_n)
H-PLA	98.1	164	1.68
M-PLA	53.2	85.2	1.60
L-PLA	19.4	35.5	1.83

5.3.2 Characterization

(1) Differential Scanning Calorimetry (DSC)

The thermal behavior of PLA samples was studied using a DSC Q2000 from TA Instruments. Temperature was calibrated before measurements using Indium as a standard material. Samples' weights were kept in the range of 5-10mg. For the non-isothermal crystallization, the samples were heated to 190 °C and then immediately cooled down to room temperature at 2 °C/min. The degree of crystallinity, X_C, of samples was calculated by the following equation:

$$X_C = \frac{\Delta H_m - \Delta H_{cc}}{\Delta H_m^o} \times 100\% \quad (9)$$

where ΔH_m is the melting enthalpy, ΔH_{cc} the cold crystallization enthalpy, and ΔH_m^o = 93.6 J/g is the melting enthalpy of 100% crystalline PLA [1].

(2) Wide-angle X-ray diffraction analysis (WAXD)

Wide-Angle X-ray Diffraction (WAXD) patterns were obtained by means of an X-ray diffractometer (D-8, Bruker) and were used to detect the crystalline phases developed at different crystallization temperatures. The samples were exposed to an X-ray beam with the X-ray generator running at 40 kV and 40 mA. The copper K_α radiation (λ=1.542Å) was selected and the scanning was carried out at 0.03 ° /s in the angular region (2θ) of 5-40°.

(3) Optical microscopy

The morphology of the non-sheared and sheared samples was observed by means of optical microscopy, on a Leica MDRX using polarized light.

(4) Rheological characterization and flow-induced crystallization

Rheological tests and flow-induced crystallization experiments were carried out using an Anton Paar rotational rheometer (MCR 502) equipped with parallel plate geometry with a diameter of 25 mm plates and gap size of 1 mm. For small amplitude oscillatory shear experiments, the experiments were carried out using a strain of 1%. It was verified that this strain was in the linear viscoelastic range by performing a strain sweep test at 10 rad/s over a strains ranging from 0.01 to 100%. The samples were prepared by compression molding of sheets with thickness of 1mm at 180 °C under 10MPa. The PLA samples were always dried overnight at 40 °C in a vacuum oven to minimize hydrolytic degradation. For the same purpose, a dry nitrogen atmosphere was used for all rheological experiments.

For flow-induced crystallization experiments, the samples were first heated up to 190 °C, maintained for 5 minutes to erase thermal history and then cooled down at 8 °C/min to the desired isothermal crystallization temperature (T_C). It was verified that virtually no crystallization took place during cooling [70,199]. Finally, a controlled continuous shear between 0.01 and 0.1s^{-1} was applied to the undercooled melt and evolution of the crystallization was monitored by the variation of viscosity versus time. Another type of experiments was carried out to monitor the effect of intensive pre-shearing (between 5 and 10s^{-1}) on crystallization. In this case, the evolution of the crystallization was assessed by monitoring the storage modulus,G', over time during oscillatory shear at $\omega = 1$rad/s and $\gamma = 1\%$.

5.4 Results and discussion

5.4.1 Shear rheology of samples

Figure 37 depicts the master curves of linear viscoelastic moduli, G' and G" as well as complex viscosity $|\eta^*|$ at the reference temperature, T_{ref} = 130 °C for the three PLA samples. Frequency sweeps were performed at 180, 160, 140 and 130 °C and Time-Temperature superposition was employed to generate the master curves. The plateau viscosity at 130 °C for H-PLA, was in the order of 10^5 Pa.s and dropped by one order of magnitude respectively for M-PLA and then L-PLA. The shear-thinning region also gradually shifted to higher frequencies as the molecular weight dropped. The storage and loss moduli, G' and G", scaled in the same way as the viscosity and respectively reached their terminal slopes of 2 and 1 on

the logarithmic representation. Furthermore, the crossover of G' and G" shifted to lower frequency decades with molecular weight.

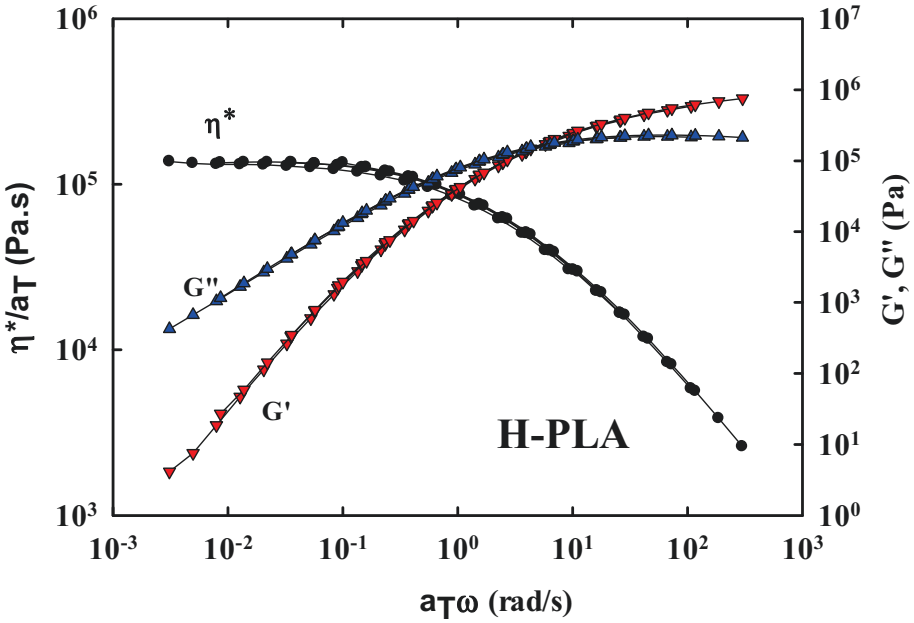

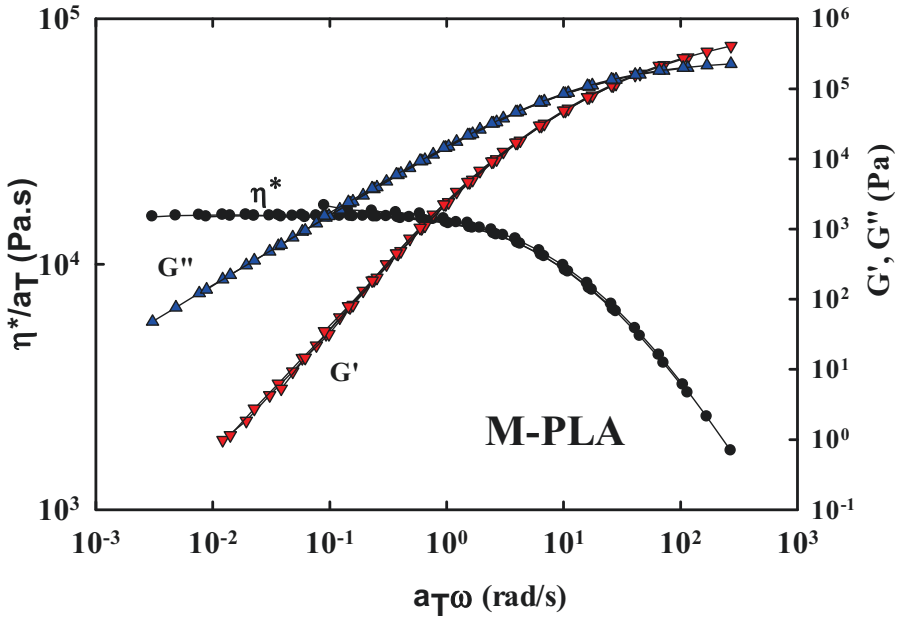

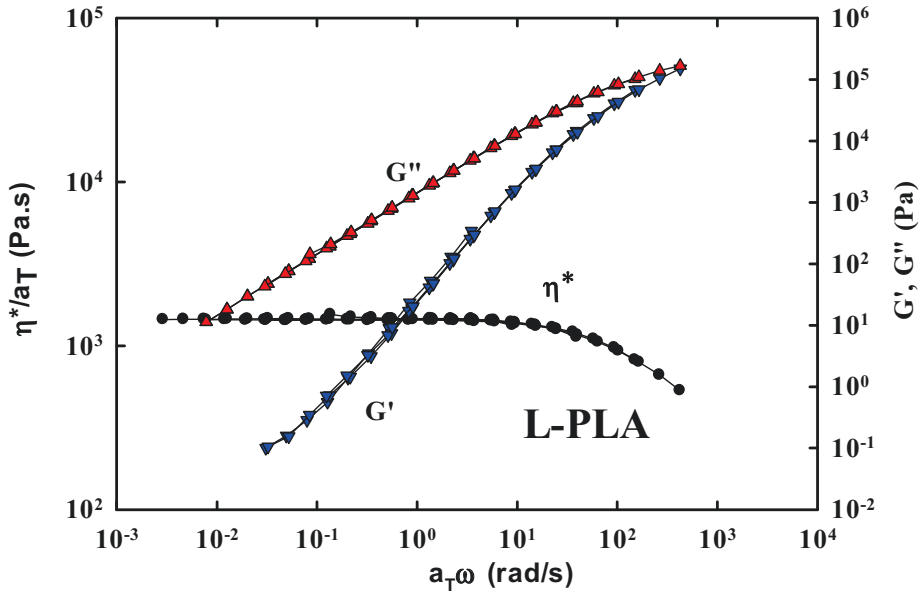

Figure 37. Rheological master curves for H-PLA, M-PLA and L-PLA at T_{ref}= 130 ° C.

The shift factors, a_T, was a function of temperature and followed a Williams-Landel- Ferry (WLF) type relationship [241]. It was well represented by the following equation:

$$a_T = \frac{exp[\frac{-C_1(T-T_r)}{C_2+T-T_r}]}{exp[\frac{-C_1(T_0-T_r)}{C_2+T_0-T_r}]} \quad (9)$$

where T is the temperature , T_0 is the reference temperature and T_r stands for the glass transition temperature, T_g. C_1=60.35 and C_2=12.54K were constants determined at T_g=333K for H-PLA, C_1=36.31 and C_2=29.7K at T_g=331K for the M-PLA, and C_1=35.61 and C_2=48.75K at T_g=327K for the L-PLA respectively. **Figure 38** depicts the variation of the ln a_T vs (1/T) for all molecular weights, showing that the relation is not linear and that the Arrhenius equation, therefore, is not applicable in this range of temperature. However, the WLF-type equation fitted the data well in the investigated temperature range.

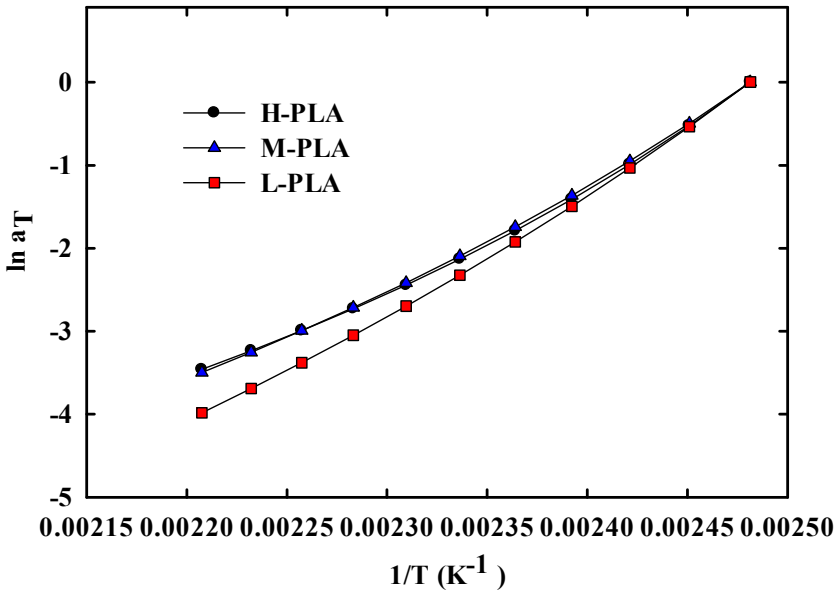

Figure 38. The ln a_T , vs (1/T) for all molecular weights at T0 = 130 °C.

Table 2 summarizes the zero-shear viscosity,η_0, of PLA samples at 130 and 180 °C. The relationship between η_0 and M_w at 180 °C can be described by:

$$\eta_0 = KM_w^{3.3} \quad (11)$$

With $K = 2.5 \times 10^{-14}$ Pa.s/(gmol)$^{3.3}$ .The exponent of 3.3, close to the expected 3.4, implied the linear structure of the studied polymers and was in good agreement with the reported data by Othman *et al.* [242] and Dorgan *et al.* [243,244,245,246] for a wide range of PLAs with different molecular weights.

Table 8. Shift factor, a_T, zero-shear viscosity, η_0, at 130 and 180 °C for PLA samples.

Sample	η_0 at 130 °C	a_T	η_0 at 180 °C
H-PLA	1.35E+05	0.0315	4.25E+03
M-PLA	1.56E+04	0.0306	4.77E+02
L-PLA	1.44E+03	0.018	2.59E+01

Figure 39 presents the normalized shear stress growth coefficient, $\eta^+ = \frac{\tau}{\dot{\gamma}}$, as a function of time for different shear rates, 0.01, 0.05 and 0.1 s^{-1} at T= 130 °C. For the sake of comparison,

the stress growth coefficient values were normalized to arbitrarily set $\eta^+ = 1$ in the constant stress growth coefficient region. As the constant shear rate was imposed, the transient stress growth coefficient of M-PLA and H-PLA increased up to a plateau followed by a sudden rise in stress growth coefficient due to crystallization. For low molecular-weight PLA, the steady state region was reached almost immediately due to its Newtonian behavior at low shear rates. In order to compare the efficiency of the different level of shear rates, an arbitrary parameter called induction time was defined. The induction time is defined as the time at which stress growth coefficient increases 20% from its steady-state value [221]. For H-PLA, the crystallization induction time was 1040 s for the lowest shear rate of $0.01s^{-1}$ and then decreased to 800 s as the shear rate was increased up to $0.1s^{-1}$. By imposing a higher shear rate, the increased chain alignment and greater nuclei density and consequently accelerated the crystallization. For M-PLA, the induction times were quite similar to those of H-PLA. The induction time for 0.01 to 0.05 s^{-1} was very close but as for H-PLA, it dropped as the shear rate was increased to $0.1s^{-1}$. Hadinata *et al.* has also reported a similar decrease in induction time with molecular weight for PB-1[231]. For the lowest molecular weight PLA, the induction period was significantly longer, around 1750 s, and was almost independent of shear rate.

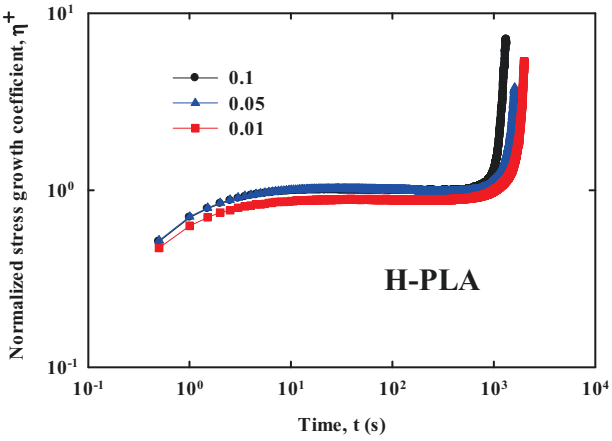

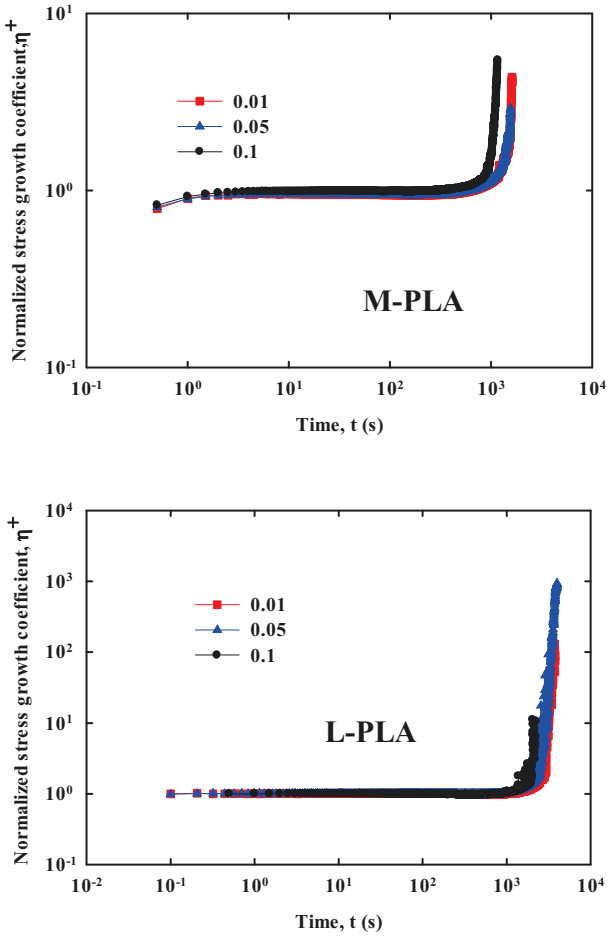

Figure 39. Normalized stress growth coefficient as a function of time at the indicated shear rates for different molecular weight PLAs at T=130 °C.

Figure 40 presents the same η^+ data as in **Figure 39** but this time as a function of strain in order to differentiate time and strain effects. Although the results of **Figure 39** suggested that the higher shear rate decreased the induction time, the results of **Figure 40** point out that a larger strain was required to observe the sharp viscosity rise associated to crystallization when the deformation rate was increased. For instance, for H-PLA, the required strain at a shear rate of $0.01s^{-1}$ was around 12 whereas at the shear rate equal to $0.1s^{-1}$, 95 unit of shear strain was needed to induce crystallization. Similar results have been reported for PP and PE [221,222].

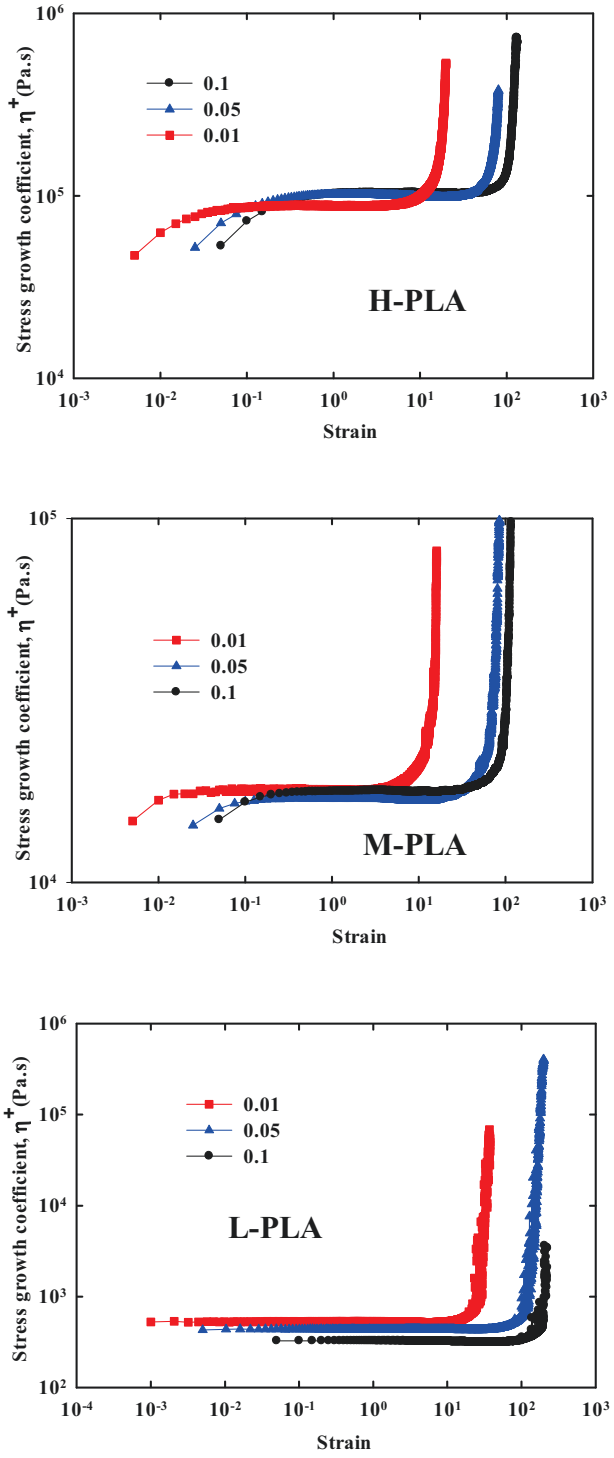

Figure 40. Transient stress growth coefficient as a function of strain at the indicated shear rates for different molecular weight PLAs at T=130 °C.

5.4.2 Rheological analysis

The Weissenberg number is one of the most frequently used dimensionless numbers in the study of viscoelastic flows as it is used to characterize the intensity of flow. The Weissenberg number is applied to measure the intensity of the shear rate and is defined by :

$$Wi = \dot{\gamma}\lambda \tag{10}$$

where $\dot{\gamma}$ is the shear rate and λ is the characteristic relaxation time. Depending on the relaxation time definition, two characteristic Weissenberg numbers, namely $W_{rep} = \dot{\gamma}\lambda_{rep}$ and $W_s = \dot{\gamma}\lambda_R$, exist. λ_{rep} and λ_R are the reptation and stretch relaxation (or Rouse time) of the polymer chains, respectively. The disengagement time is the amount of the time that it takes for the polymer chains to reptate past one another to release stress imposed by a flow. The Rouse time presents the relaxation time for a polymer chain within its tube of entanglements [226]. When W_s< 1 and W_{rep}<1, shear flow is too weak to affect the crystallization kinetics (Regime I). For W_s< 1 and W_{rep}>1, polymer chains are oriented (Regime II) and for full extension of polymer chains W_s> 1 is mandatory (Regime III) [247]. In order to compare the relaxation time of different molecular weights, the weighted relaxation spectra were calculated at 130 °C using the non-linear regression software (NLREG). The continuous relaxation spectrum, $H(\lambda)$, was determined by fitting experimental $G'(\omega)$ and $G''(\omega)$ data of the master curves (**Figure 37**) with following equations:

$$G'(\omega) = \int_{-\infty}^{\infty} H(\lambda)\, \frac{\lambda^2\omega^2}{1+\lambda^2\omega^2}\, d\ln\lambda \tag{11}$$

$$G''(\omega) = \int_{-\infty}^{\infty} H(\lambda)\, \frac{\lambda\omega}{1+\lambda^2\omega^2}\, d\ln\lambda \tag{12}$$

where ω is angular frequency and λ stands for the relaxation time. For the sake of comparison, the $\lambda H(\lambda)$ values were divided by zero shear, η_0, viscosity at 130 °C. It should be stated that a good agreement was observed between the η_0 values by Carreau-Yasuda model and the weighted relaxation method, corroborating the accuracy of the applied method to obtain the relaxation time distribution. **Figure 41** illustrates the normalized $\lambda H(\lambda)$ of samples as a function of $log\lambda$. All the molecular weights exhibited single peaks, which was attributed to the characteristic relaxation time. Additionally, these peaks shifted to longer relaxation times with

molecular weight as expected for linear polymers where the simple reptation takes place [248]. According to the tube model, proposed by Doi and Edwards [249], the relationship between λ_{rep} and λ_R is described by the equation 14:

$$\lambda_R = \frac{\lambda_{rep}}{3Z} \quad (13)$$

Where Z= M_w/M_e and M_e is the molecular mass between entanglements. According to Cooper-White [250], the estimated M_e value for PLA is about 8000 g/mol. The observed single peak for each molecular weight was considered as the λ_{rep} .**Table 9** summarizes the λ_{rep} , λ_R as well as the critical shear rate required to transit between different regimes for PLA samples at 130 °C. The critical shear rate for transition between Regime I and II, and between Regime II and III equals to $1/\lambda_{rep}$ and $1/\lambda_R$, respectively.

Table 9 results imply that for the M-PLA and L-PLA due to lower relaxation time, the Weissenberg number, W_{rep}, falls below 1. Therefore, the shear flow is too weak to accelerate the crystallization kinetics. However, for H-PLA, at shear rate equal to 0.1 s^{-1}, the Weissenberg number is above 1, providing conditions where the polymer chains can be oriented and promote the formation of crystal nuclei. $\dot{\gamma}_{I\rightarrow II}$ for the H-PLA is around 0.02 s^{-1}. Nevertheless, the transition $\dot{\gamma}_{II\rightarrow III}$ is at 1.1 s^{-1} indicating that Shish-kebab structure cannot be formed.

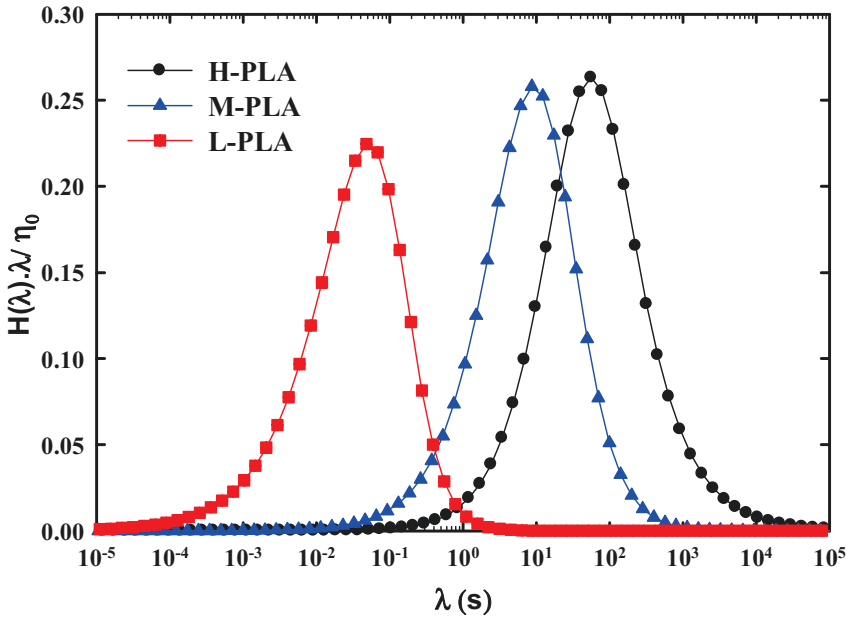

Figure 41. Normalized weighted relaxation spectra for different molecular weights at 130 °C.

Table 9. λ_{rep} , λ_R and critical shear rates for regime transition for PLA samples at 130 °C.

	T(°C)	λ_{rep} (s)	λ_R (s)	$\dot{\gamma}_{I\to II}(s^{-1})$	$\dot{\gamma}_{II\to III}(s^{-1})$
H-PLA	130	56.2	0.91	0.018	1.1
M-PLA	130	8.24	0.26	0.12	3.85
L-PLA	130	0.065	0.005	15.4	200

5.4.3Microscopy observation

Figure 42 shows optical micrographs of PLA crystallized in quiescent condition and after pre-shearing at $0.1s^{-1}$, at T= 130 °C. In quiescent condition, a spherulitic morphology was observed for all molecular weights. In the case of pre-sheared samples, the M-PLA and L-PLA also presented spherulitic morphology whereas the H-PLA showed a mixture of spherulitic morphology and cylindrite structures. The micrographs confirm that the shish-kebab structures cannot form within investigated shear rate range for the L-PLA and M-PLA. We infer from these results that the chain orientation and the formation of fully stretched chains have not reached a sufficient level of shear rate to induce the crystallization of the high molecular

weight fraction. However, for H-PLA, the Regime II is established, leading to the mixed formation of cylindrical morphology along with spherulites.

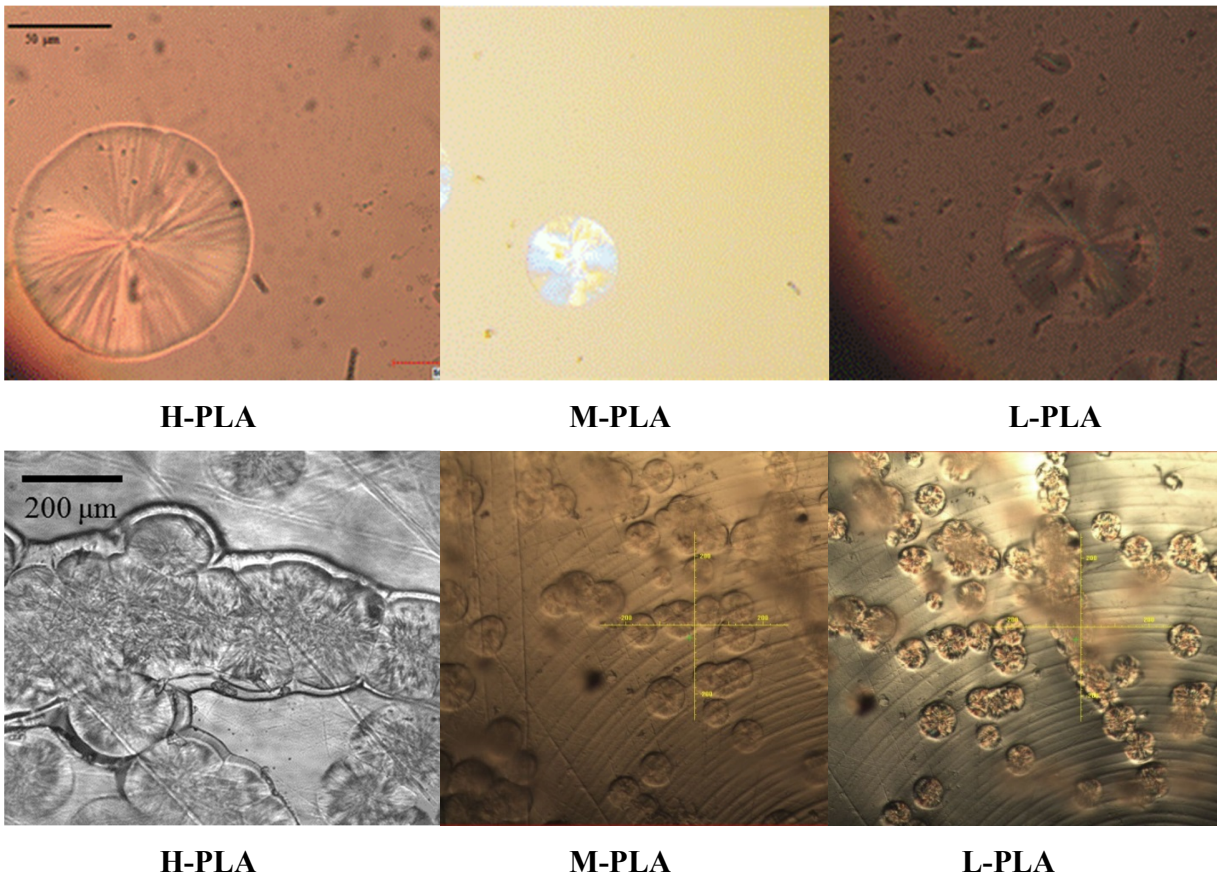

Figure 42. Optical microscopy micrographs for PLA samples: the first row at quiescent condition at 130 °C: the scale bar is 50 micrometer. The second row: sheared at 0.1 s^{-1} at 130 °C: the scale bar is 200 micrometer.

5.4.4 X-ray diffraction measurements

Samples being deformed at a rate of 0.1s^{-1} at 130 °C were rapidly quenched after cessation of shear in order to probe their crystalline modification. Sampling was carried out either in the constant transient viscosity region or in the region where the samples have started crystallization, thus after the onset of the abrupt viscosity rise (see **Figure 39**). **Figure 43** presents the WAXD patterns of the quenched H-PLA. Amorphous structure was observed for the sample quenched in the constant viscosity region. This suggests that at this stage the sample is crystal free. However, the XRD pattern of the sample quenched after crystallization exhibited peaks that were associated to the α phase of PLA at 2θ= 12.5, 14.7, 16.7, 19.1 and 22.5° [17]. The arrows on the Figure highlight these expected peak positions. It can be, thus,

concluded that the shear flow enhances the formation of the α phase. Similar results were found for M-PLA and L-PLA in identical conditions (not shown for the sake of brevity).

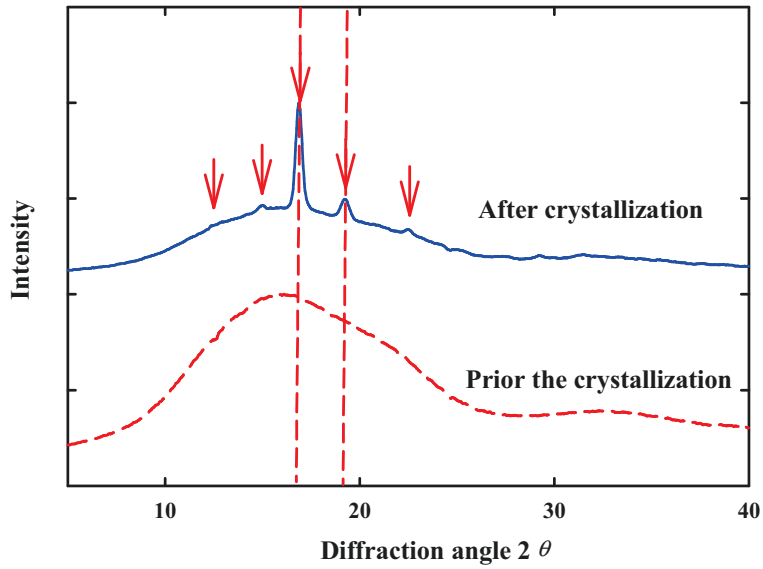

Figure 43. WAXD patterns of the sheared H-PLA in the constant viscosity region, the dash line curve, and after viscosity overshoot, the solid line curve, at 130°C.

It is also well known that PLA exhibits the α' modification when isothermally crystallized below 100 °C [1,199]. Therefore, an attempt was made to study the effect of shear flow on the crystalline structure of PLA. Because the viscosity of M-PLA and H-PLA samples below 100 ° C was out of the rheometer's measuring range, only the L-PLA was examined. To this end, the L-PLA was sheared at $\dot{\gamma} = 0.01\, s^{-1}$. **Figure 44** illustrates the XRD patterns of the L-PLA sample sheared at $\dot{\gamma} = 0.01\, s^{-1}$ for 7 minutes at T=95 °C. For comparison, the crystalline structure of the L-PLA crystallized quiescently at T=95 °C for 60 minutes is also shown in **Figure 44**. It is of great interest that while sample isothermally crystallized without shear exhibited the peaks characteristic of the α' phase, the sheared sample only presented the α characteristic peaks. It could be argued that the shear flow facilitates the chains ordering leading predominately to the α phase.

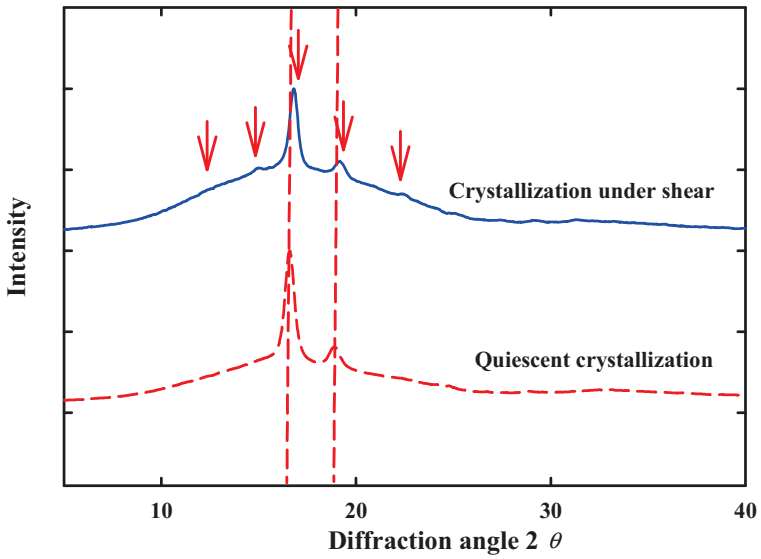

Figure 44. WAXD patterns of the L-PLA at 95 °C in quiescent condition, dash line curve, and after shearing at 0.01 s^{-1} for 7 minutes, the solid line curve.

5.4.5 Shear-induced crystallization at intensive shear flow

Up to now, the low shear rates used in the investigation did not lead to fully stretched chains. Consequently and in order to examine the effect of intensive pre-shear flows, the following procedure was used. The samples were heated up and kept at 190 °C for 5 minutes to erase thermal history, cooled down to 130 °C and sheared at 5 or 10 s^{-1} during 10 seconds. The elastic modulus was then monitored over time and was reported in **Figure 45** in normalized form, $G'(t)/G'(0)$, as a function of time. The applied pre-shearing values ensure that $W_s > 1$, for H-PLA and M-PLA, and consequently, fully stretched chains are expected upon shear. However, W_s is below 1 for L-PLA sample. The time at intersection of the slope of the ascending part of the modulus- time with the line at initial constant stage is defined as the crystallization induction time. As seen in **Figure 45**, the crystallization induction time decreased with molecular weight in intensive shear flow as observed previously for weak deformation rates. In addition, despite having the longest induction time, the L-PLA exhibited a slightly more abrupt increase in storage modulus than the H-PLA and M-PLA. It could be argued that due to low relaxation time and inelastic behavior of L-PLA, formation of crystal nuclei is rather difficult. However, as previously mentioned, the low molecular weight PLA

exhibited faster crystal growth rate [26]. That is the reason why a steeper increase in storage modulus for L-PLA was observed.

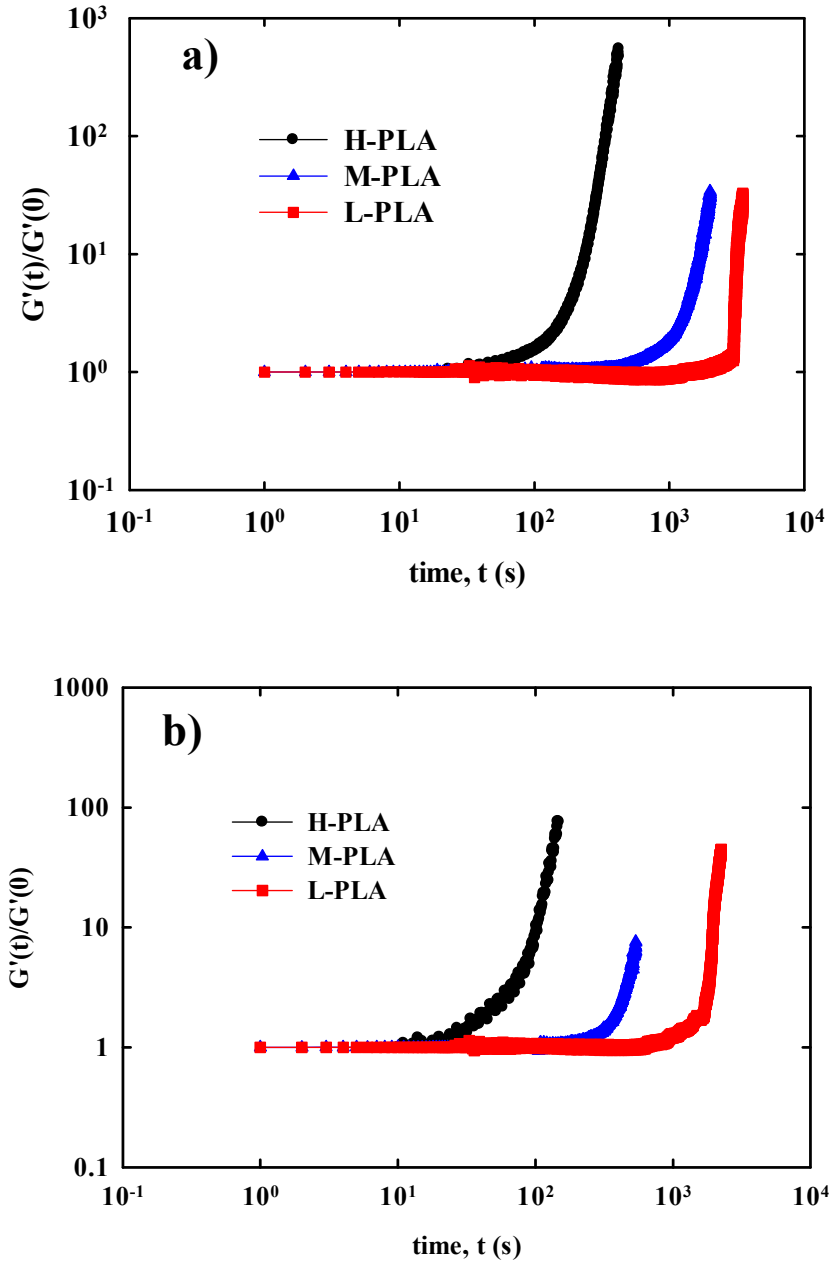

Figure 45. Development of the normalized storage modulus for different molecular weight PLA samples pre-sheared during 10 seconds at shear rates equal to a) 5 s^{-1} b) 10 s^{-1} at 130 °C.

5.4.6 Thermal analysis of sheared samples

In order to examine the impact of shear flow on the thermal behavior of PLA, the sheared samples were quenched and then analyzed by DSC. **Figure 46** shows the heating thermograms of non-sheared and sheared H-PLA. The samples were pre-sheared at 10 s^{-1} and subsequently crystallized isothermally for 10 minutes. The non-sheared H-PLA revealed a cold-crystallization temperature, T_{CC}, around 117 °C whereas the pre-sheared sample showed a T_{CC} at 110 °C. Applying the shear flow can increase the number of nuclei and, therefore, T_{CC} shifts to lower temperatures. Additionally, a small exothermic peak was detected for the sheared sample, prior the main melting peak. It could be argued that after cooling H-PLA from 190 °C to 130 °C, the undercooled melt was at rest. After a sudden shearing at a high rate, some imperfect crystals, the α' phase, might have formed at a very beginning of shear rate. These induced imperfect crystals tend to transfer to the stable phase, the α phase, through a solid-solid phase transition which is evidenced by the observed exothermic peak [26]. A similar behavior was also observed for M-PLA. The crystallinity level of the non-sheared and pre-sheared samples was determined using Eq.9 based on melting and crystallization enthalpies. The non-sheared H-PLA exhibited a low crystallinity level around 7.6%.Imposing shear just slightly increased the degree of crystallinity to 8.7%. A possible explanation is pre-shearing provides some initial nuclei ; however, most of the crystallization takes place through a quiescent process.

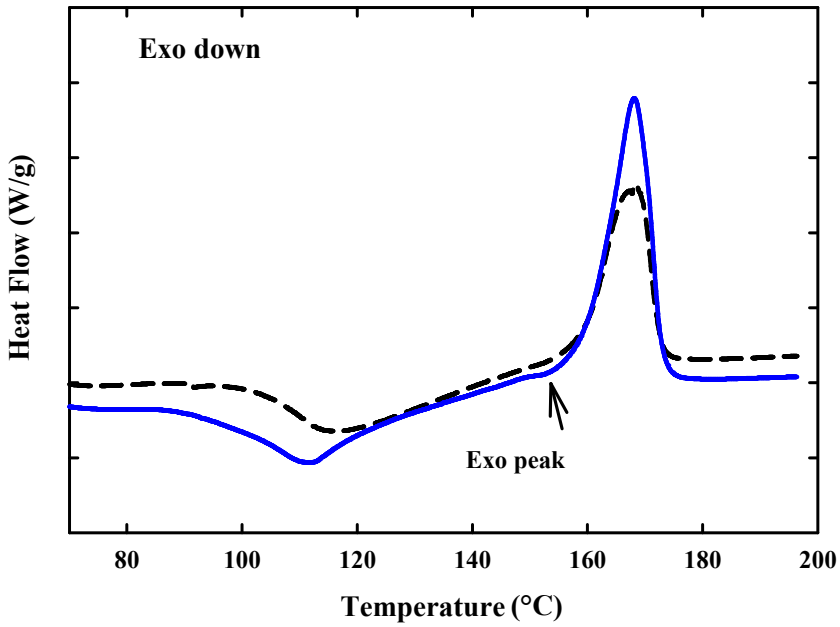

Figure 46. DSC heating micrographs for non-sheared(dashed line curve) and pre-sheared (solid line) at 10 s^{-1} for H-PLA.

Similar heating thermographs are shown in **Figure 47** but this time for L-PLA. There are two melting peaks designated low, L, and high, H. The non-sheared L-PLA exhibited a T_{CC} at 111 °C and a double melting peak at 159 and 164 °C, respectively. The first peak is ascribed to the melting of the α phase and the second one is attributed to the melting of the α' phase transferred to the α phase through the melt-recrystallization mechanism [199,251]. For the L-PLA sample pre-sheared at 10 s^{-1} and then isothermally crystallized for 10 minutes, the T_{CC} and melting peaks remained intact compared to the non-sheared sample. However, for the L-PLA pre-sheared at 33 s^{-1} for 10 seconds and then isothermally crystallized for 10 minutes, the T_{CC} shifted to 107 °C. Furthermore, the melting peak shifted to 160 and 168 °C, respectively. Additionally, the L/H peak area ratio was decreased with increasing the shear rate. A plausible reason could be that the faster the samples were sheared, the more imperfect α'crystals were formed. According to the melt-recrystallization mechanism, the imperfect crystals, therefore, transform to the stable α crystals. In terms of crystallinity level, the non-sheared L-PLA reached a value of 18%, which was noticeably higher than the non-sheared H-PLA. Pre-shearing at 10 s^{-1} and then isothermally crystallizing for 10 minutes did not change the

crystallinity level. When the pre-shearing was carried out at 33 s^{-1}, the crystallinity level was increased to 27% indicating that a significant amount of shear-induced nuclei was formed.

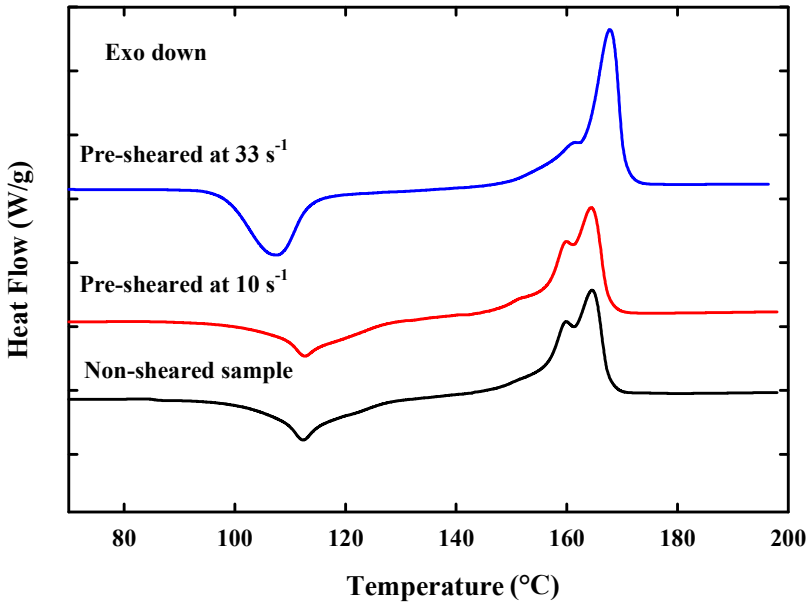

Figure 47. DSC heating micrographs for non-sheared and pre-sheared L-PLA.

Figure 48 depicts the cooling DSC scans obtained with pre-sheared samples that were isothermally crystallized at 130 °C for 1 hour and re-heated up to 190 °C. The pre-shearing was at $10s^{-1}$ for 10 seconds. The cooling was performed at a rate of 2 °C/min and was initiated as soon as the temperature reached 190 °C without the usual stabilization period used to erase thermal history. The cooling scans exhibited a peculiar double crystallization peak around 100 and 120 °C for both M-PLA and H-PLA. In our previous work, this double crystallization peak was observed for the self-nucleated PLA and was ascribed to the formation of the α and α' phases [199]. In the current study, the higher temperature peak could be ascribed to the PLA crystallized under stress while the lower temperature peak could be attributed to the PLA that crystalized quiescently. A similar result has also been reported by Zhong *et al.* [252] in which they detected a double crystallization peak for PLA upon cooling at 1 °C/min after pre-shearing at 120 °C for a few seconds. For L-PLA, a single crystallization peak around 100 °C was found. This can be explained by its smaller relaxation time, which leads to lower chain stretching.

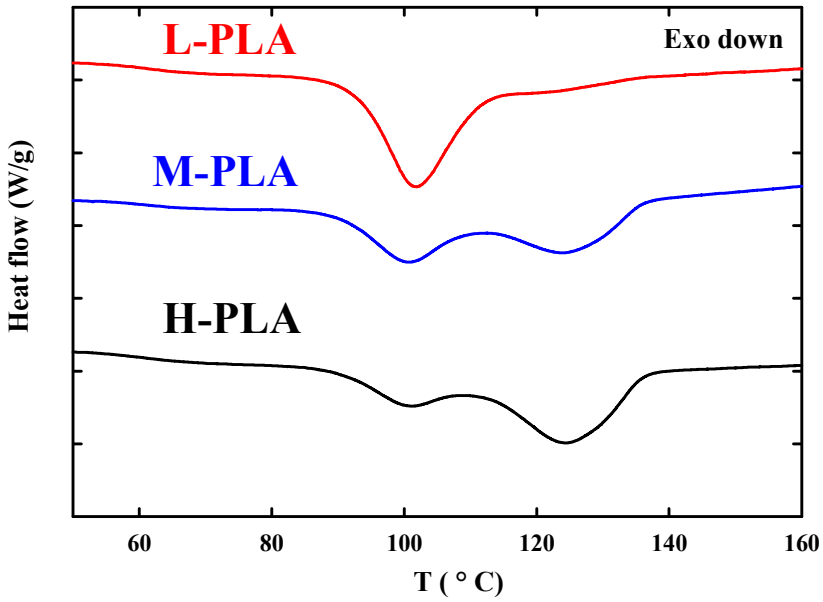

Figure 48. DSC cooling micrographs for different molecular weight PLA samples that were previously pre-sheared at 10 s^{-1} and then isothermally crystallized for 1 hour.

5.5 Conclusions

Effect of weak and strong shear flow on the crystallization of PLA with different molecular weights, M_W, was investigated. It was found that the crystallization induction time decreased with increasing the M_W in the presence of the shear flow. This was shown to be linked to the polymer relaxation time. It was also found that a higher level of strain was required to initiate the crystallization with increasing shear rate levels.

Shear flow promoted the formation of the α phase at elevated temperature, 130 °C, for all different molecular weights. X-Ray Diffraction patterns of the sheared low-molecular weight PLA also exhibited the formation of the α phase below 100 °C whereas the WAXD patterns obtained from the samples crystallized in quiescent conditions demonstrated the formation of the α' phase. Only spherulitic morphology were developed for the low and medium molecular weight PLA ; however, the high molecular weight PLA exhibited a mixture of spherulitic and cylindrite morphology. Finally, it was shown that medium and high molecular weight PLA could develop a peculiar double crystallization peak if it is pre-sheared, isothermally crystallized to full extent, then rapidly heated up, and recrystallized upon cooling. The peaks that appeared at 120 and 100 °C were ascribed respectively to nucleation by pre-formed nuclei from stretched high molecular weight fractions and nuclei formed in non-stretched (lower

molecular weight) regions. Low molecular weight PLA did not exhibit this double crystallization peak possibly the low relaxation time did not enable sufficient chain stretching.

5.6 Acknowledgment

The authors would like to thank FRQNT and NSERC for financial support. The authors also wish to express their gratitude to Mr. Edwin Rodriguez Ortega for his valuable assistance in the preparation of the samples.

CHAPTER 6 CONCLUSIONS AND RECOMMENDATION

6.1 Francais

Dans cette thèse, la cristallisation statique et induite par l'écoulement du PLA a été étudiée. Dans la première phase du projet, un procédé thermique constitué d'un chauffage et d'un refroidissement successifs, appelé auto-nucléation, a été conçu pour étudier l'efficacité et les phases du PLA cristallin, à savoir les phases α et α'. Ceci a été réalisé en comparant les températures de cristallisation lors du refroidissement après l'auto-nucléation des échantillons préalablement cristallisés isothermiquement à différentes températures allant de 80 à 130 °C. La premiere conclusion importante est un mélange de α et α' est la plus efficace en terme d'auto-nucléation du PLA. Ceci se traduit par une plus haute température de cristallisation, une plus grande densité de nucléation et une plus petite taille de sphérolites. De plus, pour la première fois dans la littérature scientifique un double pic de cristallisation particulier a été observé pour le PLA auto-nucléé, attribué à la formation des phases α et α'. En outre, en modifiant très légèrement la température dans la plage de température d'auto-nucléation, un changement de la proportion de chaque pic a été observé ce qui permet de conclure que la transition de phase α'- α s'effectue dans une plage de température très restreintes (dans la plage de fusion partielle).

Dans la deuxième partie du projet, l'effet du taux de refroidissement et de chauffage ont été étudiés. La plage de fusion partielle ainsi que le temps de maintien dans cette zone de fusion partielle, correspondant au double pic de cristallisation observé dans la première phase du projet, ont été étudié. En utilisant une déconvolution, sur la base des enthalpies de fusion et de cristallisation des pics observés, les proportions d'α et α' ont été calculés. L'effet de la masse moléculaire du PLA sur la cinétique de cristallisation et l'auto-nucléation de PLA a également été étudié. Les tests de cristallisation isothermes ont montré que le faible poids moléculaire du PLA mène à une cinétique de cristallisation plus rapide ainsi qu'un taux de croissance plus important des sphérulites. Une conclusion importante toutefois est que la création et la co-existance des phases α et α' n'est pas altérée par la masse molaire. Ceci est confirmé de différentes façons telles que la présence des doubles pics de fusion en chauffe et des doubles pics de crystallisation en refroidissement. On a également constaté que la température maximale de cristallisation après la fusion partielle est la même pour les PLA de haute et de basse masse molaire (T_{cmax} = 160 °C). Pour le PLA de masse moléculaire élevée toutefois

T_{cmax} est une fonction dépendante de la température de cristallisation isotherme préalable à la fusion partielle.

Dans la troisième et dernière étape du projet, l'effet d'un écoulement en cisaillement sur la cristallisation de PLA a été étudié en utilisant des mesures rhéologiques. Une première conclusion en cisaillement simple a été que le temps d'induction avant la cristallisation diminue avec l'augmentation de M_W. Ceci a été lié au temps de relaxation du polymère. On a également constaté qu'un niveau élevé de déformation est nécessaire pour amorcer la cristallisation avec l'augmentation des niveaux de taux de cisaillement. L'écoulement de cisaillement favorise la formation de la phase α à une température élevée (130° C) peu importe la masse moléculaire. Des diffractogrammes réalisés par diffraction des rayons X pour du PLA de faible masse moléculaire ont également montré la formation de la phase α à une température inférieure à 100 °C, tandis que les motifs de WAXD obtenus à partir des échantillons cristallisés dans des conditions statiques montraient la formation de la phase α'. Seule la morphologie sphérolitique a été formée pour des PLA de faibles et moyennes Mw ; cependant, le PLA de masse moléculaire élevée a présenté un mélange de morphologie sphérolitique et cylindrite. Enfin, il a été montré que les PLA de moyennes et hautes Mw ont pu développer un double pic de cristallisation particulier, si ces derniers ont été pré-cisaillés puis cristallisés isothermiquement à la pleine mesure, puis chauffés rapidement avant d'être recristallisés lors du refroidissement. Le pic apparu à plus haute température a été attribué à la nucléation par les noyaux préformés de fractions de longues macromolécules orientés alors que le pic à basse température a été associé à la fraction de chaines plus courtes qui a eu le temps de relaxer avant de crystalliser. Le PLA de faible masse moléculaire n'a pas montré ce double pic de cristallisation. Cela s'expliquerait pas le fait que le faible temps de relaxation n'a pas permis d'orienter suffisamment les chaines.

6.2 English

In this thesis, quiescent and flow-induced crystallization of PLA was investigated. In the first phase of the project, a successive heating and cooling thermal process, called self-nucleation, was designed to study the efficiency of the α and α' crystalline modifications of PLA. This was carried out by comparing crystallization temperatures upon cooling after self-nucleation of samples previously crystallized at various isothermal temperatures ranging from 80 °C to

130 °C. The first important conclusion is that a mixture of α and α’ crystals is the most efficient nucleant for PLA. This translates into higher crystallization temperatures, higher nuclei density and smaller spherulite size. Additionally, for the first time in the literature, a peculiar double crystallization peak was observed for the self-nucleated PLA which was ascribed to the formation of the α and α’ phases. Furthermore, by very slightly changing the temperature within the self-nucleation temperature range, a rapid change in the proportion of each peak was observed. This helped to conclude that the α'- α transition in the partial melting zone occurs in a very narrow temperature window.

In the second part of the project, it was intended to investigate the effect of the cooling and the holding time at the partial melting zone on the observed double crystallization peak in the first phase of the project. By using deconvolution, based on the melting and crystallization enthalpies of the observed peaks, the proportions of the α and α’ were calculated. Effect of molecular weight of PLA on the crystallization kinetics and the self-nucleation of PLA was also studied. Isothermal crystallization charactrization showed that the low-molecular weight PLA exhibited faster crystallization kinetics and spherulite growth rate. An important conclusion ; however, is that the generation and co-existance of α and α' phases is not modified by molecular weight. This was confirmed in many ways such as the double melting peaks upon heating and the double crystallization peaks upon cooling. It was also observed that the both low and high-molecular weight PLAs presented similar maximum crystallization temperature after partial melting , T_{cmax} = 160 °C, which is the highest reported nonisothermal crystallization temperature for PLA. For the high-molecular weight PLA T_{cmax} was a function of the isothermal crystallization temperature used prior to the partial melting step.

In the third stage of the project, the effect of steady shear and of a shear pre-treatment on the crystallization of PLA was investigated using rheological measurements. It was concluded that the crystallization induction time in steady shear decreases with increasing the M_W. This was shown to be linked to the polymer relaxation time. One important conclusion of this study is that shear flow promoted the formation of the α phase regardless of the molecular weights. X-Ray diffraction patterns of the sheared low-molecular weight PLA also confirmed the formation of the α phase below 100 °C whereas in quiscent conditions the α’ phase was favored. Another conclusion is that only spherulitic morphology can develop under shear for low molecular weight PLA. Because the rapid molecular relaxation overwhelms the effect of

the shear flow. However, for the high molecular weight PLA a mixture of spherulitic and cylindrite morphology can be generated. It is notewhorthy that for the high molecular weight PLA, the peculiar double crystallization peak observed in quiscent self-nucleation protocol was also observed when PLA was pre-sheared prior to be isothermally crystallized rapidly heated up, and recrystallized upon cooling. It was concluded that two nuclei types were present upon cooling : pre-formed nuclei from stretched long molecular macromolecules and nuclei formed in non-stretched, relaxed regions composed of the lower molecular weight material. Low molecular weight PLA did not exhibit this double crystallization peak since the rapid relaxation overwhelmed chain stretching.

6.3 Recommendations

The following topics are suggested for further investigation :

1. *Shear flow- induced crystallization of branched PLA :* As it was stated in the thesis, compared to conventional thermoplastics, a few works exist on the flow-induced crystallization of PLA. Additionally, PLA exhibits poor melt strength. To overcome this problem, branched PLA, B-PLA, is recommended. Although some works have addressed the shear-induced crystallization of the B-PLA, a systematic study on the effect of shear flow on the crystallization kinetics and on the microstructure as well as the thermal properties of the sheared B-PLA is needed.
2. *Extensional-flow induced crystallization of branched PLA* : Surprisingly, extensional-induced crystallization of PLA has yet to be carried out. Therefore, it is suggested that effect of elongational flow fields on the crystallization kinetics of PLA is explored. Potential applications include fiber spinning, film blowing, foaming and extrusion processes.
3. *Shear-induced crystallization of the nucleated PLA :* In the literature review chapter, the impact of different nucleating agents on the quiescent crystallization of PLA was comprehensively studied. These additives are normally dispersed in small amounts (less than 1% concentration) in commercial thermoplastics to shorten processing time and enhance product properties. Moreover, flow of molten polymers takes place in almost all processing operations. Hence, the crystallization occurs during the flow is of particular industrial relevance. A lack of data on the simultaneous effect of shear flow

and nucleating agents on the crystallization of PLA in the literature has been identified. Hence, influence of the shear flow on the crystallization of nucleated PLA with different types of nucleated elements needs to be explored in more details.

LIST OF REFERENCES

[1] S. Saeidlou, M.A. Huneault, L. Hongbo, C.B. Park, Poly(lactic acid) crystallization, Progress in Polymer Science 37 (2012) 1657-1677.

[2] K. Madhavan Nampoothiri, N.R. Nair, R.P. John, An overview of the recent developments in polylactide (PLA) research, Bioresource Technology 101 (2010) 8493-8501.

[3] R. Mehta, V. Kumar, H. Bhunia, S.N. Upadhyay, Synthesis of Poly(Lactic Acid): A Review, Journal of Macromolecular Science, Part C 45 (2005) 325-349.

[4] J. Menczel, B. Wunderlich, Heat capacity hysteresis of semicrystalline macromolecular glasses, Journal of Polymer Science: Polymer Letters Edition 19 (1981) 261-264.

[5] M.L. Di Lorenzo, Spherulite growth rates in binary polymer blends, Progress in Polymer Science 28 (2003) 663-689.

[6] H.D. Keith, On the relation between different morphological forms in high polymers, Journal of Polymer Science Part A: General Papers 2 (1964) 4339-4360.

[7] J.P. Armistead, J.D. Hoffman, Direct Evidence of Regimes I, II, and III in Linear Polyethylene Fractions As Revealed by Spherulite Growth Rates, Macromolecules 35 (2002) 3895-3913.

[8] M.L. Di Lorenzo, M. Raimo, E. Cascone, E. Martuscelli, Poly(3-hydroxybutyrate)-based copolymers and blends: Influence of a second component on crystalization and thermal behaviour, Journal of Macromolecular Science, Part B 40 (2001) 639-667.

[9] H.D. Keith, F.J. Padden Jr, A discussion of spherulitic crystallization and spherulitic morphology in high polymers, Polymer 27 (1986) 1463-1471.

[10] E.J. Clark, J.D. Hoffman, Regime III crystallization in polypropylene, Macromolecules 17 (1984) 878-885.

[11] H. Abe, Y. Kikkawa, Y. Inoue, Y. Doi, Morphological and Kinetic Analyses of Regime Transition for Poly[(S)-lactide] Crystal Growth, Biomacromolecules 2 (2001) 1007-1014.

[12] M.L. Di Lorenzo, Crystallization behavior of poly(l-lactic acid), European Polymer Journal 41 (2005) 569-575.

[13] W. Hoogsteen, A.R. Postema, A.J. Pennings, G. Ten Brinke, P. Zugenmaier, Crystal structure, conformation and morphology of solution-spun poly(L-lactide) fibers, Macromolecules 23 (1990) 634-642.

[14] K. De Santics, Biopolymers 6 (1987).

[15] J. Puiggali, Y. Ikada, H. Tsuji, L. Cartier, T. Okihara, B. Lotz, The frustrated structure of poly(l-lactide), Polymer 41 (2000) 8921-8930.

[16] L. Cartier, T. Okihara, Y. Ikada, H. Tsuji, J. Puiggali, B. Lotz, Epitaxial crystallization and crystalline polymorphism of polylactides, Polymer 41 (2000) 8909-8919.

[17] M. Yasuniwa, S. Tsubakihara, K. Iura, Y. Ono, Y. Dan, K. Takahashi, Crystallization behavior of poly(l-lactic acid), Polymer 47 (2006) 7554-7563.

[18] P. Pan, B. Zhu, W. Kai, T. Dong, Y. Inoue, Effect of crystallization temperature on crystal modifications and crystallization kinetics of poly(L-lactide), Journal of Applied Polymer Science 107 (2008) 54-62.

[19] M.L. Di Lorenzo, Determination of spherulite growth rates of poly(l-lactic acid) using combined isothermal and non-isothermal procedures, Polymer 42 (2001) 9441-9446.

[20] M.L. Di Lorenzo, The Crystallization and Melting Processes of Poly(L-lactic acid), Macromolecular Symposia 234 (2006) 176-183.

[21] J. Zhang, Y. Duan, H. Sato, H. Tsuji, I. Noda, S. Yan, Y. Ozaki, Crystal Modifications and Thermal Behavior of Poly(l-lactic acid) Revealed by Infrared Spectroscopy, Macromolecules 38 (2005) 8012-8021.
[22] Y. Ohtani, K. Okumura, A. Kawaguchi, Crystallization Behavior of Amorphous Poly(l-Lactide), Journal of Macromolecular Science, Part B 42 (2003) 875-888.
[23] J. Zhang, K. Tashiro, H. Tsuji, A.J. Domb, Disorder-to-Order Phase Transition and Multiple Melting Behavior of Poly(l-lactide) Investigated by Simultaneous Measurements of WAXD and DSC, Macromolecules 41 (2008) 1352-1357.
[24] J. Zhang, H. Tsuji, I. Noda, Y. Ozaki, Structural Changes and Crystallization Dynamics of Poly(l-lactide) during the Cold-Crystallization Process Investigated by Infrared and Two-Dimensional Infrared Correlation Spectroscopy, Macromolecules 37 (2004) 6433-6439.
[25] J. Zhang, H. Tsuji, I. Noda, Y. Ozaki, Weak Intermolecular Interactions during the Melt Crystallization of Poly(l-lactide) Investigated by Two-Dimensional Infrared Correlation Spectroscopy, The Journal of Physical Chemistry B 108 (2004) 11514-11520.
[26] P. Pan, W. Kai, B. Zhu, T. Dong, Y. Inoue, Polymorphous Crystallization and Multiple Melting Behavior of Poly(l-lactide): Molecular Weight Dependence, Macromolecules 40 (2007) 6898-6905.
[27] S. Tan, A. Su, W. Li, E. Zhou, New insight into melting and crystallization behavior in semicrystalline poly(ethylene terephthalate), Journal of Polymer Science Part B: Polymer Physics 38 (2000) 53-60.
[28] M. Yasuniwa, S. Tsubakihara, K. Ohoshita, S.I. Tokudome, X-ray studies on the double melting behavior of poly(butylene terephthalate), Journal of Polymer Science Part B: Polymer Physics 39 (2001) 2005-2015.
[29] M. Yasuniwa, T. Satou, Multiple melting behavior of poly(butylene succinate). I. Thermal analysis of melt-crystallized samples, Journal of Polymer Science Part B: Polymer Physics 40 (2002) 2411-2420.
[30] Z. Qiu, M. Komura, T. Ikehara, T. Nishi, DSC and TMDSC study of melting behaviour of poly(butylene succinate) and poly(ethylene succinate), Polymer 44 (2003) 7781-7785.
[31] X. Ling, J.E. Spruiell, Analysis of the complex thermal behavior of poly(L-lactic acid) film. I. Samples crystallized from the glassy state, Journal of Polymer Science Part B: Polymer Physics 44 (2006) 3200-3214.
[32] R.K. Verma, V. Velikov, R.G. Kander, H. Marand, B. Chu, B.S. Hsiao, SAXS studies of lamellar level morphological changes during crystallization and melting in PEEK, Polymer 37 (1996) 5357-5365.
[33] T.Y. Ko, E.M. Woo, Changes and distribution of lamellae in the spherulites of poly(ether ether ketone) upon stepwise crystallization, Polymer 37 (1996) 1167-1175.
[34] S. Tan, A. Su, J. Luo, E. Zhou, Crystallization kinetics of poly(ether ether ketone) (PEEK) from its metastable melt, Polymer 40 (1999) 1223-1231.
[35] R. Verma, H. Marand, B. Hsiao, Morphological Changes during Secondary Crystallization and Subsequent Melting in Poly(ether ether ketone) as Studied by Real Time Small Angle X-ray Scattering, Macromolecules 29 (1996) 7767-7775.

[36] X. Ling, J.E. Spruiell, Analysis of the complex thermal behavior of poly(L-lactic acid) film. II. Samples crystallized from the melt, Journal of Polymer Science Part B: Polymer Physics 44 (2006) 3378-3391.
[37] M. Yasuniwa, K. Iura, Y. Dan, Melting behavior of poly(l-lactic acid): Effects of crystallization temperature and time, Polymer 48 (2007) 5398-5407.
[38] M. Yasuniwa, K. Sakamo, Y. Ono, W. Kawahara, Melting behavior of poly(l-lactic acid): X-ray and DSC analyses of the melting process, Polymer 49 (2008) 1943-1951.
[39] K. Jamshidi, S.H. Hyon, Y. Ikada, Thermal characterization of polylactides, Polymer 29 (1988) 2229-2234.
[40] M. Yasuniwa, S. Tsubakihara, Y. Sugimoto, C. Nakafuku, Thermal analysis of the double-melting behavior of poly(L-lactic acid), Journal of Polymer Science Part B: Polymer Physics 42 (2004) 25-32.
[41] J.D. Hoffman, Regime III crystallization in melt-crystallized polymers: The variable cluster model of chain folding, Polymer 24 (1983) 3-26.
[42] G.R. Strobl, M.J. Schneider, I.G. Voigt-Martin, Model of partial crystallization and melting derived from small-angle X-ray scattering and electron microscopic studies on low-density polyethylene, Journal of Polymer Science: Polymer Physics Edition 18 (1980) 1361-1381.
[43] C. Migliaresi, A. De Lollis, L. Fambri, D. Cohn, The effect of thermal history on the crystallinity of different molecular weight PLLA biodegradable polymers, Clinical Materials 8 (1991) 111-118.
[44] S. Iannace, L. Nicolais, Isothermal crystallization and chain mobility of poly(L-lactide), Journal of Applied Polymer Science 64 (1997) 911-919.
[45] T. Kawai, N. Rahman, G. Matsuba, K. Nishida, T. Kanaya, M. Nakano, H. Okamoto, J. Kawada, A. Usuki, N. Honma, K. Nakajima, M. Matsuda, Crystallization and Melting Behavior of Poly (l-lactic Acid), Macromolecules 40 (2007) 9463-9469.
[46] Y. Ikada, K. Jamshidi, H. Tsuji, S.H. Hyon, Stereocomplex formation between enantiomeric poly(lactides), Macromolecules 20 (1987) 904-906.
[47] A.M. J, Kinetics of phase change-I. General Theory
Journal of Chemistry and Physics 7 (1939) 1103-1109.
[48] H. Tsuji, L. Bouapao, Stereocomplex formation between poly(L-lactic acid) and poly(D-lactic acid) with disproportionately low and high molecular weights from the melt, Polymer International 61 (2012) 442-450.
[49] H. Tsuji, F. Horii, S.H. Hyon, Y. Ikada, Stereocomplex formation between enantiomeric poly(lactic acid)s. 2. Stereocomplex formation in concentrated solutions, Macromolecules 24 (1991) 2719-2724.
[50] H. Tsuji, S.H. Hyon, Y. Ikada, Stereocomplex formation between enantiomeric poly(lactic acid)s. 3. Calorimetric studies on blend films cast from dilute solution, Macromolecules 24 (1991) 5651-5656.
[51] H. Tsuji, S.H. Hyon, Y. Ikada, Stereocomplex formation between enantiomeric poly(lactic acid)s. 4. Differential scanning calorimetric studies on precipitates from mixed solutions of poly(D-lactic acid) and poly(L-lactic acid), Macromolecules 24 (1991) 5657-5662.
[52] H. Tsuji, S.H. Hyon, Y. Ikada, Stereocomplex formation between enantiomeric poly(lactic acids). 5. Calorimetric and morphological studies on the stereocomplex formed in acetonitrile solution, Macromolecules 25 (1992) 2940-2946.

[53] H. Tsuji, F. Horii, M. Nakagawa, Y. Ikada, H. Odani, R. Kitamaru, Stereocomplex formation between enantiomeric poly(lactic acid)s. 7. Phase structure of the stereocomplex crystallized from a dilute acetonitrile solution as studied by high-resolution solid-state carbon-13 NMR spectroscopy, Macromolecules 25 (1992) 4114-4118.
[54] H. Tsuji, Y. Ikada, Blends of isotactic and atactic poly(lactide)s: 2. Molecular-weight effects of atactic component on crystallization and morphology of equimolar blends from the melt, Polymer 37 (1996) 595-602.
[55] H. Tsuji, I. Fukui, Enhanced thermal stability of poly(lactide)s in the melt by enantiomeric polymer blending, Polymer 44 (2003) 2891-2896.
[56] P. De Santis, A. Kovacs, Biopolymers 6 (1968) 299.
[57] T. Okihara, M. Tsuji, A. Kawaguchi, K.-I. Katayama, H. Tsuji, S.-H. Hyon, Y. Ikada, Crystal structure of stereocomplex of poly(L-lactide) and poly(D-lactide), Journal of Macromolecular Science, Part B 30 (1991) 119-140.
[58] H. Yamane, K. Sasai, Effect of the addition of poly(d-lactic acid) on the thermal property of poly(l-lactic acid), Polymer 44 (2003) 2569-2575.
[59] S. Inkinen, M. Stolt, A. Södergård, Effect of blending ratio and oligomer structure on the thermal transitions of stereocomplexes consisting of a D-lactic acid oligomer and poly(L-lactide), Polymers for Advanced Technologies 22 (2011) 1658-1664.
[60] J. Sun, H. Yu, X. Zhuang, X. Chen, X. Jing, Crystallization Behavior of Asymmetric PLLA/PDLA Blends, The Journal of Physical Chemistry B 115 (2011) 2864-2869.
[61] N. Rahman, T. Kawai, G. Matsuba, K. Nishida, T. Kanaya, H. Watanabe, H. Okamoto, M. Kato, A. Usuki, M. Matsuda, K. Nakajima, N. Honma, Effect of Polylactide Stereocomplex on the Crystallization Behavior of Poly(l-lactic acid), Macromolecules 42 (2009) 4739-4745.
[62] J.-R. Sarasua, R.E. Prud'homme, M. Wisniewski, A. Le Borgne, N. Spassky, Crystallization and Melting Behavior of Polylactides, Macromolecules 31 (1998) 3895-3905.
[63] S. Brochu, R.E. Prud'homme, I. Barakat, R. Jerome, Stereocomplexation and Morphology of Polylactides, Macromolecules 28 (1995) 5230-5239.
[64] H. Tsuji, Y. Ikada, Crystallization from the melt of poly(lactide)s with different optical purities and their blends, Macromolecular Chemistry and Physics 197 (1996) 3483-3499.
[65] H. Tsuji, Y. Ikada, Stereocomplex formation between enantiomeric poly(lactic acid)s. XI. Mechanical properties and morphology of solution-cast films, Polymer 40 (1999) 6699-6708.
[66] H. Tsuji, Y. Ikada, Stereocomplex formation between enantiomeric poly(lactic acids). 9. Stereocomplexation from the melt, Macromolecules 26 (1993) 6918-6926.
[67] J. Slager, A.J. Domb, Biopolymer stereocomplexes, Advanced Drug Delivery Reviews 55 (2003) 549-583.
[68] F.L. Binsbergen, Heterogeneous nucleation in the crystallization of polyolefins: Part 1. Chemical and physical nature of nucleating agents, Polymer 11 (1970) 253-267.
[69] J. Menczel, J. Varga, Influence of nucleating agents on crystallization of polypropylene, Journal of thermal analysis 28 (1983) 161-174.

[70] H. Li, M.A. Huneault, Effect of nucleation and plasticization on the crystallization of poly(lactic acid), Polymer 48 (2007) 6855-6866.
[71] M. Blomenhofer, S. Ganzleben, D. Hanft, H.-W. Schmidt, M. Kristiansen, P. Smith, K. Stoll, D. Mäder, K. Hoffmann, "Designer" Nucleating Agents for Polypropylene, Macromolecules 38 (2005) 3688-3695.
[72] J.J. Kolstad, Crystallization kinetics of poly(L-lactide-co-meso-lactide), Journal of Applied Polymer Science 62 (1996) 1079-1091.
[73] A.M. Harris, E.C. Lee, Improving mechanical performance of injection molded PLA by controlling crystallinity, Journal of Applied Polymer Science 107 (2008) 2246-2255.
[74] M. Nofar, W. Zhu, C.B. Park, J. Randall, Crystallization Kinetics of Linear and Long-Chain-Branched Polylactide, Industrial & Engineering Chemistry Research 50 (2011) 13789-13798.
[75] M.Okamoto, Recent advances in polymer/layered silicate nanocomposites: an overview from science to technology, Materials Science and Technology 22 (2006) 756-779.
[76] J.Y. Nam, S. Sinha Ray, M. Okamoto, Crystallization Behavior and Morphology of Biodegradable Polylactide/Layered Silicate Nanocomposite, Macromolecules 36 (2003) 7126-7131.
[77] M. Pluta, Melt compounding of polylactide/organoclay: Structure and properties of nanocomposites, Journal of Polymer Science Part B: Polymer Physics 44 (2006) 3392-3405.
[78] N. Najafi, M.C. Heuzey, P.J. Carreau, Crystallization behavior and morphology of polylactide and PLA/clay nanocomposites in the presence of chain extenders, Polymer Engineering & Science (2012) 1-10.
[79] P. Pan, Z. Liang, N. Nakamura, T. Miyagawa, Y. Inoue, Uracil as Nucleating Agent for Bacterial Poly[(3-Hydroxybutyrate)-co-(3-hydroxyhexanoate)] Copolymers, Macromolecular Bioscience 9 (2009) 585-595.
[80] P. Pan, J. Yang, G. Shan, Y. Bao, Z. Weng, Y. Inoue, Nucleation Effects of Nucleobases on the Crystallization Kinetics of Poly(L-lactide), Macromolecular Materials and Engineering 297 (2012) 670-679.
[81] H. Tsuji, H. Takai, N. Fukuda, H. Takikawa, Non-Isothermal Crystallization Behavior of Poly(L-lactic acid) in the Presence of Various Additives, Macromolecular Materials and Engineering 291 (2006) 325-335.
[82] M.H. Hongbo li, Crystallization of PLA/thermoplastic starch blends
International Polymer Processing 23 (2008) 412-418.
[83] O. Martin, L. Avérous, Poly(lactic acid): plasticization and properties of biodegradable multiphase systems, Polymer 42 (2001) 6209-6219.
[84] T. Ke, X. Sun, Melting behavior and crystallization kinetics of starch and poly(lactic acid) composites, Journal of Applied Polymer Science 89 (2003) 1203-1210.
[85] M.A. Huneault, H. Li, Preparation and properties of extruded thermoplastic starch/polymer blends, Journal of Applied Polymer Science 126 (2012) E96-E108.
[86] H. Tsuji, K. Tashiro, L. Bouapao, J. Narita, Polyglycolide as a Biodegradable Nucleating Agent for Poly(L-lactide), Macromolecular Materials and Engineering 293 (2008) 947-951.
[87] A. Pei, Q. Zhou, L.A. Berglund, Functionalized cellulose nanocrystals as biobased nucleation agents in poly(l-lactide) (PLLA) – Crystallization and mechanical property effects, Composites Science and Technology 70 (2010) 815-821.

[88] G. Wenz, Cyclodextrins as Building Blocks for Supramolecular Structures and Functional Units, Angewandte Chemie International Edition in English 33 (1994) 803-822.
[89] T. Dong, Y. He, B. Zhu, K.-M. Shin, Y. Inoue, Nucleation Mechanism of α-Cyclodextrin-Enhanced Crystallization of Some Semicrystalline Aliphatic Polymers, Macromolecules 38 (2005) 7736-7744.
[90] T. Dong, T. Mori, T. Aoyama, Y. Inoue, Rapid crystallization of poly(3-hydroxybutyrate-co-3-hydroxyhexanoate) copolymer accelerated by cyclodextrin-complex as nucleating agent, Carbohydrate Polymers 80 (2010) 387-393.
[91] Y. He, Y. Inoue, Effect of α-cyclodextrin on the crystallization of poly (3-hydroxybutyrate), Journal of Polymer Science Part B: Polymer Physics 42 (2004) 3461-3469.
[92] R. Zhang, Y. Wang, K. Wang, G. Zheng, Q. Li, C. Shen, Crystallization of poly(lactic acid) accelerated by cyclodextrin complex as nucleating agent, Polymer Bulletin (2012) 1-12.
[93] Z. Qiu, Z. Li, Effect of Orotic Acid on the Crystallization Kinetics and Morphology of Biodegradable Poly(l-lactide) as an Efficient Nucleating Agent, Industrial & Engineering Chemistry Research 50 (2011) 12299-12303.
[94] P. Song, G. Chen, Z. Wei, Y. Chang, W. Zhang, J. Liang, Rapid crystallization of poly(l-lactic acid) induced by a nanoscaled zinc citrate complex as nucleating agent, Polymer 53 (2012) 4300-4309.
[95] S.-F. Hsu, T.-M. Wu, C.-S. Liao, Isothermal crystallization kinetics of poly(3-hydroxybutyrate)/layered double hydroxide nanocomposites, Journal of Polymer Science Part B: Polymer Physics 44 (2006) 3337-3347.
[96] R.M. Rasal, D.E. Hirt, Toughness decrease of PLA-PHBHHx blend films upon surface-confined photopolymerization, Journal of Biomedical Materials Research Part A 88A (2009) 1079-1086.
[97] J. Zhang, H. Sato, T. Furukawa, H. Tsuji, I. Noda, Y. Ozaki, Crystallization Behaviors of Poly(3-hydroxybutyrate) and Poly(l-lactic acid) in Their Immiscible and Miscible Blends, The Journal of Physical Chemistry B 110 (2006) 24463-24471.
[98] Y. Hu, H. Sato, J. Zhang, I. Noda, Y. Ozaki, Crystallization behavior of poly(l-lactic acid) affected by the addition of a small amount of poly(3-hydroxybutyrate), Polymer 49 (2008) 4204-4210.
[99] J.Y. Nam, M. Okamoto, H. Okamoto, M. Nakano, A. Usuki, M. Matsuda, Morphology and crystallization kinetics in a mixture of low-molecular weight aliphatic amide and polylactide, Polymer 47 (2006) 1340-1347.
[100] H. Nakajima, M. Takahashi, Y. Kimura, Induced Crystallization of PLLA in the Presence of 1,3,5-Benzenetricarboxylamide Derivatives as Nucleators: Preparation of Haze-Free Crystalline PLLA Materials, Macromolecular Materials and Engineering 295 (2010) 460-468.
[101] N. Kawamoto, A. Sakai, T. Horikoshi, T. Urushihara, E. Tobita, Nucleating agent for poly(L-lactic acid)—An optimization of chemical structure of hydrazide compound for advanced nucleation ability, Journal of Applied Polymer Science 103 (2007) 198-203.
[102] L. Wen, Z. Xin, Effect of a Novel Nucleating Agent on Isothermal Crystallization of Poly(L-lactic acid), Chinese Journal of Chemical Engineering 18 (2010) 899-904.

[103] J. Cao, K. Wang, W. Cao, Q. Zhang, R. Du, Q. Fu, Combined effect of shear and nucleating agent on the multilayered structure of injection-molded bar of isotactic polypropylene, Journal of Applied Polymer Science 112 (2009) 1104-1113.
[104] Y. Feng, X. Jin, J.N. Hay, Effect of nucleating agent addition on crystallization of isotactic polypropylene, Journal of Applied Polymer Science 69 (1998) 2089-2095.
[105] W.-C. Lai, Thermal Behavior and Crystal Structure of Poly(l-lactic acid) with 1,3:2,4-Dibenzylidene-d-sorbitol, The Journal of Physical Chemistry B 115 (2011) 11029-11037.
[106] Y. Cai, S. Yan, J. Yin, Y. Fan, X. Chen, Crystallization behavior of biodegradable poly(L-lactic acid) filled with a powerful nucleating agent: N,N′-bis(benzoyl) suberic acid dihydrazide, Journal of Applied Polymer Science 121 (2011) 1408-1416.
[107] P. Song, Z. Wei, J. Liang, G. Chen, W. Zhang, Crystallization behavior and nucleation analysis of poly(l-lactic acid) with a multiamide nucleating agent, Polymer Engineering & Science 52 (2012) 1058-1068.
[108] S. Barrau, C. Vanmansart, M. Moreau, A. Addad, G. Stoclet, J.M. Lefebvre, R. Seguela, Crystallization Behavior of Carbon Nanotube−Polylactide Nanocomposites, Macromolecules 44 (2011) 6496-6502.
[109] C.-F. Kuan, H.-C. Kuan, C.-C.M. Ma, C.-H. Chen, Mechanical and electrical properties of multi-wall carbon nanotube/poly(lactic acid) composites, Journal of Physics and Chemistry of Solids 69 (2008) 1395-1398.
[110] Y. Li, H. Wu, Y. Wang, L. Liu, L. Han, J. Wu, F. Xiang, Synergistic effects of PEG and MWCNTs on crystallization behavior of PLLA, Journal of Polymer Science Part B: Polymer Physics 48 (2010) 520-528.
[111] H.-S. Xu, X.J. Dai, P.R. Lamb, Z.-M. Li, Poly(L-lactide) crystallization induced by multiwall carbon nanotubes at very low loading, Journal of Polymer Science Part B: Polymer Physics 47 (2009) 2341-2352.
[112] Y.-T. Shieh, G.-L. Liu, Effects of carbon nanotubes on crystallization and melting behavior of poly(L-lactide) via DSC and TMDSC studies, Journal of Polymer Science Part B: Polymer Physics 45 (2007) 1870-1881.
[113] Y. Li, Y. Wang, L. Liu, L. Han, F. Xiang, Z. Zhou, Crystallization improvement of poly(L-lactide) induced by functionalized multiwalled carbon nanotubes, Journal of Polymer Science Part B: Polymer Physics 47 (2009) 326-339.
[114] Z. Su, Y. Liu, W. Guo, Q. Li, C. Wu, Crystallization Behavior of Poly(Lactic Acid) Filled with Modified Carbon Black, Journal of Macromolecular Science, Part B 48 (2009) 670-683.
[115] L. Sun, W.J. Boo, D. Sun, A. Clearfield, H.-J. Sue, Preparation of Exfoliated Epoxy/α-Zirconium Phosphate Nanocomposites Containing High Aspect Ratio Nanoplatelets, Chemistry of Materials 19 (2007) 1749-1754.
[116] L.S. Brandão, L.C. Mendes, M.E. Medeiros, L. Sirelli, M.L. Dias, Thermal and mechanical properties of poly(ethylene terephthalate)/lamellar zirconium phosphate nanocomposites, Journal of Applied Polymer Science 102 (2006) 3868-3876.
[117] P. Pan, Z. Liang, A. Cao, Y. Inoue, Layered Metal Phosphonate Reinforced Poly(l-lactide) Composites with a Highly Enhanced Crystallization Rate, ACS Applied Materials & Interfaces 1 (2009) 402-411.
[118] L. Suryanegara, H. Okumura, A. Nakagaito, H. Yano, The synergetic effect of phenylphosphonic acid zinc and microfibrillated cellulose on the injection molding cycle time of PLA composites, Cellulose 18 (2011) 689-698.

[119] S. Wang, C. Han, J. Bian, L. Han, X. Wang, L. Dong, Morphology, crystallization and enzymatic hydrolysis of poly(L-lactide) nucleated using layered metal phosphonates, Polymer International 60 (2011) 284-295.
[120] H. Pan, Z. Qiu, Biodegradable Poly(l-lactide)/Polyhedral Oligomeric Silsesquioxanes Nanocomposites: Enhanced Crystallization, Mechanical Properties, and Hydrolytic Degradation, Macromolecules 43 (2010) 1499-1506.
[121] J. Yu, Z. Qiu, Preparation and Properties of Biodegradable Poly(l-lactide)/Octamethyl-Polyhedral Oligomeric Silsesquioxanes Nanocomposites with Enhanced Crystallization Rate via Simple Melt Compounding, ACS Applied Materials & Interfaces 3 (2011) 890-897.
[122] J. Yu, Z. Qiu, Effect of low octavinyl-polyhedral oligomeric silsesquioxanes loadings on the melt crystallization and morphology of biodegradable poly(l-lactide), Thermochimica Acta 519 (2011) 90-95.
[123] Z. Qiu, H. Pan, Preparation, crystallization and hydrolytic degradation of biodegradable poly(l-lactide)/polyhedral oligomeric silsesquioxanes nanocomposite, Composites Science and Technology 70 (2010) 1089-1094.
[124] R. Liao, B. Yang, W. Yu, C. Zhou, Isothermal cold crystallization kinetics of polylactide/nucleating agents, Journal of Applied Polymer Science 104 (2007) 310-317.
[125] Q. Shi, H. Mou, L. Gao, J. Yang, W. Guo, Double-Melting Behavior of Bamboo Fiber/Talc/Poly (Lactic Acid) Composites, Journal of Polymers and the Environment 18 (2010) 567-575.
[126] H. Liu, J. Zhang, Research progress in toughening modification of poly(lactic acid), Journal of Polymer Science Part B: Polymer Physics 49 (2011) 1051-1083.
[127] S. Jacobsen, H.G. Fritz, Plasticizing polylactide—the effect of different plasticizers on the mechanical properties, Polymer Engineering & Science 39 (1999) 1303-1310.
[128] W.-C. Lai, W.-B. Liau, T.-T. Lin, The effect of end groups of PEG on the crystallization behaviors of binary crystalline polymer blends PEG/PLLA, Polymer 45 (2004) 3073-3080.
[129] W.-C. Lai, W.-B. Liau, L.-Y. Yang, The effect of ionic interaction on the miscibility and crystallization behaviors of poly(ethylene glycol)/poly(L-lactic acid) blends, Journal of Applied Polymer Science 110 (2008) 3616-3623.
[130] Z. Kulinski, E. Piorkowska, Crystallization, structure and properties of plasticized poly(l-lactide), Polymer 46 (2005) 10290-10300.
[131] Z. Kulinski, E. Piorkowska, K. Gadzinowska, M. Stasiak, Plasticization of Poly(l-lactide) with Poly(propylene glycol), Biomacromolecules 7 (2006) 2128-2135.
[132] E. Piorkowska, Z. Kulinski, A. Galeski, R. Masirek, Plasticization of semicrystalline poly(l-lactide) with poly(propylene glycol), Polymer 47 (2006) 7178-7188.
[133] L.V. Labrecque, R.A. Kumar, V. Davé, R.A. Gross, S.P. McCarthy, Citrate esters as plasticizers for poly(lactic acid), Journal of Applied Polymer Science 66 (1997) 1507-1513.
[134] N. Ljungberg, B. Wesslén, The effects of plasticizers on the dynamic mechanical and thermal properties of poly(lactic acid), Journal of Applied Polymer Science 86 (2002) 1227-1234.

[135] N. Ljungberg, B. Wesslén, Preparation and Properties of Plasticized Poly(lactic acid) Films, Biomacromolecules 6 (2005) 1789-1796.
[136] H. Xiao, W. Lu, J.-T. Yeh, Effect of plasticizer on the crystallization behavior of poly(lactic acid), Journal of Applied Polymer Science 113 (2009) 112-121.
[137] Z. Jia, K. Zhang, J. Tan, C. Han, L. Dong, Y. Yang, Crystallization behavior and mechanical properties of crosslinked plasticized poly(L-lactic acid), Journal of Applied Polymer Science 111 (2009) 1530-1539.
[138] M. Takada, S. Hasegawa, M. Ohshima, Crystallization kinetics of poly(L-lactide) in contact with pressurized CO2, Polymer Engineering & Science 44 (2004) 186-196.
[139] L. Yu, H. Liu, K. Dean, Thermal behaviour of poly(lactic acid) in contact with compressed carbon dioxide, Polymer International 58 (2009) 368-372.
[140] L. Yu, H. Liu, K. Dean, L. Chen, Cold crystallization and postmelting crystallization of PLA plasticized by compressed carbon dioxide, Journal of Polymer Science Part B: Polymer Physics 46 (2008) 2630-2636.
[141] Y.-M. Corre, A. Maazouz, J. Duchet, J. Reignier, Batch foaming of chain extended PLA with supercritical CO2: Influence of the rheological properties and the process parameters on the cellular structure, The Journal of Supercritical Fluids 58 (2011) 177-188.
[142] M. Mihai, M.A. Huneault, B.D. Favis, Crystallinity development in cellular poly(lactic acid) in the presence of supercritical carbon dioxide, Journal of Applied Polymer Science 113 (2009) 2920-2932.
[143] M. Pluta, Morphology and properties of polylactide modified by thermal treatment, filling with layered silicates and plasticization, Polymer 45 (2004) 8239-8251.
[144] M. Li, D. Hu, Y. Wang, C. Shen, Nonisothermal crystallization kinetics of poly(lactic acid) formulations comprising talc with poly(ethylene glycol), Polymer Engineering & Science 50 (2010) 2298-2305.
[145] H. Xiao, L. Yang, X. Ren, T. Jiang, J.-T. Yeh, Kinetics and crystal structure of poly(lactic acid) crystallized nonisothermally: Effect of plasticizer and nucleating agent, Polymer Composites 31 (2010) 2057-2068.
[146] H.W. Xiao, P. Li, X. Ren, T. Jiang, J.-T. Yeh, Isothermal crystallization kinetics and crystal structure of poly(lactic acid): Effect of triphenyl phosphate and talc, Journal of Applied Polymer Science 118 (2010) 3558-3569.
[147] B. Fillon, A. Thierry, B. Lotz, J. Wittmann, Efficiency scale for polymer nucleating agents, Journal of Thermal Analysis and Calorimetry 42 (1994) 721-731.
[148] D.J. Blundell, A. Keller, A.J. Kovacs, A new self-nucleation phenomenon and its application to the growing of polymer crystals from solution, Journal of Polymer Science Part B: Polymer Letters 4 (1966) 481-486.
[149] C.H. Molinuevo, G.A. Mendez, A.J. Müller, Nucleation and crystallization of PET droplets dispersed in an amorphous PC matrix, Journal of Applied Polymer Science 70 (1998) 1725-1735.
[150] B. Fillon, B. Lotz, A. Thierry, J.C. Wittmann, Self-nucleation and enhanced nucleation of polymers. Definition of a convenient calorimetric “efficiency scale” and evaluation of nucleating additives in isotactic polypropylene (α phase), Journal of Polymer Science Part B: Polymer Physics 31 (1993) 1395-1405.
[151] B. Fillon, J.C. Wittmann, B. Lotz, A. Thierry, Self-nucleation and recrystallization of isotactic polypropylene (α phase) investigated by differential scanning calorimetry, Journal of Polymer Science Part B: Polymer Physics 31 (1993) 1383-1393.

[152] M.A. Sabino, G. Ronca, A.J. Müller, Heterogeneous nucleation and self-nucleation of poly(p-dioxanone), Journal of Materials Science 35 (2000) 5071-5084.
[153] M.A. Sabino, J.L. Feijoo, A.J. Müller, Crystallisation and morphology of poly(p-dioxanone), Macromolecular Chemistry and Physics 201 (2000) 2687-2698.
[154] K.S. Anderson, M.A. Hillmyer, Melt preparation and nucleation efficiency of polylactide stereocomplex crystallites, Polymer 47 (2006) 2030-2035.
[155] S.C. Schmidt, M.A. Hillmyer, Polylactide stereocomplex crystallites as nucleating agents for isotactic polylactide, Journal of Polymer Science Part B: Polymer Physics 39 (2001) 300-313.
[156] X. products., XPansion Instrument Website.
[157] M.h. Boutaous, P. Bourgin, M. Zinet, Thermally and flow induced crystallization of polymers at low shear rate, Journal of Non-Newtonian Fluid Mechanics 165 (2010) 227-237.
[158] F. Bustos, P. Cassagnau, R. Fulchiron, Effect of molecular architecture on quiescent and shear-induced crystallization of polyethylene, Journal of Polymer Science Part B: Polymer Physics 44 (2006) 1597-1607.
[159] D. Byelov, P. Panine, K. Remerie, E. Biemond, G.C. Alfonso, W.H. de Jeu, Crystallization under shear in isotactic polypropylene containing nucleators, Polymer 49 (2008) 3076-3083.
[160] A.J. Pennings, A.M. Kiel, Fractionation of polymers by crystallization from solution, III. On the morphology of fibrillar polyethylene crystals grown in solution, Kolloid-Zeitschrift und Zeitschrift für Polymere 205 (1965) 160-162.
[161] X.-j. Li, G.-j. Zhong, Z.-m. Li, Non-isothermal crystallization of poly(L-lactide) (PLLA) under quiescent and steady shear conditions, Chinese Journal of Polymer Science 28 (2010) 357-366.
[162] X.J. Li, Z.M. Li, G.J. Zhong, L.B. Li, Steady–shear-induced Isothermal Crystallization of Poly(L-lactide) (PLLA), Journal of Macromolecular Science, Part B 47 (2008) 511-522.
[163] S. Huang, H. Li, S. Jiang, X. Chen, L. An, Crystal structure and morphology influenced by shear effect of poly(l-lactide) and its melting behavior revealed by WAXD, DSC and in-situ POM, Polymer 52 (2011) 3478-3487.
[164] R.R. Lagasse, B. Maxwell, An experimental study of the kinetics of polymer crystallization during shear flow, Polymer Engineering & Science 16 (1976) 189-199.
[165] S. Naudy, L. David, C. Rochas, R. Fulchiron, Shear induced crystallization of poly(m-xylylene adipamide) with and without nucleating additives, Polymer 48 (2007) 3273-3285.
[166] M. D'Haese, P. Van Puyvelde, F. Langouche, Effect of Particles on the Flow-Induced Crystallization of Polypropylene at Processing Speeds, Macromolecules 43 (2010) 2933-2941.
[167] B. Larin, C.A. Avila-Orta, R.H. Somani, B.S. Hsiao, G. Marom, Combined effect of shear and fibrous fillers on orientation-induced crystallization in discontinuous aramid fiber/isotactic polypropylene composites, Polymer 49 (2008) 295-302.
[168] J.-Z. Xu, C. Chen, Y. Wang, H. Tang, Z.-M. Li, B.S. Hsiao, Graphene Nanosheets and Shear Flow Induced Crystallization in Isotactic Polypropylene Nanocomposites, Macromolecules 44 (2011) 2808-2818.

[169] Y.-H. Chen, G.-J. Zhong, J. Lei, Z.-M. Li, B.S. Hsiao, In Situ Synchrotron X-ray Scattering Study on Isotactic Polypropylene Crystallization under the Coexistence of Shear Flow and Carbon Nanotubes, Macromolecules 44 (2011) 8080-8092.
[170] R. Iervolino, E. Somma, M. Nobile, X. Chen, B. Hsiao, The role of multi-walled carbon nanotubes in shear enhanced crystallization of isotactic poly(1-butene), Journal of Thermal Analysis and Calorimetry 98 (2009) 611-622.
[171] H. Tang, J.-B. Chen, Y. Wang, J.-Z. Xu, B.S. Hsiao, G.-J. Zhong, Z.-M. Li, Shear Flow and Carbon Nanotubes Synergistically Induced Nonisothermal Crystallization of Poly(lactic acid) and Its Application in Injection Molding, Biomacromolecules 13 (2012) 3858-3867.
[172] Z. Xia, H.-J. Sue, Z. Wang, C.A. Avila-Orta, B.S. Hsiao, Determination of crystalline lamellar thickness in poly(ethylene terephthalate) using small-angle X-Ray scatering and transmission electron microscopy*, Journal of Macromolecular Science, Part B 40 (2001) 625-638.
[173] H. Fang, Y. Zhang, J. Bai, Z. Wang, Shear-Induced Nucleation and Morphological Evolution for Bimodal Long Chain Branched Polylactide, Macromolecules 46 (2013) 6555-6565.
[174] J. Bai, J. Wang, W. Wang, H. Fang, Z. Xu, X. Chen, Z. Wang, Stereocomplex Crystallite-Assisted Shear-Induced Crystallization Kinetics at a High Temperature for Asymmetric Biodegradable PLLA/PDLA Blends, ACS Sustainable Chemistry & Engineering 4 (2016) 273-283.
[175] H. Xu, L. Xie, M. Hakkarainen, Beyond a Model of Polymer Processing-Triggered Shear: Reconciling Shish-Kebab Formation and Control of Chain Degradation in Sheared Poly(l-lactic acid), ACS Sustainable Chemistry & Engineering 3 (2015) 1443-1452.
[176] M. Mihai, M.A. Huneault, B.D. Favis, H. Li, Extrusion Foaming of Semi-Crystalline PLA and PLA/Thermoplastic Starch Blends, Macromolecular Bioscience 7 (2007) 907-920.
[177] W. Zhai, Y. Ko, W. Zhu, A. Wong, C. Park, A Study of the Crystallization, Melting, and Foaming Behaviors of Polylactic Acid in Compressed CO2, International Journal of Molecular Sciences 10 (2009) 5381-5397.
[178] G. Kokturk, E. Piskin, T.F. Serhatkulu, M. Cakmak, Evolution of phase behavior and orientation in uniaxially deformed polylactic acid films, Polymer Engineering & Science 42 (2002) 1619-1628.
[179] H. Li, M.A. Huneault, Comparison of sorbitol and glycerol as plasticizers for thermoplastic starch in TPS/PLA blends, Journal of Applied Polymer Science 119 (2011) 2439-2448.
[180] R. Pantani, F. De Santis, A. Sorrentino, F. De Maio, G. Titomanlio, Crystallization kinetics of virgin and processed poly(lactic acid), Polymer Degradation and Stability 95 (2010) 1148-1159.
[181] J. Zhang, K. Tashiro, A.J. Domb, H. Tsuji, Confirmation of Disorder α Form of Poly(L-lactic acid) by the X-ray Fiber Pattern and Polarized IR/Raman Spectra Measured for Uniaxially-Oriented Samples, Macromolecular Symposia 242 (2006) 274-278.
[182] P. Pan, B. Zhu, W. Kai, T. Dong, Y. Inoue, Polymorphic Transition in Disordered Poly(l-lactide) Crystals Induced by Annealing at Elevated Temperatures, Macromolecules 41 (2008) 4296-4304.

[183] J.P. Kalish, K. Aou, X. Yang, S.L. Hsu, Spectroscopic and thermal analyses of α′ and α crystalline forms of poly(l-lactic acid), Polymer 52 (2011) 814-821.
[184] X. Chen, J. Kalish, S.L. Hsu, Structure evolution of α′-phase poly(lactic acid), Journal of Polymer Science Part B: Polymer Physics 49 (2011) 1446-1454.
[185] B. Lotz, α and β phases of isotactic polypropylene: a case of growth kinetics `phase reentrency' in polymer crystallization, Polymer 39 (1998) 4561-4567.
[186] B. Fillon, A. Thierry, J.C. Wittmann, B. Lotz, Self-nucleation and recrystallization of polymers. Isotactic polypropylene, β phase: β-α conversion and β-α growth transitions, Journal of Polymer Science Part B: Polymer Physics 31 (1993) 1407-1424.
[187] S. Schneider, X. Drujon, B. Lotz, J.C. Wittmann, Self-nucleation and enhanced nucleation of polyvinylidene fluoride (α-phase), Polymer 42 (2001) 8787-8798.
[188] L. Marquez, I. Rivero, A.J. Müller, Application of the SSA calorimetric technique to characterize LLDPE grafted with diethyl maleate, Macromolecular Chemistry and Physics 200 (1999) 330-337.
[189] M. Arnal, V. Balsamo, G. Ronca, A. Sánchez, A. Müller, E. Cañizales, C. Urbina de Navarro, Applications of Successive Self-Nucleation and Annealing (SSA) to Polymer Characterization, Journal of Thermal Analysis and Calorimetry 59 (2000) 451-470.
[190] R.M. Michell, A.J. Müller, G. Deshayes, P. Dubois, Effect of sequence distribution on the isothermal crystallization kinetics and successive self-nucleation and annealing (SSA) behavior of poly(ε-caprolactone-co-ε-caprolactam) copolymers, European Polymer Journal 46 (2010) 1334-1344.
[191] F. De Santis, R. Pantani, G. Titomanlio, Nucleation and crystallization kinetics of poly(lactic acid), Thermochimica Acta 522 (2011) 128-134.
[192] R. Androsch, H.M.N. Iqbal, C. Schick, Non-isothermal crystal nucleation of poly (l-lactic acid), Polymer 81 (2015) 151-158.
[193] S. Saeidlou, M.A. Huneault, H. Li, P. Sammut, C.B. Park, Evidence of a dual network/spherulitic crystalline morphology in PLA stereocomplexes, Polymer 53 (2012) 5816-5824.
[194] P. Supaphol, J.E. Spruiell, Crystalline memory effects in isothermal crystallization of syndiotactic polypropylene, Journal of Applied Polymer Science 75 (2000) 337-346.
[195] K. Wasanasuk, K. Tashiro, Structural Regularization in the Crystallization Process from the Glass or Melt of Poly(l-lactic Acid) Viewed from the Temperature-Dependent and Time-Resolved Measurements of FTIR and Wide-Angle/Small-Angle X-ray Scatterings, Macromolecules 44 (2011) 9650-9660.
[196] D. Garlotta, A Literature Review of Poly(Lactic Acid), Journal of Polymers and the Environment 9 (2001) 63-84.
[197] B. Gupta, N. Revagade, J. Hilborn, Poly(lactic acid) fiber: An overview, Progress in Polymer Science 32 (2007) 455-482.
[198] P. Pan, B. Zhu, W. Kai, T. Dong, Y. Inoue, Macromolecules 41 (2008) 4296.
[199] A. Jalali, M.A. Huneault, S. Elkoun, Effect of thermal history on nucleation and crystallization of poly(lactic acid), Journal of Materials Science (2016) 1-12.
[200] P. Zhu, D. Ma, Double cold crystallization peaks of poly(ethylene terephthalate)—1. Samples isothermally crystallized at low temperature, European Polymer Journal 33 (1997) 1817-1818.

[201] Z. Pingping, M. Dezhu, Study on the double cold crystallization peaks of poly(ethylene terephthalate) 3. The influence of the addition of calcium carbonate (CaCO3), European Polymer Journal 36 (2000) 2471-2475.
[202] F.J. Díez, C. Alvariño, J. López, C. Ramírez, M.J. Abad, J. Cano, S. García-Garabal, L. Barral, Influence of the stretching in the crystallinity of biaxially oriented polypropylene (BOPP) films, Journal of Thermal Analysis and Calorimetry 81 (2005) 21-25.
[203] J. Varga, J. Menczel, A. Solti, Double crystallization of biaxially oriented polypropylene, Journal of Thermal Analysis and Calorimetry 20 (1981) 23-32.
[204] G. Gorrasi, R. Pantani, Effect of PLA grades and morphologies on hydrolytic degradation at composting temperature: Assessment of structural modification and kinetic parameters, Polymer Degradation and Stability 98 (2013) 1006-1014.
[205] H. Tsuji, K. Nakahara, Poly(L-lactide). IX. Hydrolysis in acid media, Journal of Applied Polymer Science 86 (2002) 186-194.
[206] E.J. Rodriguez, B. Marcos, M.A. Huneault, Hydrolysis of polylactide in aqueous media, Journal of Applied Polymer Science (2016),In press.
[207] Y. Yamamoto, Y. Inoue, T. Onai, C. Doshu, H. Takahashi, H. Uehara, Deconvolution Analyses of Differential Scanning Calorimetry Profiles of β-Crystallized Polypropylenes with Synchronized X-ray Measurements, Macromolecules 40 (2007) 2745-2750.
[208] T.-Y. Cho, G. Strobl, Temperature dependent variations in the lamellar structure of poly(l-lactide), Polymer 47 (2006) 1036-1043.
[209] A.T. Lorenzo, M.L. Arnal, J.J. Sánchez, A.J. Müller, Effect of annealing time on the self-nucleation behavior of semicrystalline polymers, Journal of Polymer Science Part B: Polymer Physics 44 (2006) 1738-1750.
[210] R. Datta, M. Henry, Lactic acid: recent advances in products, processes and technologies — a review, Journal of Chemical Technology & Biotechnology 81 (2006) 1119-1129.
[211] H.S. Myung, W.J. Yoon, E.S. Yoo, B.C. Kim, S.S. Im, Effect of shearing on crystallization behavior of poly(ethylene terephthalate), Journal of Applied Polymer Science 80 (2001) 2640-2646.
[212] A.J. Pennings, Bundle-like nucleation and longitudinal growth of fibrillar polymer crystals from flowing solutions, Journal of Polymer Science: Polymer Symposia 59 (1977) 55-86.
[213] R. Pantani, V. Nappo, F. De Santis, G. Titomanlio, Fibrillar Morphology in Shear-Induced Crystallization of Polypropylene, Macromolecular Materials and Engineering 299 (2014) 1465-1473.
[214] N.V. Pogodina, V.P. Lavrenko, S. Srinivas, H.H. Winter, Rheology and structure of isotactic polypropylene near the gel point: quiescent and shear-induced crystallization, Polymer 42 (2001) 9031-9043.
[215] C. Duplay, B. Monasse, J.M. Haudin, J.L. Costa, Shear-induced crystallization of polypropylene: Influence of molecular weight, Journal of Materials Science 35 (2000) 6093-6103.
[216] F. Jay, J.M. Haudin, B. Monasse, Shear-induced crystallization of polypropylenes: effect of molecular weight, Journal of Materials Science 34 (1999) 2089-2102.
[217] R.H. Somani, L. Yang, B.S. Hsiao, T. Sun, N.V. Pogodina, A. Lustiger, Shear-Induced Molecular Orientation and Crystallization in Isotactic Polypropylene: Effects of the Deformation Rate and Strain, Macromolecules 38 (2005) 1244-1255.

[218] R.H. Somani, L. Yang, L. Zhu, B.S. Hsiao, Flow-induced shish-kebab precursor structures in entangled polymer melts, Polymer 46 (2005) 8587-8623.
[219] C.K. Chai, N.M. Dixon, D.L. Gerrard, W. Reed, Rheo-Raman studies of polyethylene melts, Polymer 36 (1995) 661-663.
[220] J. Vega, D. Hristova, G. Peters, Flow-induced crystallization regimes and rheology of isotactic polypropylene, Journal of Thermal Analysis and Calorimetry 98 (2009) 655-666.
[221] M. Derakhshandeh, S.G. Hatzikiriakos, Flow-induced crystallization of high-density polyethylene: the effects of shear and uniaxial extension, Rheologica Acta 51 (2012) 315-327.
[222] M. Derakhshandeh, A.K. Doufas, S.G. Hatzikiriakos, Quiescent and shear-induced crystallization of polyprophylenes, Rheologica Acta 53 (2014) 519-535.
[223] J.-W. Housmans, G.M. Peters, H.H. Meijer, Flow-induced crystallization of propylene/ethylene random copolymers, Journal of Thermal Analysis and Calorimetry 98 (2009) 693-705.
[224] J.-W. Housmans, R.J.A. Steenbakkers, P.C. Roozemond, G.W.M. Peters, H.E.H. Meijer, Saturation of Pointlike Nuclei and the Transition to Oriented Structures in Flow-Induced Crystallization of Isotactic Polypropylene, Macromolecules 42 (2009) 5728-5740.
[225] M. Sentmanat, O. Delgadillo-Velázquez, S.G. Hatzikiriakos, Crystallization of an ethylene-based butene plastomer: the effect of uniaxial extension, Rheologica Acta 49 (2010) 931-939.
[226] E. Bischoff White, H. Henning Winter, J. Rothstein, Extensional-flow-induced crystallization of isotactic polypropylene, Rheologica Acta 51 (2012) 303-314.
[227] J.-M. Haudin, C. Duplay, B. Monasse, J.-L. Costa, Shear-induced crystallization of polypropylene. Growth enhancement and rheology in the crystallization range, Macromolecular Symposia 185 (2002) 119-133.
[228] H. Tsuji, H. Takai, S.K. Saha, Isothermal and non-isothermal crystallization behavior of poly(l-lactic acid): Effects of stereocomplex as nucleating agent, Polymer 47 (2006) 3826-3837.
[229] A. Nogales, B.S. Hsiao, R.H. Somani, S. Srinivas, A.H. Tsou, F.J. Balta-Calleja, T.A. Ezquerra, Shear-induced crystallization of isotactic polypropylene with different molecular weight distributions: in situ small- and wide-angle X-ray scattering studies, Polymer 42 (2001) 5247-5256.
[230] R.H. Somani, L. Yang, B.S. Hsiao, Effects of high molecular weight species on shear-induced orientation and crystallization of isotactic polypropylene, Polymer 47 (2006) 5657-5668.
[231] C. Hadinata, C. Gabriel, M. Ruellman, H.M. Laun, Comparison of shear-induced crystallization behavior of PB-1 samples with different molecular weight distribution, Journal of Rheology 49 (2004) 327-349.
[232] D. Dikovsky, G. Marom, C.A. Avila-Orta, R.H. Somani, B.S. Hsiao, Shear-induced crystallization in isotactic polypropylene containing ultra-high molecular weight polyethylene oriented precursor domains, Polymer 46 (2005) 3096-3104.

[233] P. Jerschow, H. Janeschitz-Kriegl, The Role of Long Molecules and Nucleating Agents in Shear Induced Crystallization of Isotactic Polypropylenes, International Polymer Processing 12 (1997) 72-77.
[234] Y. Ogino, H. Fukushima, G. Matsuba, N. Takahashi, K. Nishida, T. Kanaya, Effects of high molecular weight component on crystallization of polyethylene under shear flow, Polymer 47 (2006) 5669-5677.
[235] G. Matsuba, S. Sakamoto, Y. Ogino, K. Nishida, T. Kanaya, Crystallization of Polyethylene Blends under Shear Flow. Effects of Crystallization Temperature and Ultrahigh Molecular Weight Component, Macromolecules 40 (2007) 7270-7275.
[236] C.A. Avila-Orta, C. Burger, R. Somani, L. Yang, G. Marom, F.J. Medellin-Rodriguez, B.S. Hsiao, Shear-induced crystallization of isotactic polypropylene within the oriented scaffold of noncrystalline ultrahigh molecular weight polyethylene, Polymer 46 (2005) 8859-8871.
[237] J. Baert, P. Van Puyvelde, Effect of molecular and processing parameters on the flow-induced crystallization of poly-1-butene. Part 1: Kinetics and morphology, Polymer 47 (2006) 5871-5879.
[238] C. Stern, A. Frick, G. Weickert, Relationship between the structure and mechanical properties of polypropylene: Effects of the molecular weight and shear-induced structure, Journal of Applied Polymer Science 103 (2007) 519-533.
[239] F. Zuo, J.K. Keum, L. Yang, R.H. Somani, B.S. Hsiao, Thermal Stability of Shear-Induced Shish-Kebab Precursor Structure from High Molecular Weight Polyethylene Chains, Macromolecules 39 (2006) 2209-2218.
[240] S. Acierno, B. Palomba, H. Winter, N. Grizzuti, Effect of molecular weight on the flow-induced crystallization of isotactic poly(1-butene), Rheologica Acta 42 (2003) 243-250.
[241] M.L. Williams, R.F. Landel, J.D. Ferry, The Temperature Dependence of Relaxation Mechanisms in Amorphous Polymers and Other Glass-forming Liquids, Journal of the American Chemical Society 77 (1955) 3701-3707.
[242] N. Othman, A. Acosta-Ramírez, P. Mehrkhodavandi, J.R. Dorgan, S.G. Hatzikiriakos, Solution and melt viscoelastic properties of controlled microstructure poly(lactide), Journal of Rheology 55 (2011) 987-1005.
[243] J.R. Dorgan, J.S. Williams, D.N. Lewis, Melt rheology of poly(lactic acid): Entanglement and chain architecture effects, Journal of Rheology 43 (1999) 1141-1155.
[244] L. Palade, H.J. Lehermeier, J.R. Dorgan, Melt Rheology of High l-Content Poly(lactic acid), Macromolecules 34 (2001) 1384-1390.
[245] J.R. Dorgan, J. Janzen, M.P. Clayton, S.B. Hait, D.M. Knauss, Melt rheology of variable L-content poly(lactic acid), Journal of Rheology 49 (2005) 607-619.
[246] J.R. Dorgan, J. Janzen, D.M. Knauss, S.B. Hait, B.R. Limoges, M.H. Hutchinson, Fundamental solution and single-chain properties of polylactides, Journal of Polymer Science Part B: Polymer Physics 43 (2005) 3100-3111.
[247] J. van Meerveld, G.M. Peters, M. Hütter, Towards a rheological classification of flow induced crystallization experiments of polymer melts, Rheologica Acta 44 (2004) 119-134.
[248] L.J. Fetters, D.J. Lohse, S.T. Milner, W.W. Graessley, Packing Length Influence in Linear Polymer Melts on the Entanglement, Critical, and Reptation Molecular Weights, Macromolecules 32 (1999) 6847-6851.

[249] M. Doi, S.F. Edwards, Dynamics of concentrated polymer systems. Part 2.-Molecular motion under flow, Journal of the Chemical Society, Faraday Transactions 2: Molecular and Chemical Physics 74 (1978) 1802-1817.
[250] J.J. Cooper-White, M.E. Mackay, Rheological properties of poly(lactides). Effect of molecular weight and temperature on the viscoelasticity of poly(l-lactic acid), Journal of Polymer Science Part B: Polymer Physics 37 (1999) 1803-1814.
[251] P. Pan, Y. Inoue, Polymorphism and isomorphism in biodegradable polyesters, Progress in Polymer Science 34 (2009) 605-640.
[252] Y. Zhong, H. Fang, Y. Zhang, Z. Wang, J. Yang, Z. Wang, Rheologically Determined Critical Shear Rates for Shear-Induced Nucleation Rate Enhancements of Poly(lactic acid), ACS Sustainable Chemistry & Engineering 1 (2013) 663-672.